

D I S S E R T A T I O N

Isomerization of n-alkanes over Pt containing sulfated zirconia

**Isomerisierung von n-Alkanen über Pt h ltigem sulfatisierten
Zirkonoxid**

ausgef hrt zum Zwecke der Erlangung des akademischen Grades eines Doktors
der technischen Wissenschaften unter der Leitung von

A.o. Univ. - Prof. Dr. Hannelore Vinek

E 165

Institut f r Materialchemie

eingereicht an der Technischen Universit t Wien

Fakult t f r Technische Chemie

von

Dipl.-Ing. Karin F ttinger

Matrikelnummer 9525250

Kalvarienberggasse 18/1/1

1170 Wien

Wien, am 23.05.2005

KURZFASSUNG

Gesättigte Kohlenwasserstoffe, Hauptbestandteile von Rohöl, sind bis heute noch immer die wichtigste Quelle für die Herstellung von Treibstoffen. Da geradkettige n-Alkane eine sehr niedrige Oktanzahl aufweisen, müssen sie zu verzweigten Alkanen (hohe OZ) isomerisiert werden. Als Katalysatoren für die Isomerisierung werden bifunktionelle Katalysatoren mit sauren und metallischen Zentren eingesetzt. Sulfatisiertes Zirkonoxid (SZ) hat großes Interesse hervorgerufen, da es eine ausgezeichnete Aktivität für die Isomerisierung von kurzkettigen Alkanen bei tiefen Temperaturen aufweist. Allerdings ist die Art der aktiven Zentren von SZ noch ungeklärt.

Das Ziel dieser Arbeit war es, die Art der aktiven Zentren und den Einfluß des Sulfatgehalts mit Hilfe von in situ IR Spektroskopie, IR Messungen nach Adsorption von Sondenmolekülen wie CO und Pyridin, thermogravimetrischen Messungen (TG), Temperatur-programmierter Desorption (TPD) sowie der Isomerisierung von n-Hexan und n-Heptan als kinetische Testreaktionen zu untersuchen.

Um einen aktiven Katalysator zu erhalten, müssen die folgenden Anforderungen erfüllt sein: die Sulfatgruppen müssen auf ein Zirkonhydroxid als Ausgangsmaterial aufgebracht werden, das Material muß anschließend bei 600-650°C calciniert werden und das SZ muß in der tetragonalen Modifikation vorliegen.

Während der Reaktion von n-Hexan und n-Heptan deaktiviert SZ ohne Pt sehr rasch aufgrund von Kohlenstoffablagerungen (Coke) am Katalysator. Durch Abbrennen des Cokes kann der Katalysator regeneriert werden und weist wieder die gleiche Anfangsaktivität auf.

Das gleiche Verhalten findet man, wenn die Reaktion über Pt hältigem SZ in Helium oder Stickstoff als Trägergas durchgeführt wird. Es konnte gezeigt werden, dass die oxidative Dehydrierung des Alkans ein plausibler Initiierungsschritt der Reaktion in Inertgasatmosphäre ist. Die gebildeten Alkene können in weiterer Folge an der Oberfläche oligomerisieren und Coke bilden. Erst in Gegenwart von Wasserstoff und Pt findet man eine sehr stabile Aktivität über eine längere Zeit. Für die Isomerisierung von n-Hexan wurde eine ausgezeichnete Isomerisierungsselektivität beobachtet. Hingegen bei der Reaktion von n-Heptan fand hauptsächlich Cracken zu Propan und iso-Butan statt, was auf einen säurekatalysierten Crackmechanismus hinweist.

Die katalytische Aktivität konnte durch Oxidation in Luft bei 500°C komplett wiederhergestellt werden. Wenn die Regeneration jedoch im Inertgas durchgeführt wird, wird der Katalysator inaktiv und kann durch thermische Behandlung nicht wieder reaktiviert werden. Das kann durch einen Verlust eines Teils der Sulfatgruppen zwischen 300 und 500°C erklärt werden, was anhand von TG, TPD und IR Messungen beobachtet wurde. Pyridinadsorption ergab, dass ein inaktives Material nur Lewis saure Zentren (LS) besitzt, während ein aktiver Katalysator sowohl Brønsted saure Zentren (BS) als auch LS aufweist.

Es ist jedoch möglich, einen inaktiven Katalysator, der einen Teil der Sulfatgruppen verloren hat, durch Resulfatisierung zu reaktivieren. Eine Erhöhung des Sulfatgehalts führt wieder zu einem aktiven Katalysator, der BS besitzt. Allerdings konnte nicht mehr die gleiche Aktivität wie vorher erreicht werden, was wahrscheinlich auf die Bildung einer kleinen Menge an monokliner Phase zurückzuführen ist, die als inaktiv angesehen wird.

Außerdem wurde der Einfluß des Sulfatgehalts auf die katalytische Aktivität untersucht. Vier Proben mit unterschiedlicher Sulfatbelegung (zwischen 0.46 und 0.63 einer Monolage) wurden miteinander verglichen. Ein Anstieg der Aktivität mit steigendem Sulfatgehalt wurde beobachtet. Die Probe, die weniger als eine halbe Monolage an Sulfaten an der Oberfläche besitzt, war vollständig inaktiv, und Pyridinadsorption ergab, dass dieses Material keine BS besitzt.

Man kann daraus schließen, dass es zumindest zwei verschiedene Arten von Sulfatgruppen an der Oberfläche von SZ gibt. Eine Spezies, die nach einem reduktiven Schritt schwächer an der Oberfläche gebunden ist und daher beim Aufheizen im Inertgas schon bei tieferen Temperaturen (zwischen 300 und 500°C) weggeht, ist verantwortlich für die katalytische Aktivität, während die Sulfatgruppen, die unter den gleichen Bedingungen erst bei höheren Temperaturen oberhalb von 600°C weggehen, inaktiv für die Umsetzung von n-Alkanen sind. Als aktive Spezies werden Pyrosulfatgruppen $\text{S}_2\text{O}_7^{2-}$ diskutiert, die erst bei einer Bedeckung mit mehr als einer halben Monolage Sulfaten gebildet werden.

Die metallische Komponente muß direkt auf das SZ aufgebracht werden, das Zumischen von Pt auf einem inerten Trägermaterial führte zu einer signifikant schlechteren Aktivität und Isomerisierungselektivität. Daraus kann geschlossen werden, daß eine möglichst große Nähe der sauren und metallischen Zentren zueinander gegeben sein muß. Ensembles, die Brønsted saure Zentren an Pyrosulfatgruppen und benachbarte Metallzentren besitzen, werden als aktive Zentren für die n-Alkanisomerisierung angenommen.

Die folgenden Anforderungen müssen erfüllt sein, um einen aktiven Katalysator zu erhalten:

- (i) die Zugabe von Pt
- (ii) die Gegenwart von Wasserstoff
- (iii) mehr als eine halbe Monolage Sulfatgruppen an der Oberfläche und das Vorhandensein von Brønsted und Lewis sauren Zentren.

ABSTRACT

Saturated hydrocarbons as the main components of raw oil are one of the most important sources of fuels. Since n-alkanes possess a low octane number isomerization to branched alkanes is necessary. Noble metal containing acid catalysts and strong acid catalysts are used for isomerization. Among the solid acid catalysts sulfated zirconia (SZ) has reached a lot of interest due to its high activity for the isomerization of light alkanes at low temperatures. Until now a discussion exists about the nature of the active sites on SZ.

The aim of this thesis is to investigate the nature of active sites and the influence of the sulfate content on the activity by means of in situ infrared spectroscopy (IR), adsorption of probe molecules (CO, pyridine) followed by IR measurements, thermogravimetric measurements (TG), temperature-programmed desorption (TPD) and kinetic measurements using n-hexane and n-heptane conversion as test reaction.

For obtaining an active catalyst the following requirements have to be fulfilled: zirconium hydroxide must be used as precursor for sulfation, the material has to be calcined at 600-650°C and tetragonal SZ is regarded as the active modification.

During the conversion of n-hexane and n-heptane SZ without Pt deactivates very fast due to carbon deposition on the catalyst. By burning off the coke the catalyst could be regenerated to its initial activity.

The same behavior was observed when the reaction was carried out over Pt containing SZ catalysts using nitrogen or helium as carrier gas. It can be shown that a plausible initiation step of alkane activation in inert gas atmosphere is the oxidative dehydrogenation. The formed alkenes remain on the surface and can oligomerize into coke. A stable and high activity was only observed in the presence of hydrogen and Pt. The selectivity to isomerization was excellent for hexane, whereas for n-heptane it was small and the main reaction products were propane and isobutane indicating an acid catalyzed cracking mechanism.

The activity of the Pt/SZ catalyst could be completely restored by oxidation in air at 500°C. However, if regeneration was done in inert gas, the catalyst was inactive for alkane conversion and could not be reactivated by thermal treatment. This can be explained by a loss of a part of sulfates between 300 and 500°C observed by TG, TPD and IR. Pyridine adsorption on an inactive

sample showed only the presence of Lewis acid sites (LS), whereas active samples possess both – Brønsted (BS) and Lewis acid sites.

It is possible to reactivate an inactive catalyst, which had lost a part of the sulfates, by resulfation. Increasing the sulfate content leads again to an active catalyst, where BS are present on the surface. However, it was not possible to reach the same catalytic activity as before, probably due to the formation of a small amount of the monoclinic phase, which is regarded as an inactive phase.

Furthermore the influence of the sulfate content on the catalytic activity was investigated. Four samples with different sulfate coverage (between 0.46 and 0.63 of a monolayer) were compared. An increase of the activity with increasing sulfate content was observed. The sample containing less than half a monolayer was completely inactive, and pyridine adsorption showed no BS present on this sample.

It can be concluded that there are at least two different sulfate species present on the surface of sulfated zirconia. The sulfate species, which are more weakly bonded to the surface after a reductive step and are thus evolved at lower temperatures (between 300 and 500°C) in inert gas, are essential for catalytic activity, whereas the sulfate groups, which are removed at temperatures above 600°C under the same conditions, are inactive for n-alkane conversion. As active species pyrosulfate groups $\text{S}_2\text{O}_7^{2-}$ are proposed, which are formed at sulfate loadings of more than half a monolayer.

The metal component should be impregnated directly on the SZ. A mechanical mixture of SZ and Pt supported on an inert carrier material shows a significantly lower activity and isomerization selectivity. A close vicinity of the metal and acidic sites leads to a significantly better performance of the catalyst. Thus, ensembles containing Brønsted acid sites connected to pyrosulfate species and adjacent metal sites are suggested as active sites for n-alkane conversion.

It was found that the following requirements have to be fulfilled for obtaining an active catalyst:

- (i) addition of Pt
- (ii) presence of hydrogen
- (iii) more than half a monolayer of sulfates on the surface and presence of both Brønsted and Lewis acid sites.

ICH DANKE ...

- HANNELORE VINEK
FÜR IHRE UNTERSTÜTZUNG UND IHRE WERTVOLLE HILFE IN ALLEN
BELANGEN
- ALLEN MITGLIEDERN DER ARBEITSGRUPPE UND DES INSTIUTS
FÜR IHRE HILFSBEREITSCHAFT, DAS NETTE UMFELD UND DAFÜR,
DASS SIE MIR DIE ZEIT AM INSTITUT NICHT NUR ERLEICHTERT,
SONDERN AUCH BEREICHERT HABEN
- MEINEN ELTERN
FÜR IHRE LIEBEVOLLE UNTERSTÜTZUNG
- MEINEN FREUNDEN
DAFÜR, DASS SIE ES SIND
- DR. ERICH HALWAX
FÜR DIE XRD MESSUNGEN
- MEL CHEMICALS
FÜR DIE BEREITSTELLUNG DER PROBEN
- DEM FWF (FONDS ZUR FÖRDERUNG DER WISSENSCHAFTLICHEN
FORSCHUNG)
FÜR DIE FINANZIELLE UNTERSTÜTZUNG
- UND ALL JENEN, DIE HIER NOCH NICHT GENANNT SIND, DENEN ICH
JEDOCH NICHT WENIGER ZU DANK VERPFLICHTET BIN

Table of contents

1	Introduction.....	1
1.1	Alkane isomerization and its importance for refining.....	1
1.2	Reactions of hydrocarbons over acidic and bifunctional catalysts.....	7
1.2.1	Reactions of alkanes over acidic catalysts	
1.2.2	Reactions of hydrocarbons over bifunctional catalysts in the presence of hydrogen	
1.3	Sulfated zirconia.....	12
1.3.1	Preparation methods	
1.3.2	Strength of acid sites	
1.3.3	Nature of active sites and structure of the sulfate groups	
1.3.4	Promotors	
1.3.5	Other sulfated oxides	
2	Catalyst preparation and experimental methods.....	23
2.1	Introduction.....	23
2.2	Catalyst preparation.....	23
2.3	Characterization methods.....	24
2.3.1	Structural and morphological characterization	
2.3.2	Thermogravimetric measurements	
2.3.3	Temperature programmed desorption (TPD)	
2.3.4	Infrared spectroscopy	
2.3.4.1	Adsorption of probe molecules	
2.3.4.2	In situ FT-IR measurements	
2.3.4.3	Diffusion measurements	
2.4	Kinetic studies.....	29
3	Characterization of the commercial Mel catalysts.....	31
3.1	Introduction.....	31
3.2	Results and discussion.....	33
3.2.1	Structural and morphological properties and chemical composition	
3.2.2	Characterization of surface sites	
3.2.2.1	Characterization with TPD	

3.2.2.2	Characterization with IR spectroscopy	
3.2.3	Diffusion measurements	
3.2.4	Calorimetric studies	
3.3	Conclusions and summary.....	50
4	n-Alkane hydroisomerization over commercial Pt/Mel catalysts....	52
4.1	Introduction.....	52
4.2	Results and discussion.....	53
4.2.1	Activity and selectivity of bifunctional Pt/Mel	
4.2.2	Comparison of sulfated zirconia and zeolite HBEA	
4.3	Conclusions and summary.....	67
5	In situ IR investigation of n-hexane isomerization over sulfated zirconia and Pt containing sulfated zirconia – Influence of the carrier gas.....	69
5.1	Introduction.....	69
5.2	In situ IR measurements.....	70
5.3	Results and discussion.....	71
5.3.1	In situ IR measurements of the n-hexane isomerization over Pt/SZ and SZ	
5.3.2	Characterization of the coked catalysts	
5.4	Conclusions and summary.....	80
6	Deactivation and Regeneration of Pt containing sulfated zirconia and sulfated zirconia.....	82
6.1	Introduction.....	82
6.2	Results and discussion.....	84
6.2.1	Deactivation and regeneration of SZ and Pt/SZ studied by TG, TPD and in situ IR spectroscopy	
6.2.2	Characterization of the inactive catalyst	
6.2.3	Reactivation of an inactive catalyst	
6.3	Conclusions.....	95

7	Influence of the sulfate content on the activity of Pt containing sulfated zirconia.....	98
7.1	Introduction.....	98
7.2	Results and discussion.....	99
7.3	Conclusions.....	111
8	General conclusions.....	114

Lebenslauf

Publikationsliste

1 INTRODUCTION

1.1 Alkane isomerization and its importance for refining

General introduction:

Crude oil is the most important source of energy and fuels. Despite of the limited availability it will not lose importance in the near future. The demand for energy and fuels is continuously increasing, mainly due to the economic growth especially in developing countries. It can be easily foreseen that private transportation and conveyance of goods will continue to grow in the next years and decades. Total world oil consumption is expected to increase by 1.9 % per year, from 77 million barrels per day in 2001 to nearly 121 million barrels per day in 2025 [1]. The transportation sector is the largest part of worldwide oil use today, and it is expected to account for an increasing share of total oil consumption in the future. Although there are enormous efforts to find sustainable and more environmentally friendly ways for producing energy, there are currently no alternative energy sources that compete economically with oil for transportation uses.

Table 1.1: World total energy consumption by region and fuel [1]

Region/Country	Total energy consumption 2001 (quadrillion Btu) *	World oil consumption 2001 (million barrels per day)	Average annual % change, 2001-2025			
			Oil	Natural Gas	Coal	Total
United States	97.0	19.6	1.5	1.4	1.6	1.4
Western Europe	68.2	14.0	0.5	2.0	-0.9	0.7
Japan	21.9	5.4	0.3	1.6	0.8	0.8
Former Soviet Union	41.9	3.9	2.1	1.9	-0.1	1.5
Eastern Europe	11.4	1.4	1.7	3.6	-1.2	1.4
China	39.7	5.0	4.0	6.9	2.9	3.5
India	12.8	2.1	3.9	4.8	2.2	3.2
Middle East	20.8	5.4	2.2	1.8	1.7	2.1
Africa	12.4	2.6	2.5	3.0	1.4	2.3
Central + South America	20.9	5.2	2.4	3.8	2.7	2.4
Total world	403.9	77.1	1.9	2.2	1.6	1.8

* Btu = British thermal unit; 1 Btu = 1054 J; energy unit; defined as energy required for heating 1 pound of water by 1 degree Fahrenheit

Besides, there is an increasing demand for high quality fuels, mostly due to environmental reasons. Cleaner fuels, containing fewer compounds, which can form pollutants during combustion, lead to a reduction of harmful emissions.

Crude oil refining:

Crude oil is a complex mixture of different hydrocarbons, mainly linear alkanes, cycloalkanes and aromatics, and small amounts of organic compounds containing sulfur, oxygen, nitrogen or metals (mainly nickel and vanadium).

Distillation of crude oil yields several fractions, which find different applications. Chemical processing is used to convert these fractions into valuable products. The straight-run gasoline fraction (also called naphtha) mainly consists of linear alkanes and possesses a low octane number (ON), therefore it cannot be directly used and further treatment is necessary.

The ON is the most important characteristic for gasoline describing the anti-knock properties of the fuel. This number is the percentage by volume of iso-octane (ON 100) in a blend with n-heptane (ON 0) that matches the gasoline in knock characteristics in a standard engine run under standard conditions. The following table shows examples for the ON of different hydrocarbons [2].

Table 1.2: Research Octane Numbers (RON) of pure hydrocarbons

Hydrocarbon	RON
n-Butane	113
iso-Butane	122
n-Pentane	62
2-Methylbutane	99
n-Hexane	19
2-Methylpentane	83
2,3-Dimethylbutane	96
n-Heptane	0
2-Methylhexane	41
2,3-Dimethylpentane	87
2,2,3-Trimethylbutane	113
n-Octane	-19
2,2,4-Trimethylpentane (iso-octane)	100
1-Pentene	91
Cyclohexane	110
Benzene	99
Toluene	124
MTBE	117

As it can be seen in Table 1.2, substances with high ON include aromatics, highly branched alkanes, cyclic hydrocarbons, alkenes and short-chain hydrocarbons. The content of aromatics should be reduced because of environmental and health reasons (e.g. benzene is toxic). Consequently, the maximum concentration of aromatics, especially benzene, has been limited in many countries by government regulations. In the European Union the content of aromatics is limited to 35 vol% with a maximum benzene concentration of 1.0 vol% (Directive 2003/17/EC of the European Parliament and of the Council). In 1990 the RFG program (reformulated gasoline) was started in the USA introducing a cleaner burning gasoline [3], which limits the aromatics concentration to 22 vol% and the benzene content to 0.8 vol% (RFG Phase II). Alkenes are not wanted in gasoline because they can polymerize and form deposits, and short-chain alkanes should be avoided due to their high vapor pressure. Therefore the most favorable components are iso-alkanes and oxygen-containing additives (oxygenates), such as MTBE (methyl-*tert*-butylether).

For obtaining high-octane gasoline the most important refining processes are isomerization, alkylation, catalytic cracking and reforming. Figure 1.1 shows the composition of gasoline [4].

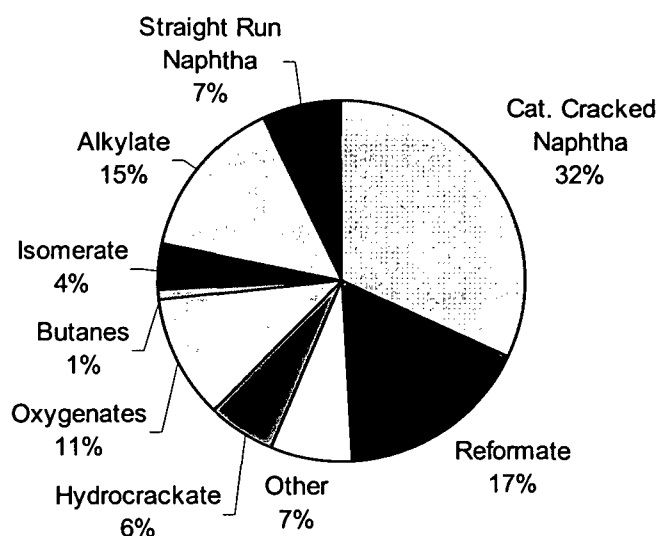


Figure 1.1: Composition of gasoline

The values are for US gasoline, but it should be similar worldwide. Catalytically cracked gasoline is the largest part and is also the major source of unwanted sulfur. Cracking is a process that converts long-chain alkanes into shorter alkanes. Since the amount of gasoline obtained by distillation of crude oil is in general less than the amount required by the market, it is necessary to transform heavier cuts into gasoline by cracking processes. A second major component is produced by reforming, a process that converts aliphatics into aromatics. Reformate possesses a high ON due to its high aromatics content, but there is regulatory pressure to reduce it. Oxygenates are another significant component, mainly ethers such as MTBE. The addition of oxygenated compounds promotes a more complete combustion of gasoline because of the presence of oxygen. Unfortunately, MTBE is being restricted in some countries due to its toxicity and water solubility. The next significant part is isomerate, the product of C_5 and C_6 isomerization. These iso-alkanes are sulfur-free. The last big part is alkylate, which consists mainly of C_8 isomers. It is very clean and possesses a very high ON, therefore it could be an ideal blending component for gasoline. However, commercial alkylation processes use hydrofluoric and sulfuric acid as catalysts, both of them are very corrosive and not easy and safe to handle. The development of new processes based on strong solid acid catalysts to replace HF and H_2SO_4 is strongly needed for environmental and safety considerations.

Strategies for obtaining iso-alkanes:

The most favorable way to increase the octane number of gasoline is to increase the amount of branched alkanes in the fuel. There are two main strategies for producing multi-branched hydrocarbons: alkylation of iso-butane with $C_3 - C_5$ alkenes and isomerization of linear alkanes. Isomerization technologies are used for several refining applications. Low octane light straight-run naphtha, comprised of a mixture of pentanes and hexanes, is isomerized to produce a high octane blending component that is free of sulfur and aromatics. Another application is the isomerization of n-butane to iso-butane, which is needed as feed for alkylation process units and for the production of ethers like MTBE.

If isomerization is carried out in the presence of hydrogen this process is called hydroisomerization. The presence of hydrogen is necessary to prevent coking and deactivation of the catalyst.

Very active catalysts are necessary to overcome the low reactivity of n-alkanes. For hydroisomerization bifunctional catalysts are used, which possess two functions: an acidic and a

metal function. As metal components mainly noble metals like Pt and Pd or transition metals like Ni, Mo, Co, W (the latter as sulfides) are used. Typical acidic materials are zeolites or modified oxides.

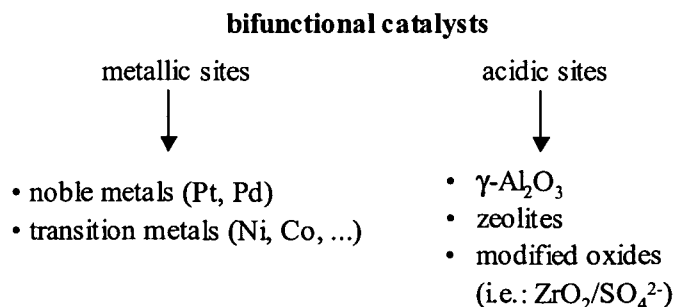


Figure 1.2: Bifunctional catalysts

In industrial processes the two major catalysts used for isomerization are halogenated aluminas and zeolites, both with noble metal.

Pt supported on chlorided alumina ($\text{Pt/Cl}/\text{Al}_2\text{O}_3$) shows a very high activity, therefore the reaction can be carried out at relatively low temperatures (around 150°C), which is thermodynamically favorable for obtaining branched isomers. However, a chlorine-containing organic compound has to be continuously supplied during operation to compensate the loss of chloride species that leach slowly during the reaction. The chlorine source is necessary to maintain the catalytic activity, but it causes corruptions. Another disadvantage of chlorided alumina catalysts is the sensitivity to contaminants such as water or oxygenates. Well-known processes using $\text{Pt/Cl}/\text{Al}_2\text{O}_3$ catalysts are the UOP Penex Process [5] for isomerization of C_5 and C_6 and the Butamer Process (for butane isomerization, since 1959).

Other commercial processes (for example Shell's Hysomer process) use Pt on zeolites as catalysts, mainly HMOR (Mordenite). This material is less active, therefore significantly higher reaction temperatures are necessary. As a consequence, the octane number of isomerate produced by this process is lower due to equilibrium limitation.

Current technology for alkylation processes uses hydrofluoric and sulfuric acid as catalysts, which have many drawbacks such as high toxicity and corrosivity and the inherent risk of handling large amounts of hazardous acids. The development of new processes based on strong solid acid catalysts to replace HF and H_2SO_4 is strongly needed for environmental and safety considerations.

Thus, improvements in catalysts and processes are urgently searched for. New materials should fulfill the following requirements. They should be

- (i) active at low temperatures, which shifts the thermodynamic equilibrium towards the desired branched products (see Figure 1.3),
- (ii) selective and
- (iii) environmentally benign, non-corrosive, easy and safe to handle.

Among the most promising are sulfated zirconia (SZ) and tungstated zirconia (WO_3/ZrO_2). The exceptionally high activity of SZ made it attractive as a catalyst for hydroisomerization, hydrocracking, alkylation and oligomerization.

In 1996 the first commercial application of a Pt promoted SZ catalyst was accomplished in the refinery of Flying J Company in Salt Lake City, USA. This catalyst was developed by researchers from Cosmo Oil Co. and Mitsubishi Heavy Industries [6], and the technology has been released and licensed by UOP as Par-Isom process [7]. The activity of the Pt/SZ catalyst is higher than that of zeolites but lower than the chlorided alumina catalyst. In contrary to the latter, Pt/SZ is robust, not permanently deactivated by water or oxygenates and fully regenerable by oxidation procedure.

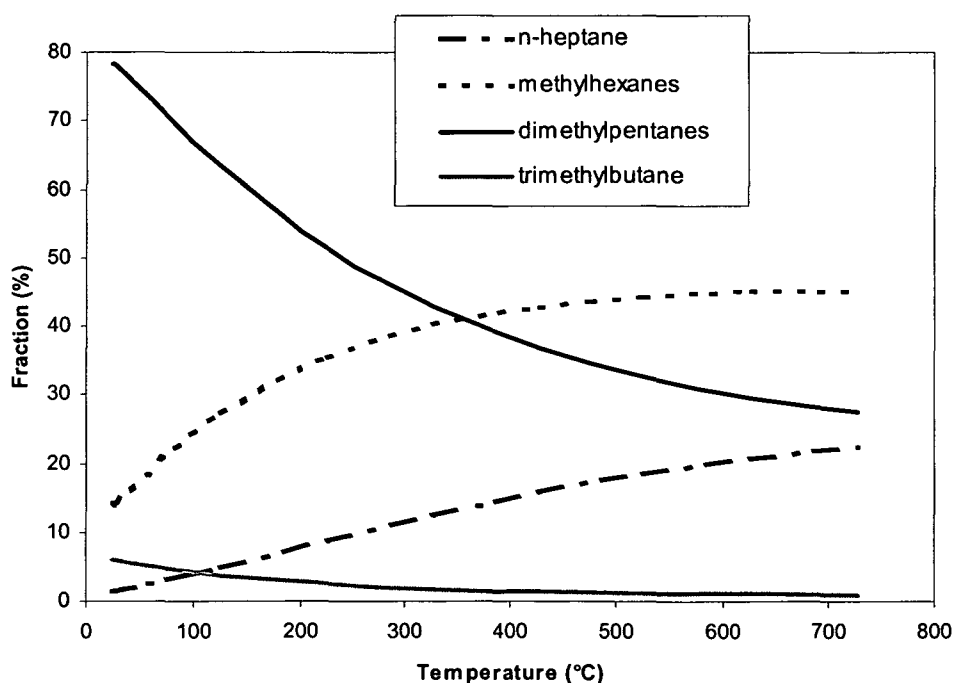


Figure 1.3: Equilibrium distribution of heptane isomers versus temperature

1.2 Reactions of hydrocarbons over acidic and bifunctional catalysts

1.2.1 Reactions of alkanes over acidic catalysts

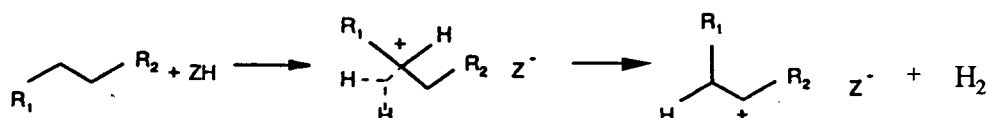
Mechanistic studies have led to general agreement on carbenium ions and/or alkoxy species as reaction intermediates in acid-catalyzed hydrocarbon conversion. Different mechanisms have been proposed for the formation of surface carbenium ions, which is regarded as the initial step of the skeletal isomerization reaction. Due to the lack of experimental proof the mechanism of formation of such an active species is still under discussion.

Concerning carbocations one has to distinguish between 3-fold coordinated carbenium ions and carbonium ions containing a 5-fold coordinated carbon atom. The concept of carbonium ions was originally developed for reactions in liquid superacids, which means acids stronger than 100% sulfuric acid, and then further adapted for solid superacids by Tanabe et al. [8].

Carbenium ions formed on oxidic surfaces can interact with neighboring oxygen atoms and thus form surface-bound alkoxy species.

Suggestions for carbenium ion formation from alkanes were summarized by Sommer and coworkers [9]:

Mechanism 1: Protolysis of a C-H or C-C bond



Mechanism 2: Hydride abstraction by a Lewis acid site on the solid



Mechanism 3: Protonation of traces of alkenes present in the feed by Brønsted acid sites



The protolysis of C-H or C-C bonds by solid acids with subsequent decomposition under cleavage of hydrogen was suggested on the basis of methane and hydrogen formation during

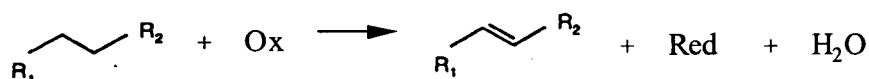
cracking of alkanes over the zeolite H-ZSM5 at high temperatures (500°C) [10]. However, the formation of carbonium ions was not directly demonstrated.

So far no experimental evidence has been found for hydride abstraction at a Lewis acid site. Besides, the formation of a weak metal-hydrogen bond from a strong C-H bond is not thermodynamically favorable under acidic conditions [9].

The protonation of traces of olefin impurities in the feed by Brønsted acid sites (BS) was also proposed as starting reaction. Tabora et al. [11] reported that sulfated zirconia (SZ) loses all catalytic activity for n-butane isomerization when butene impurities were removed from the feed. However, Li et al. [12] still found catalytic activity of sulfated zirconia for n-butane skeletal isomerization after careful purification using an olefin trap, which leads to the assumption that olefins can be formed on the catalytic surface during the reaction.

For catalysts with oxidizing properties an additional mechanism was suggested: the direct oxidation of the alkane. This mechanism of alkane activation is limited to systems containing strong oxidants, such as sulfated oxides. The oxidative power of sulfated zirconia towards alkanes was reported by Farcasiu and coworkers [13,14]. They suggested a one-electron oxidation of the hydrocarbon by the sulfate groups.

Mechanism 4: Oxidation of the C-H bond



The formed alkenes can then be protonated at the Brønsted acid sites.

After initialization the reaction can proceed via hydride transfer from an n-alkane to an isomerized carbenium ion, which then desorbs as an iso-alkane. Desorption of surface carbenium ions can occur either as paraffins via hydride transfer or as olefins, which leads to the restoration of the acid site and to a chain termination.

For n-butane skeletal isomerization an intra-molecular (or monomolecular) and an inter-molecular (or bimolecular) mechanism are discussed. The inter-molecular mechanism proceeds via formation of C₈ intermediates followed by isomerization and cracking. An argument in favor of the inter-molecular pathway is the involvement of a primary carbenium ion in the case of a monomolecular reaction, which is very energetically demanding to form. The kinetic results of n-

butane isomerization also suggested a prevailing inter-molecular reaction route, since the reaction order of n-butane was reported to be higher than 1 [15]. However, the labeled carbon distribution of ^{13}C labeled n-butane isomerization revealed the intra-molecular pathway [16].

For linear alkanes with a chain length $> \text{C}_4$ there is general agreement that the reaction proceeds via the intra-molecular mechanism. The intra-molecular rearrangement can proceed via protonated cyclic intermediates without the necessity of forming highly energetic primary carbenium ions, as in the case of n-butane.

1.2.2 Reactions of hydrocarbons over bifunctional catalysts in the presence of hydrogen

For hydroconversion of n-alkanes bifunctional catalysts are used, which possess an acidic and a metal function. The metallic sites provide the activation of hydrogen and hydrogenation/dehydrogenation of hydrocarbons. The equilibrium concentration of alkenes is very low. Activated hydrogen is necessary to keep the surface concentration of unsaturated intermediates low and thus avoid catalyst coking.

The classical reaction scheme was first proposed by Weisz and Swegler [17] and is shown in Figure 1.4. According to this model, the first step is the dehydrogenation of the alkane on the metallic sites. The formed alkenes diffuse to the acidic sites where they can be adsorbed as carbenium ions. The carbenium ions can then undergo isomerization or cracking reactions. The products finally desorb as alkenes and are hydrogenated on the metallic sites.

Cracking and isomerization reactions can be classified according to the stability of the involved carbenium ions, which was done by Weitkamp and Jacobs [18]. The heat of formation of the carbenium ions decreases with the degree of branching on the positively charged carbon atom. Considering this, the relative reaction rates of cracking reactions can be sorted in ascending order from type A $>$ type B $>$ type C $>$ type D. The different cracking mechanisms are summarized in Table 1.3 and Figure 1.5. Type D cracking reactions are energetically demanding and thus very slow due to the involvement of primary carbenium ions.

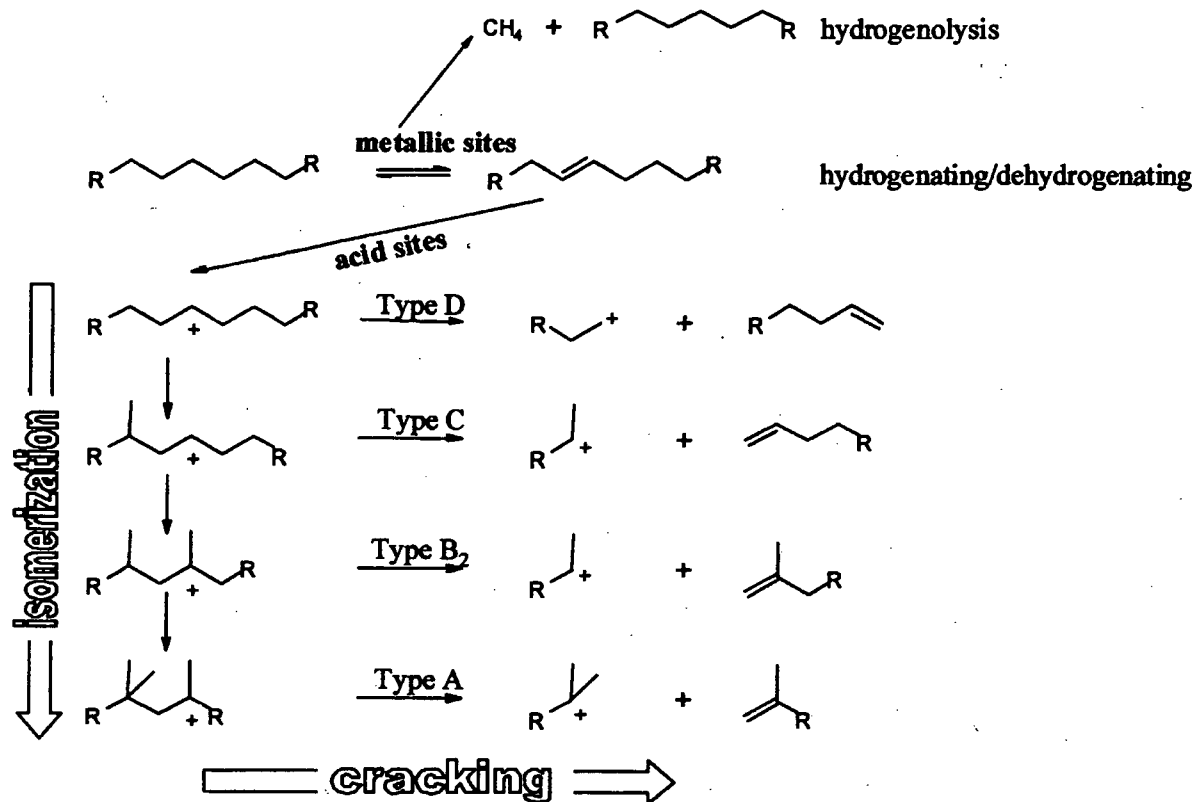
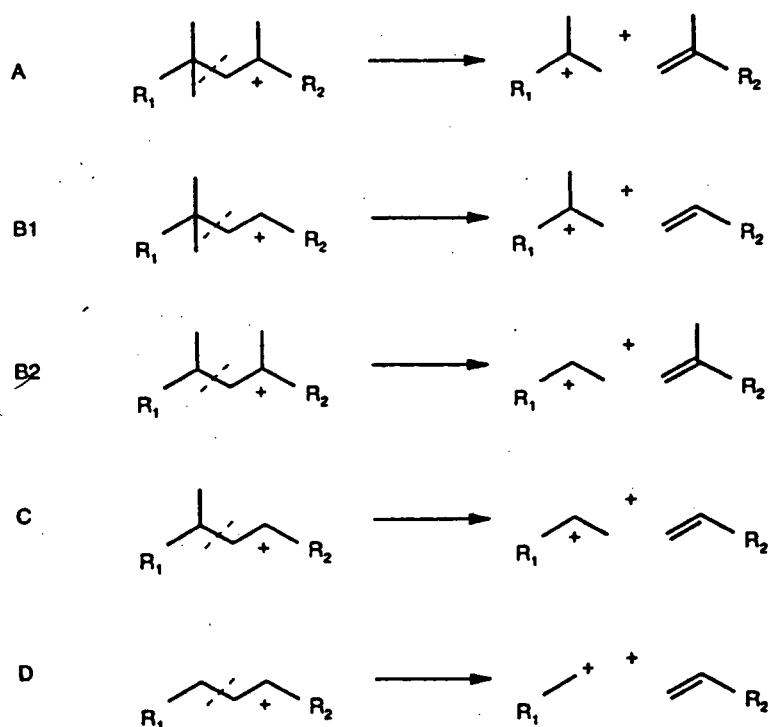


Figure 1.4: Reaction scheme for the hydroconversion of n-alkanes over bifunctional catalysts

Table 1.3: Classification of β -cracking mechanisms

type	carbenium ion *)			minimum number of C-atoms
	start	→	end	
A	tertiary		tertiary	8
B ₁	secondary		tertiary	7
B ₂	tertiary		secondary	7
C	secondary		secondary	6
D	secondary		primary	4

*) at the beginning (start) respectively at the end of the reaction

Figure 1.5: Classification of β -cracking mechanisms

Within the classical model only classical carbenium ions are considered as reaction intermediates, however it is possible that the reaction proceeds via non-classical ions (carbonium ions) and cyclic intermediates. A cyclopropyl-cation was suggested as intermediate [19] (see Figure 1.6). Sie et al. [19,20,21] presented a reaction mechanism, which allowed the interpretation that cracking and isomerization can occur as parallel reactions and share a common intermediate. With this model experimental data for monofunctional cracking as well as bifunctional hydroconversion can be explained. However, so far there is no direct experimental evidence for the formation of protonated cyclic intermediates during the catalytic reaction.

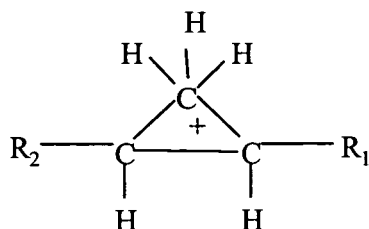


Figure 1.6: Protonated cyclopropane (PCP)

1.3 Sulfated zirconia

Sulfated zirconia (SZ) has attracted a lot of interest due to its exceptionally high activity for acid-catalyzed reactions. There are several promising applications of SZ as acidic catalyst, such as hydroisomerization, hydrocracking, alkylation, Fischer-Tropsch Synthesis, methanol conversion, acylation and oligomerization [22].

First reports date back to 1962 from Holm and Baily [23], but detailed studies did not appear until 1979. In that year Arata et al. [24,25] reported that zirconia treated with sulfuric acid or ammonium sulfate exhibits extremely strong acidity and is able to catalyze the isomerization of n-butane to iso-butane at room temperature. This catalytic performance is unique compared to typical solid acid catalysts, such as zeolites, which show no activity for this reaction at such low temperatures. Since then numerous studies have been published about the preparation, physico-chemical properties and catalytic performance of SZ in various chemical reactions.

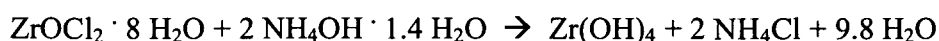
However, the strength and nature of acid sites, the reaction mechanism, the role of Brønsted and Lewis acid sites as well as the structure of the sulfate groups are still controversial.

SZ deactivates rapidly during the reaction with hydrocarbons. The rapid deactivation limits the use of bare SZ for industrial applications. Thus, usually a noble metal function is added and the reaction is carried out under hydrogen atmosphere.

1.3.1 Preparation methods

The catalytic performance of sulfated zirconia depends significantly on the preparation method. A variety of synthesis methods have been reported. The classical approach, which is used most often, is a two-step procedure, based on the method of Arata et al. [24,25]. The first step is the preparation of a zirconium hydroxide, followed by sulfation as second step.

The zirconium hydroxide can be prepared by hydrolysis of a soluble zirconium salt, e.g. ZrOCl_2 or $\text{ZrO}(\text{NO}_3)_2$, with aqueous ammonia. The hydrolysis of $\text{ZrOCl}_2 \cdot 8 \text{H}_2\text{O}$ with 28 wt% aqueous ammonia solution (this corresponds to $\text{NH}_4\text{OH} \cdot 1.4 \text{H}_2\text{O}$) can be represented in the following way [26]:



The pH has a strong influence on the crystalline structure of the material and on the catalytic properties. Usually a final pH of 9 – 10 is reached.

The $\text{Zr}(\text{OH})_4$ can also be prepared by a sol-gel method. In this method a metal alkoxide undergoes hydrolysis and subsequent condensation in an alcohol solvent, forming a polymeric oxide network, a so-called alcogel. Removal of the solvent under conventional air drying generates a liquid – vapor interface inside the pores, the high surface tension collapses the porous network, resulting in a material with reduced surface area called a xerogel. The formation of the liquid – vapor interface can be avoided by supercritical drying, resulting in a so-called aerogel [27].

As sulfating agents sulfuric acid or ammonium sulfate are usually used. The sulfation can be carried out by pouring H_2SO_4 on the $\text{Zr}(\text{OH})_4$ held on a filter paper, by immersing the hydroxide into the solution under stirring or by impregnation. The solid is usually separated from the liquid by filtration or centrifugation and then dried without washing. Best results were obtained with 1N H_2SO_4 , typical ratios of acid solution to solid vary from 2 to 10 ml/g.

Other synthesis methods have also been developed, among them one-step preparation methods. Ward and Ko [28] and Signoretto et al. [29] reported one-step preparation methods by sol-gel technique, where zirconium propoxide and sulfuric acid in propanol were mixed with another solution containing water and propanol. The mixture was gelled and dried supercritically to obtain an aerogel with the sulfate ions trapped in the bulk of the aerogel. Ward and Ko found that during calcination and crystallization sulfate is expelled to the surface and transformed into catalytically active species.

Then the resulting sulfated zirconias have to be calcined at 550 – 650°C to generate acidity. The calcination temperature influences the sulfur content, the surface area and the crystal structure of the catalyst. ZrO_2 can exist in three different phases: monoclinic (stable below 1373 K), tetragonal (stable between 1373 and 2173 K) and cubic (stable above 2173 K); the latter two can be generated as metastable structures at lower temperatures. Sulfate ions stabilize the surface area and the tetragonal phase of zirconia. Calcination of a pure $\text{Zr}(\text{OH})_4$ results in a mixture of monoclinic and tetragonal phase, with decreasing fraction of the tetragonal phase with increasing calcination temperature, until about 650°C where only the monoclinic phase was observed [26]. On the contrary, for sulfated $\text{Zr}(\text{OH})_4$ only the tetragonal phase existed until about 800°C. Increasing calcination temperature results in a decreasing sulfur content. It was reported that the

amorphous zirconium hydroxide must be used as precursor for sulfation [24]. Sulfation of a crystalline oxide leads to a much less active or inactive material [30]. However, some exceptions are reported [31,32]. Morterra et al. [33] demonstrated that sulfation of zirconia in the tetragonal phase stabilized by incorporation of Y_2O_3 resulted in an active material, whereas sulfation of a monoclinic ZrO_2 did not generate active sites. Therefore they concluded that the metastable tetragonal and cubic phase are the active phases. The calcination step is crucial for getting an active catalyst. Two reasons were given in literature. First, the inactive amorphous hydroxide is transformed into the active tetragonal zirconia. A second important function of the calcination proposed by Morterra et al. [34,35] is to selectively eliminate part of the sulfate groups and thus create strong Lewis acid sites.

1.3.2 Strength of acid sites

Sulfated zirconia was long considered a solid superacid, which means an acid stronger than 100% sulfuric acid. However, more and more authors came to the conclusion that the acidity of SZ is similar to sulfuric acid or to some acidic zeolites [36, 37, 38]. A variety of techniques have been applied to estimate the acid strength, but the acidity of SZ catalysts is still a subject of debate.

Using Hammett indicators Hino and Arata [24,25] first claimed that SZ is an acid 10^4 times stronger than sulfuric acid and therefore a superacid. The strength of an acid can be characterized by the so-called Hammett acidity function $-H_0$. This method uses a base as indicator, and the color changes of the indicator are observed visually. The method was established for acidity measurements in solution and later extended to solid acids. It is assumed that the indicators are in adsorption equilibrium with the surface acid sites and are distributed uniformly over the surface. However, these assumptions and generally the use of the Hammett indicator method for the determination of the acidity of solid acids have been questioned by several authors [37,39]. The use of UV spectroscopy instead of the visual observation of color changes in Hammett titrations showed that the acid strength of SZ is similar to 100% sulfuric acid [40].

Another method for the determination of acid strength is the use of test reactions. The skeletal isomerization of light paraffins is widely accepted as suitable test reaction for strong acidity. n-Butane can be isomerized to iso-butane at room temperature over SZ, which is not the case for sulfuric acid or zeolites as catalysts. However, other factors than the strength of the acid sites are discussed to be the cause of the high activity. Above a certain level of acid strength the activity of a catalyst is dominated by the nature of intermediates and the energetics associated with the

reaction pathway. Liu et al. [41] proposed that an exceptionally active catalyst for an acid catalyzed reaction does not necessarily need to be an extremely strong acid. Instead, the reaction can proceed via a less energy intensive bimolecular mechanism for small alkanes.

Temperature programmed desorption (TPD) of an adsorbed base, like NH_3 or pyridine, was also used for characterizing the amount and strength of acid sites. However, a major drawback of this method is the strong interaction between the adsorbate molecules and the sulfate groups, which can lead to an oxidative decomposition of adsorbed species during heating.

IR spectroscopy was used for characterization of the acidity of SZ catalysts. The Brønsted acidity can be estimated by adsorption of a weak base like benzene. The interaction with the base leads to a shift of the band of the acidic OH groups to lower frequencies. This shift can be taken as a measure for the Brønsted acid strength. Kustov et al. [36] reported a shift of 200 cm^{-1} for SZ, which is significantly larger than that for unsulfated zirconia, but smaller than that for acidic zeolites, such as HY or HZSM-5. Similar results were reported by Adeeva et al. [37]. They compared the shift of the OH band after adsorption of CD_3CN and found that the Brønsted acid sites of SZ were weaker than those of zeolite HY and HZSM-5. Characterization of Lewis acid sites was done by IR measurements after CO adsorption. Adeeva et al. [37] compared the shift of the stretching frequency of CO adsorbed on SZ with that of CO adsorbed on Al^{3+} ions on the surface of $\gamma\text{-Al}_2\text{O}_3$ and concluded that the Lewis acidity of SZ is weaker.

Additionally nuclear magnetic resonance (NMR) was used for estimating the acid strength of SZ catalysts. ^1H chemical shifts were correlated with the acidity of surface OH groups. Riemer et al. [32] reported that the ^1H chemical shift of SZ was higher than that of HZSM-5, indicating that SZ has stronger Brønsted acid sites than the zeolite. However, Adeeva et al. [37] questioned the use of ^1H chemical shifts in the absence of a base as a measure for acidity, because the chemical shifts depend not only on the acidity, but also on H-bonding of the protons. Comparison of the ^1H shifts upon adsorption of bases, such as CD_3CN and CCl_3CN , showed that the acid strength of Brønsted sites on SZ is less than on HZSM-5 [37].

With electron paramagnetic resonance (EPR) strong ionizing sites on solid acid catalysts can be characterized using probe molecules, which are difficult to ionize, such as benzene [42]. The formation of paramagnetic carbocations by charge transfer between surface sites and probe molecules can be detected by EPR. Vedrine and coworkers [42] reported a correlation between the ionizing ability and the catalytic activity.

1.3.3 Nature of active sites and structure of the sulfate groups

Although the nature of acid sites and the structure of the sulfate groups were the focus of numerous studies, they remain a subject of debates.

The role of Brønsted (BS) and Lewis acid sites (LS) has been debated for a long time, but no consensus has yet been reached. Several authors observed the highest catalytic activity when LS were dominantly present on the surface of SZ [43,42]. Yamaguchi et al. [44] proposed LS as active sites, because after activation at 500°C they observed the highest activity, but only LS were found after adsorption of pyridine under these pretreatment conditions. However, it was suggested that BS may be generated by interaction of hydrocarbon molecules or water with Lewis acid sites. Under reaction conditions water could be formed during the reaction or traces of water can be present in the feed. Coordinatively unsaturated metal sites were suggested as LS, with the Lewis acid strength of Zr^{4+} sites remarkably enhanced by the electron inductive effect of adjacent S=O groups. The detrimental effect of hydration and CO on the catalytic activity supported LS as active sites. However, Kobe et al. [45] observed that a small amount of adsorbed water, which may transform LS into BS, is beneficial for the catalytic activity. Babou et al. found a volcano-shaped curve for activity versus amount of adsorbed water [38]. Reversible transformation of LS into BS by adsorption of water molecules was observed by Arata and coworkers [46] and by Morterra et al. [47]. The negative effect of CO on the isomerization rate was attributed to a blocking of Lewis sites [48]. However, Adeeva et al. [49] reported that the rate of activity restoration after removal of CO from the feed does not correlate with the CO desorption from LS. The authors suggested the formation of oxo-carbenium ions from CO and adsorbed carbenium ions instead of a poisoning of Lewis acid sites. From IR spectra of pyridine adsorbed on a spent catalyst Watanabe and coworkers [50] concluded that LS are responsible for the catalytic activity in n-pentane isomerization.

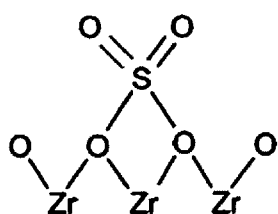
A crucial role of BS has been reported by Lunsford et al. [51] for the alkylation of iso-butane with butanes and by Li et al. [12] for the isomerization of n-butanes. Ward and Ko [28] proposed that the strong BS are Zr-OH surface hydroxyl groups whose proton donating ability is increased by the electron withdrawing effect of the S=O groups. On the other hand Kustov et al. [36] and Adeeva et al. [37] proposed that surface bisulfate species instead of Zr-OH are responsible for BS.

Nascimento et al. [52] argue that both BS and LS are important for butane isomerization over SZ. Several authors suggested a synergistic effect of both types of acid sites [53,54].

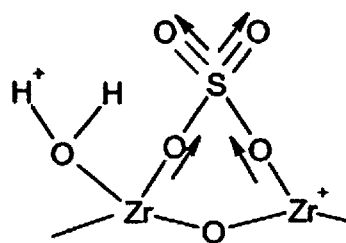
Different models have been proposed concerning the structure and state of the sulfate groups including mono-, bi- or tridentate structures, sulfates chelating a single Zr atom or bridging across two Zr atoms, bisulfate species or sulfuric acid grafted on the oxidic surface.

The oxidation state of sulfur in catalysts showing high activity was S^{6+} , which was determined by XPS [44]. Catalysts containing sulfur in a lower oxidation state were inactive. Covalent S=O bonds are necessary for the generation of strong acidity.

Yamaguchi et al. [44] proposed that the sulfate chelates the Zr (model 1). In contrast Arata and Hino [24] considered that a bidentate sulfate is bridging across two Zr atoms (model 2).



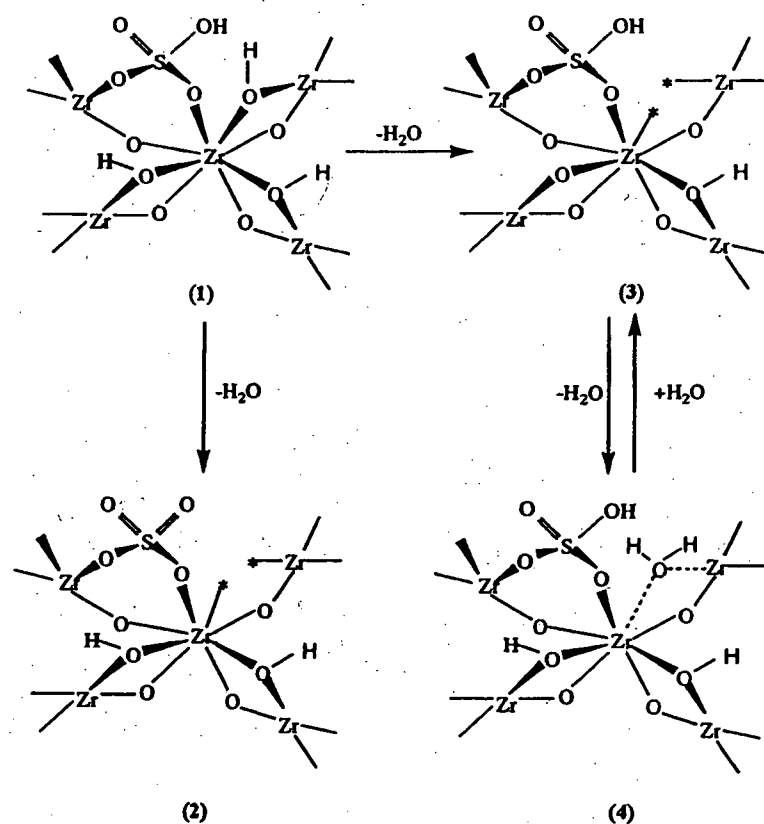
Model 1 (Yamaguchi et al. [44])



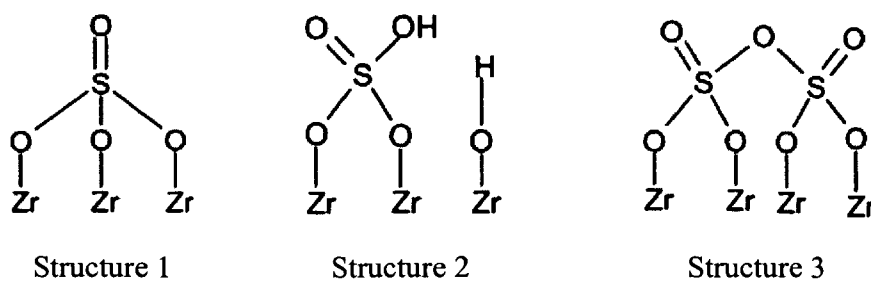
Model 2 (Arata et al. [24])

Clearfield et al. [53] excluded the possibility of chelation of a Zr by sulfate and proposed model 3, which is able to explain the simultaneous presence of LS and BS. During calcination of the uncalcined catalyst (model 3, structure 1) water is lost and the structures 2 and 3 can be formed. In both structures LS are present (indicated by asterisks), but in 3 the bisulfate group (HSO_4^-) remains intact, which results in a LS adjacent to a S-O-H group. This bisulfate group can act as strongly acidic BS with the neighboring LS tending to withdraw electrons from the bisulfate group, thus weakening the SO-H bond.

Lavalley [55,56] carried out ^{18}O exchange experiments with $H_2^{18}O$ vapor followed by IR spectroscopic measurements for determining the structure of the sulfate groups. For dehydrated SZ with a low sulfate loading a tridentate structure was proposed (model 4, structure 1), which forms a bridged bidentate species in the presence of moisture (structure 2). They suggested polysulfate structures on SZ with higher sulfate contents (structure 3). Morterra et al. [47] supported the structural models put forward by Lavalley.



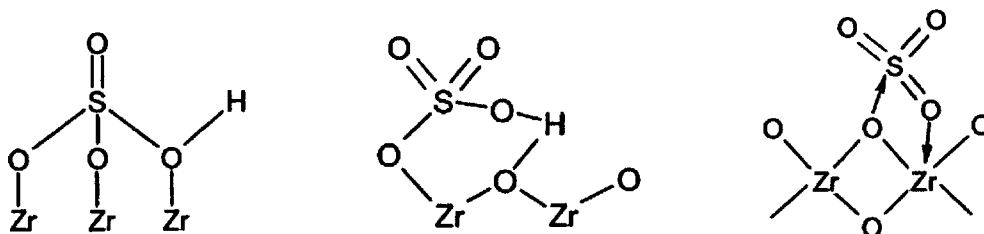
Model 3 (Clearfield et al. [53])



Model 4 (Lavalley et al. [55,56])

By use of ^1H NMR, Raman and IR spectroscopy, Riemer et al. [32] proposed a tridentate model structure involving only one $\text{S}=\text{O}$ group (model 5). Monodentate bisulfate species with the OH group H-bonded to a surface oxygen atom of zirconia were proposed by Adeeva and coworkers [37] (model 6). Based on quantum mechanical studies Babou et al. [57] considered SZ as sulfuric acid grafted at the surface of zirconia (model 7) in a state very sensitive to hydration/dehydration.

On a dehydrated sample $(\text{SO}_3)_{\text{ads}}$ species are formed, which exhibit strong Lewis acidity. At intermediate dehydration degrees H_3O^+ and HSO_4^- species induce Brønsted acidity. Therefore, the nature of acid sites on SZ depends critically on the water content.



Model 5 (Riemer et al. [32])

Model 6 (Adeeva et al. [37])

Model 7 (Babou et al. [57])

Sauer et al. [58] calculated the structures and stabilities of different surface species by DFT (density-functional theory) for an increasing loading of H_2SO_4 or SO_3 and H_2O adsorbed from the gas phase on the (101) surface of tetragonal ZrO_2 . Assuming H_2SO_4 and H_2O present in the gas phase, the pyrosulfate phase ($\text{S}_2\text{O}_7^{2-}$) is the prevailing structure for wide temperature and partial pressure ranges. If equilibrium is assumed with SO_3 and H_2O in the gas phase, the proton-free SO_3 structure dominates over a wide range.

1.3.4 Promoters

Doping of SZ with Pt results in an improvement of stability and catalytic activity, when the reaction is carried out in a flow of hydrogen. The role and state of Pt are not yet fully clarified. Pt can dissociate hydrogen homolytically. The dissociated hydrogen hydrogenates carbonaceous residues, removes them from the surface and thus prevents deactivation. Additionally, Hattori [59] proposed that dissociated hydrogen can spill over to the SZ surface, lose an electron at a LS and form a H^+ which can act as BS. Drago et al. [60] and Xu and coworkers [61] showed that doping SZ with Pt does not change the acidity.

The promoting effect of Fe and Mn was first discovered by Hsu et al. [62]. They reported that SZ doped with Fe and Mn (FMSZ) was two or three orders of magnitude more active for n-butane isomerization. Comparative studies of the acidity of promoted and unpromoted SZ catalysts carried out by different researchers revealed similar acid strength and acid site density [63,64] or even less acidity [60]. Hypotheses to explain the higher activity of FMSZ compared to SZ are that the presence of transition metal oxides leads to (i) the intermediate formation of butenes, or (ii) to

a better stabilization of transition state complexes, such as alkoxy groups or alkyl sulfates. Fe alone shows a significant promoting effect, but Mn alone showed negligible promoting effect [64], FMSZ was the most active. Coelho et al. [64] observed a maximum in the plot activity versus Fe concentration, the decreasing activity with increasing Fe loading was attributed to Fe agglomeration. Considering this, the main role of Mn would be to stabilize the dispersion of Fe. Using EXAFS, Tabora and Davis [65] found that on a sample prepared by coprecipitation method both Fe and Mn are not incorporated into the lattice of zirconia but are present as small clusters on the surface of ZrO_2 . Adeeva et al. [37] interpreted the promoting effect of Fe and Mn as an enhancement of the oxidative properties of SZ.

Additionally, Al and Ga were found to have a promoting effect on the catalytic activity and the stability of the catalyst [66,67].

1.3.5 Other sulfated oxides

Other sulfated metal oxides, e.g. Fe_2O_3 , TiO_2 , Al_2O_3 , SiO_2 and SnO_2 , have also been found to be active in n-alkane isomerization [24,46].

Jin et al. [68] compared different sulfated metal oxides using cyclopropane isomerization. They found the highest activity for sulfated ZrO_2 , Fe_2O_3 and TiO_2 , less activity for sulfated Al_2O_3 and SnO_2 , and sulfated SiO_2 was inactive. Using IR spectroscopy, they found a correlation between the catalytic activity and the shift of the S=O band after pyridine adsorption.

Electronegativity and coordination number of the metal cation in a metal oxide affect the acid strength [44]. The metal oxides, which show strong acidity by introducing sulfur compounds, are considered to have cations of high electronegativity and high coordination number. The most active sulfated oxides ZrO_2 , TiO_2 and Fe_2O_3 are classified as oxides, which have highly electronegative cations, while SnO_2 and Al_2O_3 have intermediate electronegative cations. The cations of all those oxides are 6- or 7-coordinated. Though Si^{4+} has a high electronegativity, its coordination number is 4. Thus it seems that Si^{4+} has difficulty in forming stable active sites or to provide coordinatively unsaturated sites.

References

-
- [1] Energy Information Administration, *International Energy Outlook 2004*, <http://www.eia.doe.gov/>
 - [2] G. Antos, A. Aitani, J. Parera, *Catalytic Naphtha Reforming: Science and Technology*, Marcel Dekker, New York (1995)
 - [3] U.S. Environmental Protection Agency, <http://www.epa.gov/>
 - [4] F.M. Dautzenberg, P.J. Angevine, *Catalysis Today* 93-95 (2004) 3.
 - [5] UOP website
 - [6] T. Kimura, *Cat. Today* 81 (2003) 57.
 - [7] C. Gosling, R. Rosin, P. Bullen, T. Shimizu, T. Imai, *Petrol. Technol. Quart.* (1997/98) 55.
 - [8] H. Hattori, O. Takahashi, K. Tanabe, *J. Catal.* 68 (1981) 132.
 - [9] J. Sommer, R. Jost, M. Hachoumy, *Cat. Today* 38 (1997) 309.
 - [10] W.O. Haag, R.M. Dessau, *Proc. 8th Int. Congress on Catalysis, Berlin (1984) Vol. 2*, p. 305.
 - [11] J.E. Tabora, R.J. Davis, *J. Am. Chem. Soc.* 118 (1996) 12240.
 - [12] X. Li, K. Nagaoka, L.J. Simon, J.A. Lercher, *J. Catal.* 227 (2004) 130.
 - [13] R. Srinivasan, R.A. Keogh, A. Ghenciu, D. Farcasiu, B.H. Davis, *J. Catal.* 158 (1996) 502.
 - [14] D. Farcasiu, A. Ghenciu, L.J. Qi, *J. Catal.* 158 (1996) 116.
 - [15] H. Liu, V. Adeeva, G.D. Lei, W.M.H. Sachtler, *J. Mol. Catal. A* 100 (1995) 35.
 - [16] F. Garin, L. Seyfried, P. Girard, G. Maire, A. Abdulsamad, J. Sommer, *J. Catal.* 151 (1995) 26.
 - [17] P.B. Weisz, E.W. Swegler, *Science* 126 (1957) 31.
 - [18] J. Weitkamp, P.A. Jacobs, J.A. Martens, *Appl. Cat.* 8 (1983) 123.
 - [19] S.T. Sie, *Ind. Eng. Chem. Res.* 31 (1992) 1881.
 - [20] S.T. Sie, *Ind. Eng. Chem. Res.* 32 (1993) 397.
 - [21] S.T. Sie, *Ind. Eng. Chem. Res.* 32 (1993) 403.
 - [22] G.D. Yadav, J.J. Nair, *Microp. Mesop. Mat.* 33 (1999) 1.
 - [23] V.C.F. Holm, G.C. Baily, U.S. Patent 3032599 (1962).
 - [24] M. Hino, S. Kobayashi, K. Arata, *J. Am. Chem. Soc.* 101 (1979) 6439.
 - [25] M. Hino, K. Arata, *J. Chem. Soc. Chem. Commun.* 851 (1980).
 - [26] X. Song, A. Sayari, *Catal. Rev. – Sci. Eng.* 38 (3), (1996) 329.
 - [27] D.A. Ward, E.I. Ko, *Ind. Eng. Chem. Res.* 34 (1995) 421.
 - [28] D.A. Ward, E.I. Ko, *J. Catal.* 150 (1994) 18.
 - [29] M. Signoretto, F. Pinna, G. Strukul, G. Cerrato, C. Morterra, *Catal. Lett.* 36 (1996) 129.
 - [30] R.A. Comelli, C.R. Vera, J.M. Parera, *J. Catal.* 151 (1995) 96.
 - [31] D.A. Ward, E.I. Ko, *J. Catal.* 157 (1994) 321.
 - [32] T. Riemer, D. Spielbauer, M. Hunger, G.A.H. Mekheimer, H. Knözinger, *J. Chem. Soc. Chem. Comm.* (1994) 1181.
 - [33] C. Morterra, G. Cerrato, F. Pinna, M. Signoretto, *J. Catal.* 157 (1995) 109.
 - [34] C. Morterra, G. Cerrato, M. Signoretto, *Catal. Lett.* 41 (1996) 101.
 - [35] C. Morterra, G. Cerrato, G. Meligrana, M. Signoretto, F. Pinna, G. Strukul, *Catal. Lett.* 73 (2001) 113.
 - [36] L.M. Kustov, V.B. Kazansky, F. Figueras, D. Tichit, *J. Catal.* 150 (1994) 143.
 - [37] V. Adeeva, J.W. de Haan, J. Jänchen, G.D. Lei, G. Schünemann, L.J.M. van de Ven, W.M.H. Sachtler, R.A. van Santen, *J. Catal.* 151 (1995) 364.
 - [38] F. Babou, B. Bigot, G. Coudurier, P. Sautet, J.C. Vedrine, *Stud. Surf. Sci. Catal.* 90 (1994) 519.

-
- [39] M. Deeba, W.K. Hall, *J. Catal.* 60 (1979) 417.
 - [40] B. Umansky, J. Engelhardt, W.K. Hall, *J. Catal.* 127 (1991) 128.
 - [41] H. Liu, V. Adeeva, G.D. Lei, W.M.H. Sachtler, *J. Mol. Catal. A* 146 (1996) 165.
 - [42] F.R. Chen, G. Coudurier, J.F. Joly, J.C. Vedrine, *J. Catal.* 143 (1993) 616.
 - [43] C. Morterra, G. Cerrato, F. Pinna, M. Signoretto, G. Strukul, *J. Catal.* 149 (1994) 181.
 - [44] T. Yamaguchi, *Appl. Cat.* 61 (1990) 1.
 - [45] J.M. Kobe, M.R. Gonzalez, K.B. Fogash, J.A. Dumesic, *J. Catal.* 164 (1996) 459.
 - [46] K. Arata, *Adv. Catal.* 37 (1990) 165.
 - [47] C. Morterra, G. Cerrato, C. Emanuel, V. Bolis, *J. Catal.* 142 (1993) 349.
 - [48] F. Pinna, M. Signoretto, G. Strukul, G. Cerrato, C. Morterra, *Catal. Lett.* 26 (1994) 339.
 - [49] V. Adeeva, H. Liu, B. Xu, W.M.H. Sachtler, *Topics in Catalysis* 6 (1998) 61.
 - [50] K. Watanabe, N. Oshio, T. Kawakami, T. Kimura, *Appl. Cat. A* 272 (2004) 281.
 - [51] J. Lunsford, H. Sang, S.M. Campbell, C.H. Liang, R.G. Anthony, *Catal. Lett.* 27 (1994) 305.
 - [52] P. Nascimento, C. Akrapoulou, M. Oszagyan, G. Coudurier, C. Travers, J.F. Joly, J.C. Vedrine, *Stud. Surf. Sci. Catal.* 75 (1993) 1185.
 - [53] A. Clearfield, G.P.D. Serrette, A.H. Khazi-Syed, *Cat. Today* 20 (1994) 295.
 - [54] C. Morterra, G. Cerrato, V. Bolis, S. Di Ciero, M. Signoretto, *J. Chem. Soc., Faraday Trans.* 93 (1997) 1179.
 - [55] M. Bensitel, O. Saur, J.C. Lavalley, B.A. Morrow, *Mater. Chem. Phys.* 19 (1988) 147.
 - [56] O. Saur, M. Bensitel, A.B.M. Saad, J.C. Lavalley, C.P. Tripp, B.A. Morrow, *J. Catal.* 99 (1986) 104.
 - [57] F. Babou, G. Coudurier, J.C. Vedrine, *J. Catal.* 152 (1995) 341.
 - [58] A. Hofmann, J. Sauer, *J. Phys. Chem. B* 108 (2004) 14652.
 - [59] H. Hattori, *Stud. Surf. Sci. Catal.* 77 (1993) 69.
 - [60] R.S. Drago, N. Kob, *J. Phys. Chem. B* 101 (1997) 3360.
 - [61] B.Q. Xu, W.M.H. Sachtler, *J. Catal.* 167 (1997) 224.
 - [62] C.Y. Hsu, C.R. Heimbuch, C.T. Armes, B.C. Gates, *J. Chem. Soc. Chem. Commun.* (1992) 1645.
 - [63] J.E. Tabora, R.J. Davis, *J. Chem. Soc. Faraday Trans.* 91 (1995) 1825.
 - [64] M.A. Coelho, D.E. Resasco, E.C. Sikabwe, R.L. White, *Catal. Lett.* 32 (1995) 256.
 - [65] J.E. Tabora, R.J. Davis, *J. Chem. Soc. Faraday Trans.* 91 (1995) 1825.
 - [66] Z. Gao, Y. Xia, W. Hua, C. Miao, *Top. Catal.* 6 (1998) 101.
 - [67] J.A. Moreno, G. Poncelet, *J. Catal.* 203 (2001) 453.
 - [68] T. Jin, T. Yamaguchi, K. Tanabe, *J. Phys. Chem.* 90 (1986) 4797.

2 CATALYST PREPARATION AND EXPERIMENTAL METHODS

2.1 Introduction

The experimental work on the alkane hydroisomerization over bifunctional SZ catalysts consists of three major parts: (i) preparation of the catalysts, (ii) catalyst characterization and (iii) kinetic test reactions. In the following part the catalyst preparation and the methods applied for characterization and kinetic measurements are described. Characterization techniques comprise methods for structural, morphological and chemical description of the samples, methods for characterization of surface sites and techniques contributing to the understanding of the catalytic reaction, such as diffusion and adsorption measurements. A combination of a variety of methods can lead to a better understanding of the relationship between the chemical and physico-chemical properties and the performance of a catalyst.

2.2 Catalyst preparation

Two different commercial sulfated zirconium hydroxide materials were used in this study, both obtained from MEL Chemicals: XZO 1077 (in the following work called Mel 1) and XZO 1249/1 (called Mel 2). The two materials differ slightly in the nominal sulfate content and the surface area.

To obtain pure sulfated zirconium oxide the hydroxides were calcined at 600°C for 3 hours in static air.

For the preparation of the bifunctional catalysts the hydroxides as starting materials were impregnated with the desired amount of Pt (2.5 wt%) by dispersing the catalyst in an aqueous solution of PtCl_4 and evaporation of the water. After drying at 100°C over night, the material was calcined at 600°C for 3 h.

Additionally, a series of four samples was synthesized with different sulfate content. For this a two-step procedure was applied. In the first step zirconium hydroxide was produced from an aqueous solution of ZrOCl_2 (from Aldrich) by adding dropwise ammonium hydroxide (25% solution) under heavy stirring until a pH of 10 was reached. The obtained solid material was dried at 100°C and then sulfated in a second step. This was done by adding a defined amount of 1N H_2SO_4 , which would lead to a theoretical coverage of 1/3, 2/3, 1 and 2 monolayers of sulfate

groups. Calcination and impregnation with Pt was done in the same way as for the commercial Mel samples.

Table 2.1: Synthesis of SZ catalysts with different sulfate content

theoretical coverage fraction of a monolayer	wt% SO ₄	weight Zr(OH) ₄ *	amount 1 N H ₂ SO ₄ **
		(g)	(ml)
1/3	1.19	5.01	1.17
2/3	2.37	4.99	2.38
1	3.56	5.00	3.61
2	7.11	5.02	7.49

* specific surface area after calcination at 600°C: 58 m²/g

** used for sulfation

2.3 Characterization methods

2.3.1 Structural and morphological characterization

Structural analysis was done by X-ray powder diffraction (XRD) with a Philips X'Pert PRO diffractometer using Cu K_α radiation.

The particle size and shape was determined by Transmission Electron Microscopy (TEM) for the commercial samples Mel 1 and Mel 2. The samples were dispersed in ethanol and placed on a grid. Measurements were carried out on a 200 kV FEI Tecnai F20 S-Twin microscope with a field emission gun and CCD camera or on a 100 kV JEOL 100CX.

The specific surface area of the catalysts was determined according to the BET method from an adsorption isotherm of nitrogen at 77 K. The isotherm was obtained in a Quantasorb apparatus equipped with a thermal conductivity detector (TCD) using different helium/N₂ mixtures flowing over the sample. Adsorption was started by cooling the sample to 77 K, desorption by removing the liquid nitrogen bath and heating the sample fast with a hair-dryer. Calibration of the amount of adsorbed nitrogen was done by injection of a defined amount of adsorbate with a gas-tight syringe. Prior to the measurement the samples were activated in flowing nitrogen at 200°C for one hour.

2.3.2 Thermogravimetric measurements

Thermogravimetric studies were carried out on a combined TG/DSC apparatus (Netzsch STA 409 Luxx, see Figure 2.1).

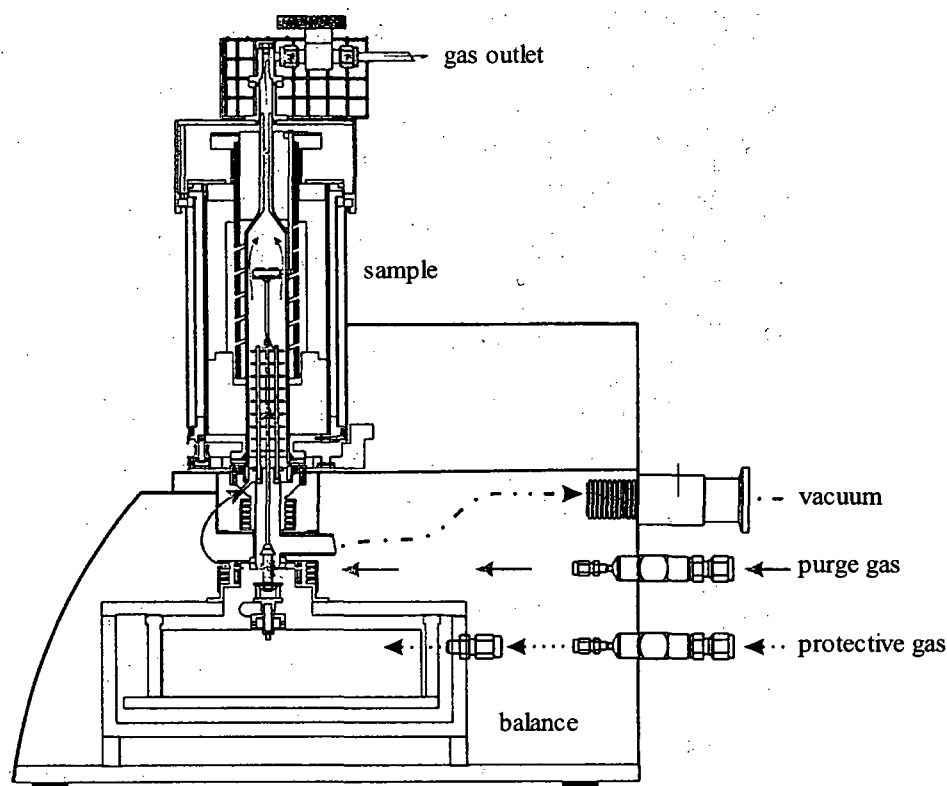
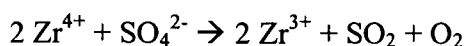


Figure 2.1: Netzsch STA 409 Luxx combined TG/DSC apparatus (from [1])

This method was used for the determination of the sulfate content, from which the surface coverage could be calculated.

At higher temperatures the sulfate groups decompose to form SO_2 . A possible pathway for this decomposition was suggested by Chen et al. [2] as:



Typically, around 100 mg sample were heated up with a heating rate of $10^\circ/\text{min}$ under a helium flow of 40 ml/min adjusted with mass flow controllers. Sulfate decomposition started above 600°C . From the mass change above this temperature the sulfate content was determined. The sulfate density ($\text{SO}_4^{2-} \text{ nm}^{-2}$) can be calculated assuming a surface area of 0.25 nm^2 for a sulfate group [2].

Additionally, TG analysis was used for the determination of the amount of coke formed during the reaction by heating a coked sample in an oxidizing atmosphere. For these measurements a heating rate of 10°/min and a flow of 40 ml/min He mixed with 10 ml/min O₂ were applied.

With the help of DSC measurements (Differential Scanning Calorimetry) the heat of adsorption of the reactants and different basic probe molecules could be measured. As reference an empty pan was used. The measurements were carried out isothermally at room temperature in helium. The addition of the liquid n-heptane was done via a saturator in pulses. Before the measurement the samples were activated in helium flow at 500°C.

2.3.3 Temperature programmed desorption (TPD)

The system for TPD measurements consists of a quadrupole mass spectrometer (Balzers QMG 200) operated under high vacuum with a turbomolecular pump (Pfeiffer TMU 065). The sample is placed either in a gas flow system connected to the MS via a heated capillary or in a rough-vacuum system with a rotary vane pump (Balzers DUO M). In the latter case a valve serves as connection to the MS, with which a constant leaking rate can be adjusted. Up to 60 different masses of interest (m/e) can be followed online. A pressure of 10⁻⁶ mbar was adjusted for the measurements.

NH₃-TPD: The amount of acid sites can be determined by temperature programmed desorption of adsorbed basic probe molecules, such as ammonia. Ammonia adsorption was carried out at 80°C in He flow, using a mixture of 10 vol% NH₃ in He and a total flow of 20 ml/min. After flushing the sample with pure He at 80°C for one hour in order to remove physisorbed NH₃ the TPD was carried out in He flow with a linear heating rate of 10°C/min. The desorbing species were detected by the quadrupole mass spectrometer. The amount of adsorbed ammonia can be calculated by integration of the mass peak. For quantification of the number of acid sites the peak area has to be compared to a reference material with a known amount of acid sites under assumption of a certain adsorption stoichiometry.

TPR: With the same experimental setup temperature programmed reduction (TPR) can be carried out. For this the samples were heated with 10°/min in a flow of helium containing 5 vol% hydrogen. Reduction processes can be observed by a decreasing concentration of hydrogen and by formation of water at the same time.

2.3.4 Infrared spectroscopy

IR spectroscopy is a very useful and widespread method for the investigation of surface groups, directly or indirectly via adsorption of probe molecules. FT-IR measurements were performed on a Bruker IFS 28 FT-IR spectrometer equipped with a MCT detector. Transmission spectra were recorded in the range of $4000 - 1200 \text{ cm}^{-1}$ with a resolution of 4 cm^{-1} . Measurements could be carried out either in a vacuum cell or in a flow cell, both equipped with CaF_2 windows. The latter is connected to the system for kinetic studies and the gas chromatograph (see also Fig. 2.3).

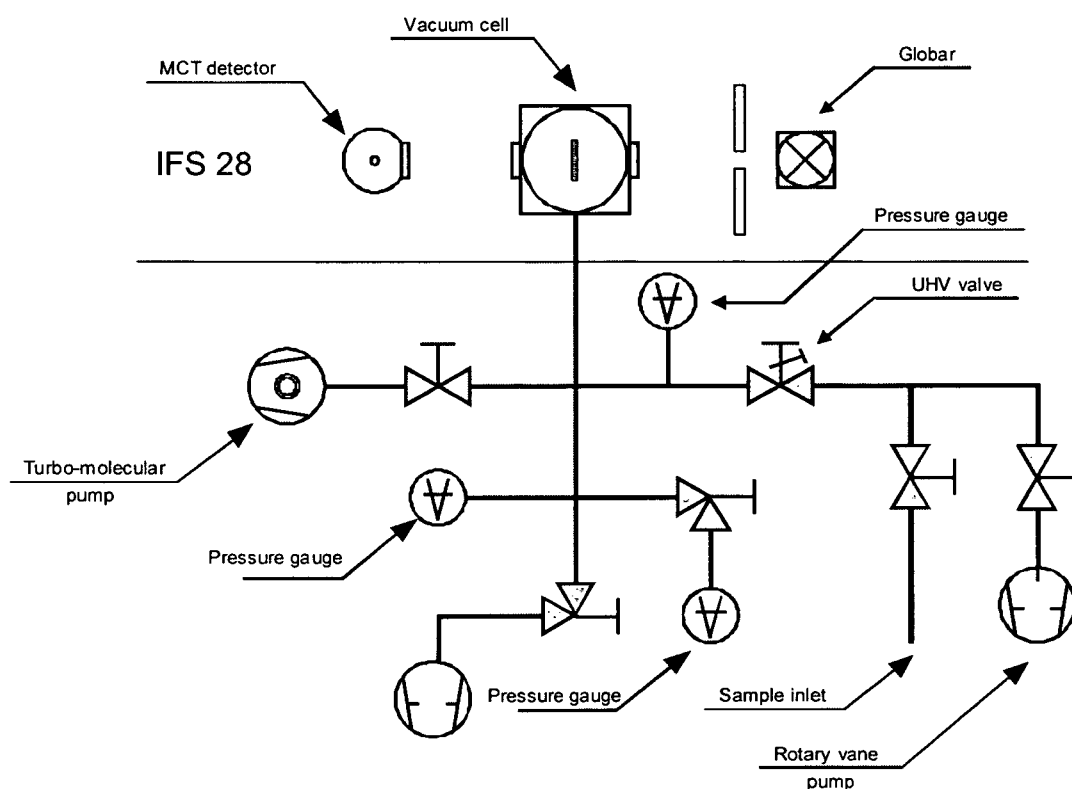


Figure 2.2: Experimental setup of the vacuum cell for FT-IR measurements

2.3.4.1 Adsorption of probe molecules

For characterization of the metallic and acidic sites the adsorption of different probe molecules, such as water, pyridine, CD_3CN and CO , followed by infrared measurements was carried out. These adsorption experiments were done in the vacuum cell after pretreatment either in vacuum, in flowing synthetic air at 500°C or by activation in air followed by reduction at 200°C . The adsorption was then carried out under static conditions in vacuum. The infrared spectra were recorded on a Bruker IFS 28 FT-IR spectrometer equipped with a MCT detector. The samples

were prepared as self-supporting wafers (2 cm diameter and typically 7–8 mg/cm²) and placed inside the cell, which allowed heating the samples up to 600°C.

2.3.4.2 In situ FT-IR measurements

The in situ FT-IR experiments were carried out in a flow cell approximating a continuously stirred tank reactor ($V = 1.5 \text{ cm}^3$). The samples were pressed into self-supporting wafers and placed inside a ring shaped furnace. The partial pressure of n-heptane (15 mbar) or n-hexane (60 mbar) was adjusted via a saturator kept at 0°C. Prior to the reaction the samples were activated in synthetic air at 500°C for 1 hour, cooled to 200°C and then reduced at this temperature for (at least) 15 min. During the reaction (200°C and the reagents flowing through the cell) IR spectra were recorded and the gas phase was analyzed by a gas chromatograph (HP 5980 II) equipped with an Al₂O₃/KCl or a HP-5 (phenyl-methylsilicone) column and a flame ionization detector. The reaction was carried out at atmospheric pressure in a H₂ flow of 40 ml/min. For n-hexane isomerization a reaction temperature of 250°C was used, whereas for n-heptane the typical reaction temperature was 200°C.

2.3.4.3 Diffusion measurements

Diffusion and transport phenomena are of great importance in heterogeneous catalysis. Diffusion measurements were carried out by time resolved IR spectroscopy in the vacuum cell. The aim was to investigate the residence time of the reactants on the surface of the catalyst.

After activation of the catalyst in vacuum at 500°C the adsorption of n-hexane or n-heptane (0.005 mbar) was started and spectra were recorded every 10 seconds, until equilibrium was reached. Desorption was started by evacuation to 10⁻⁶ mbar and again IR spectra were collected every 10 seconds during desorption. Analysis was done by integration of the bands of the C-H stretching vibration (3000 – 2700 cm⁻¹), which were taken as a measure for the amount of adsorbed hydrocarbon. The fractional uptake, which is the actual uptake divided by the uptake at equilibrium, is plotted against the square root of the time. From the linear part of this plot the diffusion coefficient can be estimated according to Fick's law for cubic and spheric particles [3]:

$$\frac{M_t}{M_{equ}} = \frac{6}{r \cdot \sqrt{\pi}} \sqrt{D \cdot t}$$

M_t/M_{equ} is the fractional uptake, r the mean radius (in cm), t is the time (in s) and D is the diffusion coefficient (in cm²/s).

2.4 Kinetic studies

For kinetic measurements a system was used which consisted of a gas supply, a saturator, a heatable reactor and a gas chromatograph for analysis of the reaction products. With the setup used in this work the test reaction could be carried out either in a plug flow reactor or in a flow cell for in situ IR measurements.

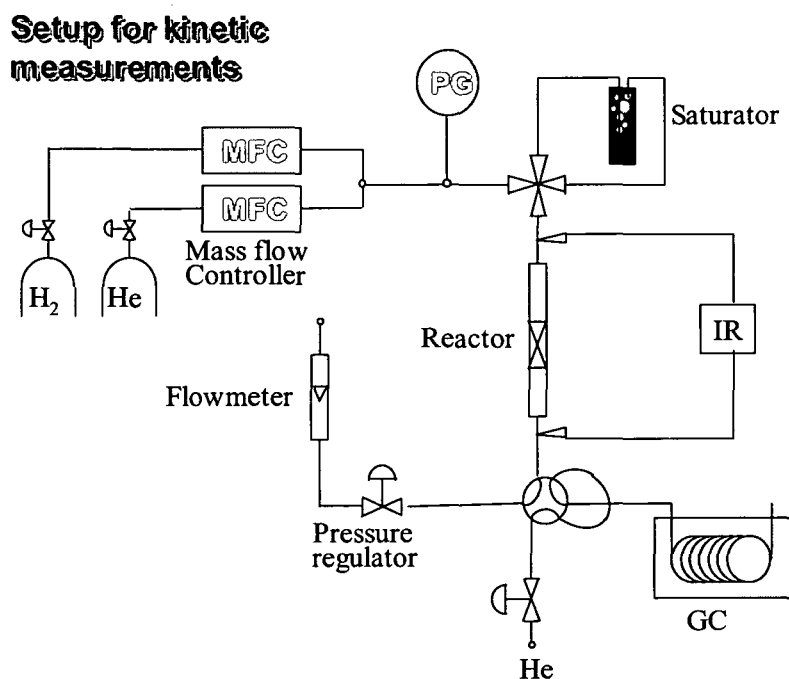


Figure 2.3: Experimental setup for kinetic measurements

For reaction kinetic studies n-alkane conversion was carried out in a down-stream fixed-bed plug flow reactor. About 15 mg of the catalyst were loaded in the reactor and activated in flowing synthetic air at 500°C for one hour. Then the catalyst was cooled down to 200°C and reduced in a flow of hydrogen (40 ml/min) at this temperature. After the reduction the reaction was started by passing the n-alkane either in He or H_2 (Messer, 5.0) as carrier gas over the catalyst bed. Usually a total flow of 40 ml/min was used, and the total pressure could be adjusted from 1 to 5 bar with a back pressure regulator. The n-alkane was added via a saturator kept at 0°C, which leads to a partial pressure of 15 mbar n-heptane or 60 mbar n-hexane. Alternatively, the liquid reactant could also be added with a syringe pump. The products were analyzed by a gas chromatograph (HP 5890 II) equipped with a capillary column (either Al_2O_3/KCl or HP-5 (phenyl-methylsilicone)) and a flame ionization detector.

Evaluation and determination of kinetic parameters:

The setup was designed to comply the assumption of an ideal plug flow reaction system. At low conversions (< 10 %) a constant flow of reactants and products and a constant temperature in the whole reaction zone can be assumed - these differential conditions were the basis for the calculation of the kinetic parameters.

The reaction rate was calculated according to the formula

$$r_i = X_i \cdot \frac{F_R}{W_{cat}}$$

In this equation r_i is the rate of formation (in $\text{mol} \cdot \text{g}^{-1} \cdot \text{s}^{-1}$) of the substance i ; X_i the conversion (in mol per 100 mol reactant) to the product i ; F_R is the molar flow (in $\text{mol} \cdot \text{s}^{-1}$) of the reactant and W_{cat} is the weight of the catalyst (in g).

The conversion X_i was estimated by dividing the normalized FID response of the substance i through the total normalized FID response. Normalization of the FID signal was carried out according to ref. [4]: the FID signal increases linearly with the number of carbon atoms within a homologue series of hydrocarbons, thus it is possible to normalize the FID response to the number of carbon atoms and consequently the conversion X_i was calculated according to:

$$X_i = \frac{C_i}{C_n} = \frac{A_i \cdot f_i \cdot n_i}{\sum_{j=1}^{j=n_{total}} A_j \cdot f_j \cdot n_j}$$

In this formula C is the normalized FID signal, A is the measured peak area in the chromatogram, f the correction factor (depending on the substance and detector) and n the number of carbon atoms in the hydrocarbon.

The selectivity S_i is calculated as the ratio of the amount of product i to the sum of all products.

References

-
- [1] Manual Netzsch STA 409 Luxx
 - [2] F.R. Chen, G. Coudurier, J.F. Joly, J.C. Vedrine, J. Catal. 143 (1993) 616.
 - [3] J. Crank, *Mathematics of Diffusion*, Oxford University Press, London (1956) 62.
 - [4] R. Kaiser, *Chromatographie in der Gasphase*, Hochschultaschenbücherverlag, Mannheim, IV/2 (1969), 201

3 CHARACTERIZATION OF THE COMMERCIAL MEL CATALYSTS

3.1 Introduction

The properties of a catalyst determine substantially the performance in the catalytic reaction. The knowledge of as many influence factors as possible and their impact on the catalytic reaction are decisive for a better understanding of catalytic reactions and the operation of catalysts.

The identification of the active sites is the main focus of the catalyst characterization. The determination of the nature, strength and number of the sites responsible for the conversion are critical for the understanding of the catalytic properties. Although a great number of studies deal with the active sites of sulfated zirconia catalysts, there are still debates on the nature and strength of acid sites, the state of the sulfates and the influence of the zirconia support. This is contrary to zeolites, where it seems to be quite clear which are the active sites and what are their properties.

Among the solid acid catalysts sulfated zirconia (SZ) has reached a lot of interest due to its high activity for the isomerization of light alkanes at low temperatures [1].

SZ was first considered to be a solid superacid [2], however, more recent studies have shown that the catalyst does not possess superacid strength [1,3]. Until now there is a serious controversy about the interpretation of the acidic properties of SZ. A further complication occurred by the nature of SZ, showing different reactivities according to the preparation method and activation conditions [4]. For example Tichit et al. [5] found SZ prepared by a one step sol-gel method more active for n-hexane isomerization than SZ prepared in two steps. The actual nature of the catalytic sites, as well as the mechanism through which the catalytic sites are produced, is still subject of debate [6].

The most convincing evidence of the superacidic character of a solid would be its ability to reversibly protonate an alkane via a Brønsted acid site (BS) or its ability to abstract a hydride via a Lewis acid site (LS). Unfortunately, there exist no experimental evidences for carbenium ions or for the existence of Zr-hydrides. It is generally admitted that the Lewis acid sites on SZ play an important role in enhancing the acidity of neighboring Brønsted sites [7]. Bolis et al. [6] found that upon sulfation the overall surface concentration of LS decreases but their acidic strength increases provided that the sample had been calcined at a proper temperature. It was proposed by

3. Characterization of the commercial Mel catalysts

Morterra et al. [8,9] that the calcination step allows selective elimination of sulfates located on the side terminations of the crystallites, thus forming low-coordinated Zr cations, which can act as Lewis acid sites.

Various model structures for the adsorbed sulfate groups such as doubly bonded structures with two S=O groups, triply bonded structures that contain only one S=O group, bisulfate –like doubly bonded structures were discussed in the literature [1,10]. After the model of Clearfield [11], uncalcined SZ contains protons as bisulfate groups and as hydroxyl groups bridging two zirconium ions. During calcination water is removed from the surface and Lewis acid sites are formed. But when the bisulfate group remains intact, a Lewis acid site adjacent to a S-OH group results. These bisulfate groups can act as highly acidic Brønsted acid sites because the neighboring Lewis acid sites tend to withdraw electrons from the bisulfate group, thus weakening the SO-H bond. This model can explain the presence of both Brønsted and Lewis acid sites and the reversible transformation between these two sites upon the degree of hydration/dehydration.

Due to the large number of parameters we decided to use a commercial SZ catalyst as a standard material in order to focus on some important influence factors.

In general a description of acidity requires the determination of the nature, strength and number of acid sites. Different methods can be applied, which can provide partial information. Suitable techniques are IR measurements, calorimetric measurements and temperature programmed desorption of basic molecules. Especially IR spectroscopy is a very valuable method for obtaining information on surface groups and their interaction with probe molecules.

Some properties of the SZ catalysts were compared to those of the zeolite HBEA. This was done because both materials – zeolites and sulfated zirconia – are commercially used for n-alkane isomerization.

3.2 Results and discussion

3.2.1 Structural and morphological properties and chemical composition

The crystal structure of the catalysts Mel 1 and Mel 2 was determined by X-ray powder diffraction. Both showed the pure tetragonal structure, which is assumed to be the catalytically active phase. Impregnation with Pt had no measurable effect on the crystal structure. Only very small reflexes from Pt were found in the XRD patterns.

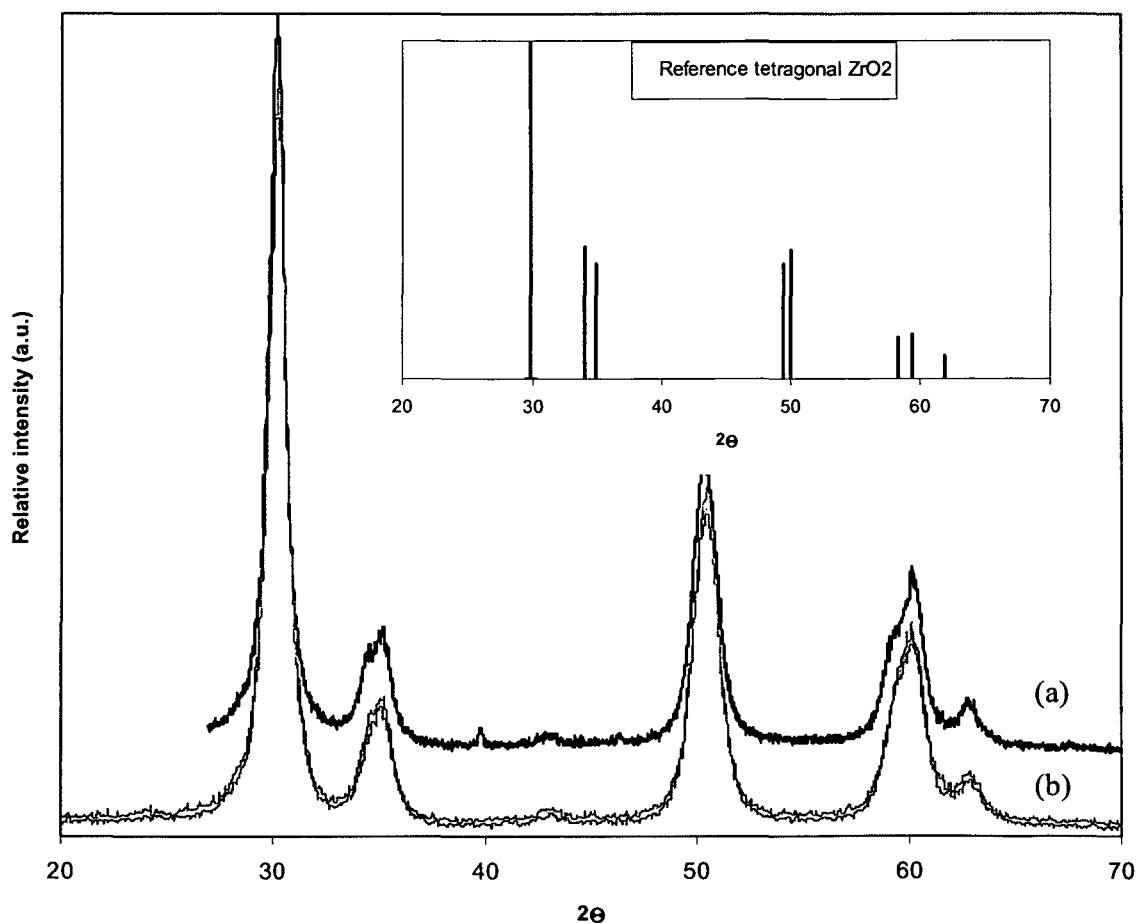


Figure 3.1: XRD patterns of Mel 1 (a) and Mel 2 (b)

For investigation of the particle size TEM pictures (transmission electron microscopy) were collected. They revealed particles of around 10 nm (see Figure 3.2).

3. Characterization of the commercial Mel catalysts

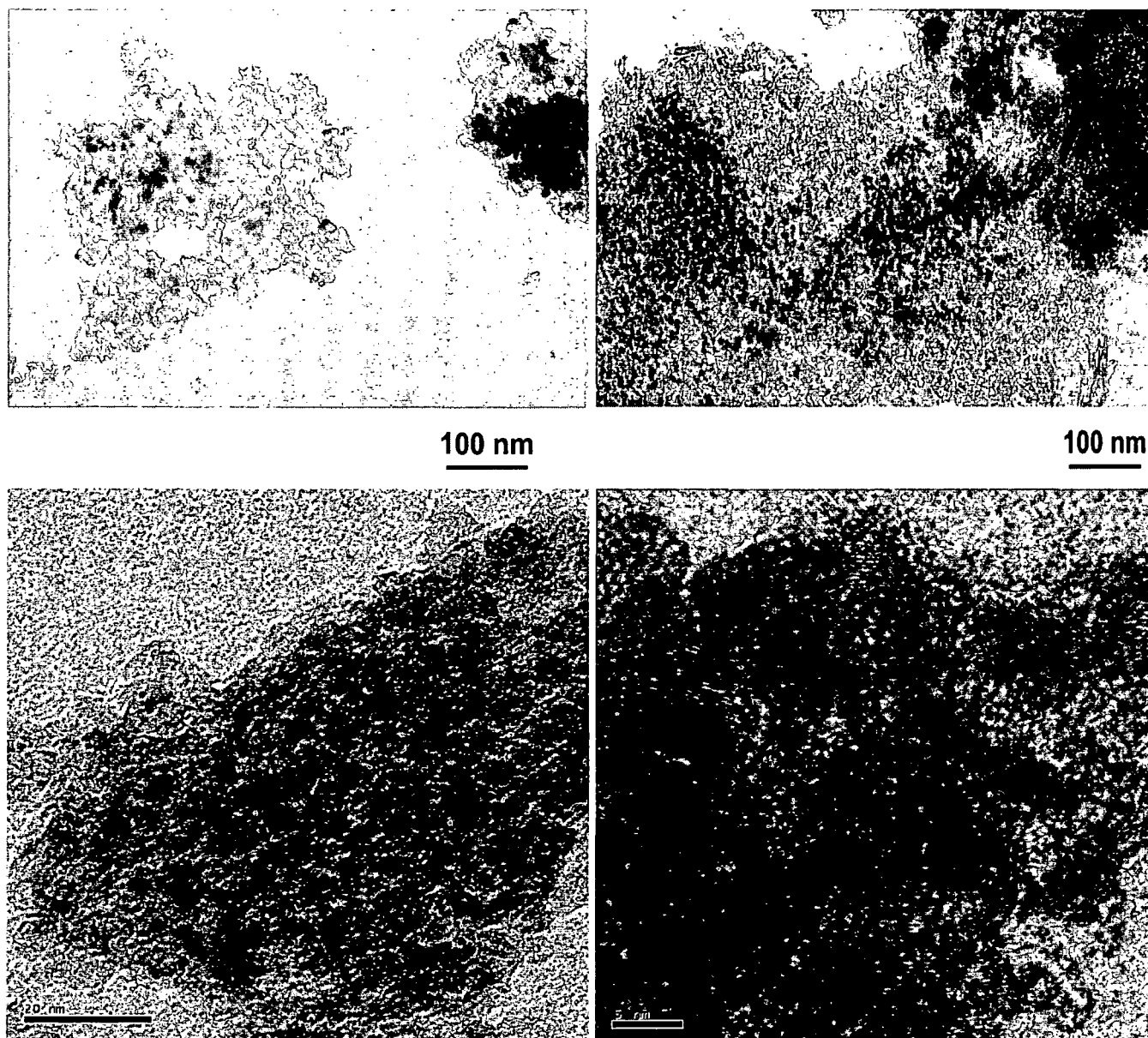


Figure 3.2: TEM pictures of Pt/Mel catalysts

Surface area, sulfate content and surface coverage by sulfate groups were determined by means of BET adsorption isotherms and thermogravimetric analysis (TG). The results for Mel 1 and Mel 2 are summarized in Table 3.1. Two mass steps were observed by TG (see Figure 3.3 A). The first mass decline up to 300°C can be attributed to the removal of water, and the second mass loss above 600°C is due to the decomposition of the sulfate groups. The two processes can be

3. Characterization of the commercial Mel catalysts

assigned by comparison with TPD measurements carried out under the same conditions (Figure 3.3 B). For the calculation of the sulfate density ($\text{SO}_4^{2-} \text{ nm}^{-2}$) and surface coverage a surface area of 0.25 nm^2 was assumed for a sulfate group [12].

Table 3.1: Physico-chemical properties of the commercial SZ catalysts Mel 1 and Mel 2

Catalyst	Specific surface area (m^2/g)	wt% SO_4^{2-}	wt% S	mmol/g SO_4^{2-}	Surface coverage	Sulfate density (nm^{-2})
Mel 1	111	5.0	1.67	0.52	0.71	2.8
Mel 2	155	5.7	1.9	0.59	0.58	2.3

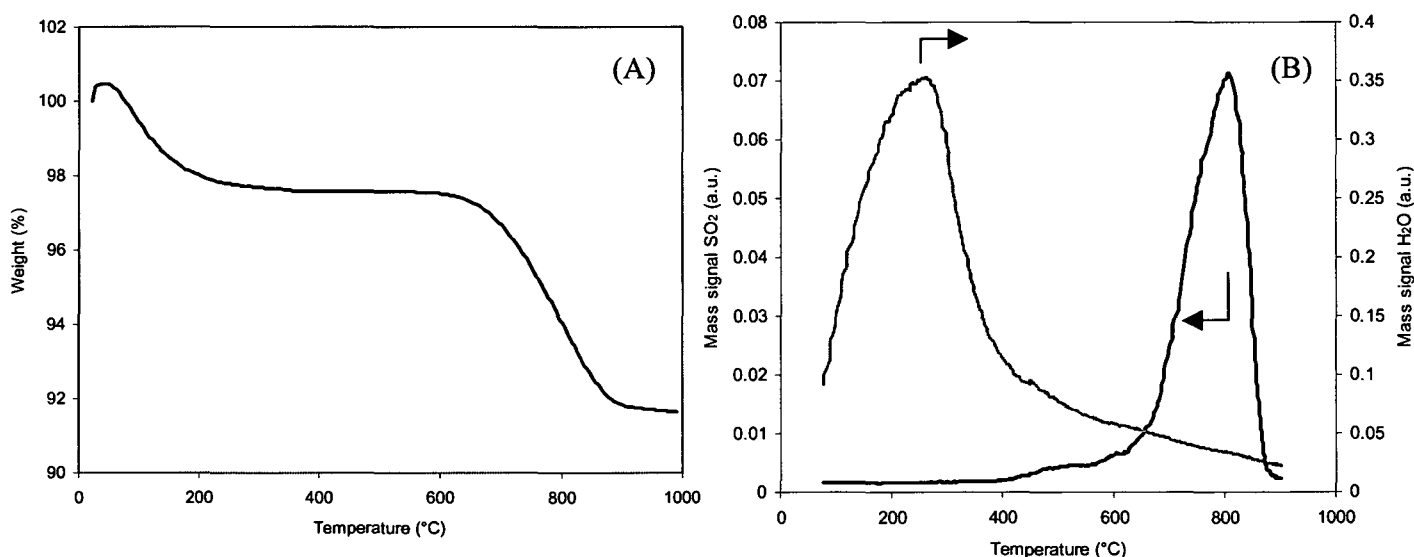


Figure 3.3: (A) TG curve of the commercial Mel 2 catalyst in He; (B) TPD of Mel 2 in He

3.2.2 Characterization of surface sites

3.2.2.1 Characterization with TPD

TPD (temperature programmed desorption) of basic probe molecules such as ammonia provide information about the number of acid sites from the amount of adsorbed NH_3 molecules and the strength of acid sites from the temperature of desorption.

NH_3 TPD spectra are shown in Fig. 3.4. SZ catalysts are characterized by a broad desorption peak with a maximum below 200°C spanning in the range of $100 - 400^\circ\text{C}$ and asymmetric on the high temperature side. The broad peak indicates a broad variety of sites of different acid strength. This

3. Characterization of the commercial Mel catalysts

is in contrary to zeolites, which usually show very sharp and defined desorption peaks. From this it can be concluded that the acid sites on sulfated zirconia are rather heterogeneous. Concerning the desorption temperature the TPD of NH_3 does not hint to strong acid sites.

Ammonia TPD for determining the acidity of SZ catalysts is certainly not suitable, because ammonia decomposes sulfate at higher temperatures. However, for qualitative investigation of the strength of the acid sites this process is straightforward. Following the decomposition of sulfates two desorption maxima are observed when ammonia was adsorbed before. Without ammonia only one maximum at the higher temperature due to the loss of sulfate groups was detected when SZ is heated up to 1000°C (see Figure 3.3 (B)). Therefore, it can be assumed that ammonia adsorption-desorption induces a (partial) reduction of sulfates.

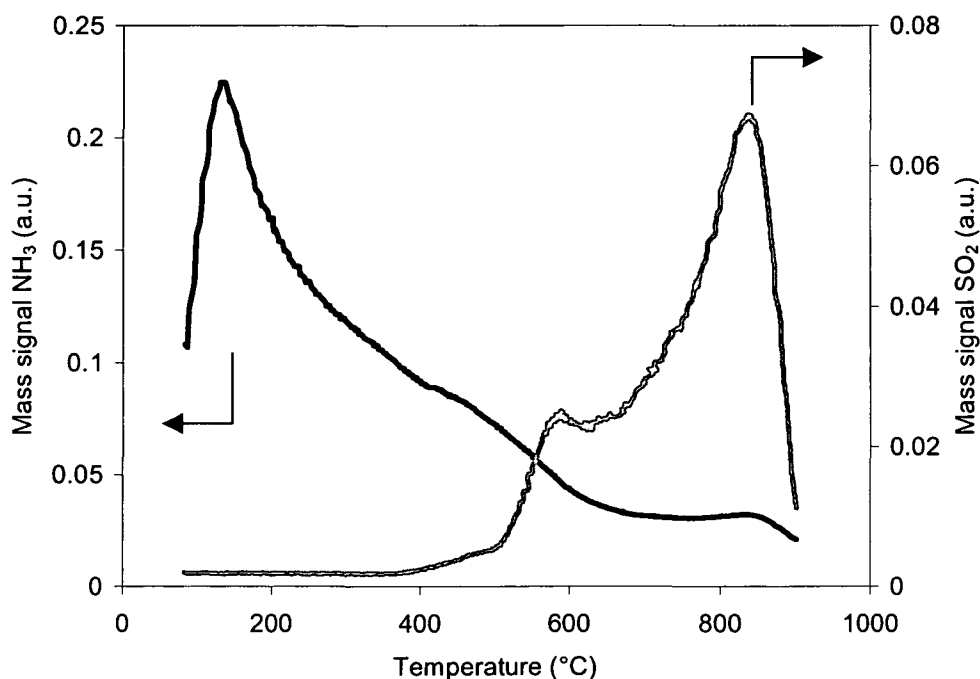


Figure 3.4: Ammonia TPD on a Mel 2 catalyst

3.2.2.2 Characterization with IR spectroscopy

IR spectroscopy is a very useful technique. Much information can be obtained: information about number, strength, location and accessibility of surface sites and about the interaction with different probe molecules and the reactants.

Surface hydroxyl and sulfate groups of the activated samples, reversible adsorption and desorption of water

The IR spectrum of Pt/SZ (Fig. 3.5) activated in air shows four bands in the OH stretching region, at 3743, 3640, 3582 cm^{-1} and a very broad band with a maximum around 3200 cm^{-1} . In the literature [13,14] the first two bands are described as isolated ZrOH groups and as hydroxyl groups coordinated to more than one Zr cation respectively, the low frequency band at 3582 cm^{-1} can be attributed to non-specified hydroxyl groups present in sulfated zirconia, which is not found in the spectrum of tetragonal zirconia [15]. Kustov et al. [14] assigned the broad band around 3200 cm^{-1} to protons resulting from the substitution of terminal Zr-OH groups by HSO_4^- anions.

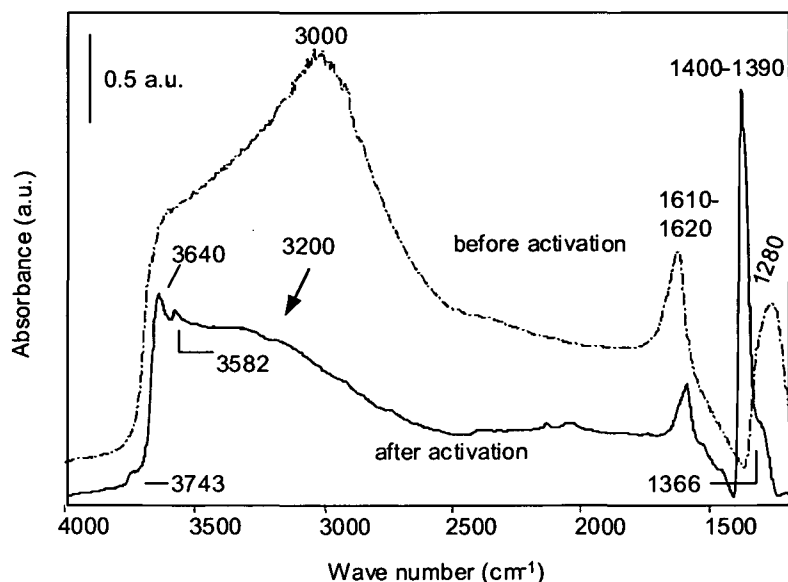


Figure 3.5: IR spectra of Pt/SZ before and after activation in synthetic air at 500°C

In the region between 1610 and 1620 cm^{-1} the deformation vibration of adsorbed water was observed, even after activation at 500°C in air. Also Moreno and Poncelet [16] found a small water band at 1620 cm^{-1} in the IR spectrum after activation of SZ at 450°C in air. However, if the activation was carried out under vacuum or in He the intensity of the band assigned to adsorbed

3. Characterization of the commercial Mel catalysts

water was found to be very small. The residual water content of synthetic air was determined to be around 10 ppm, which can be the reason for the more intense water band. The OH region in the IR spectrum of Pt/SZ before activation showed only a huge band with a maximum at 3000 cm^{-1} .

The band at 1400 - 1390 cm^{-1} can be ascribed to the stretching vibration of S=O [15,17]. The position of this band depends strongly on the water content. Bands at lower wave numbers, 1366, 1280 cm^{-1} , are assigned to adsorbed forms of sulfuric acid. After evacuation and heating the bands stemming from adsorbed water decreased and the S=O band at 1395 cm^{-1} increased strongly. Addition of a controlled amount of water to dehydrated SZ shifted the S=O band downwards and the bands near 1370 and 1280 cm^{-1} developed. After desorption of water the opposite behavior was observed, the S=O band was restored, the broad band around 3200 cm^{-1} and the band around 1615 cm^{-1} decreased in intensity. Higher wave numbers of the S=O stretching vibration indicate a higher S=O bond order and a more covalent character of the bond.

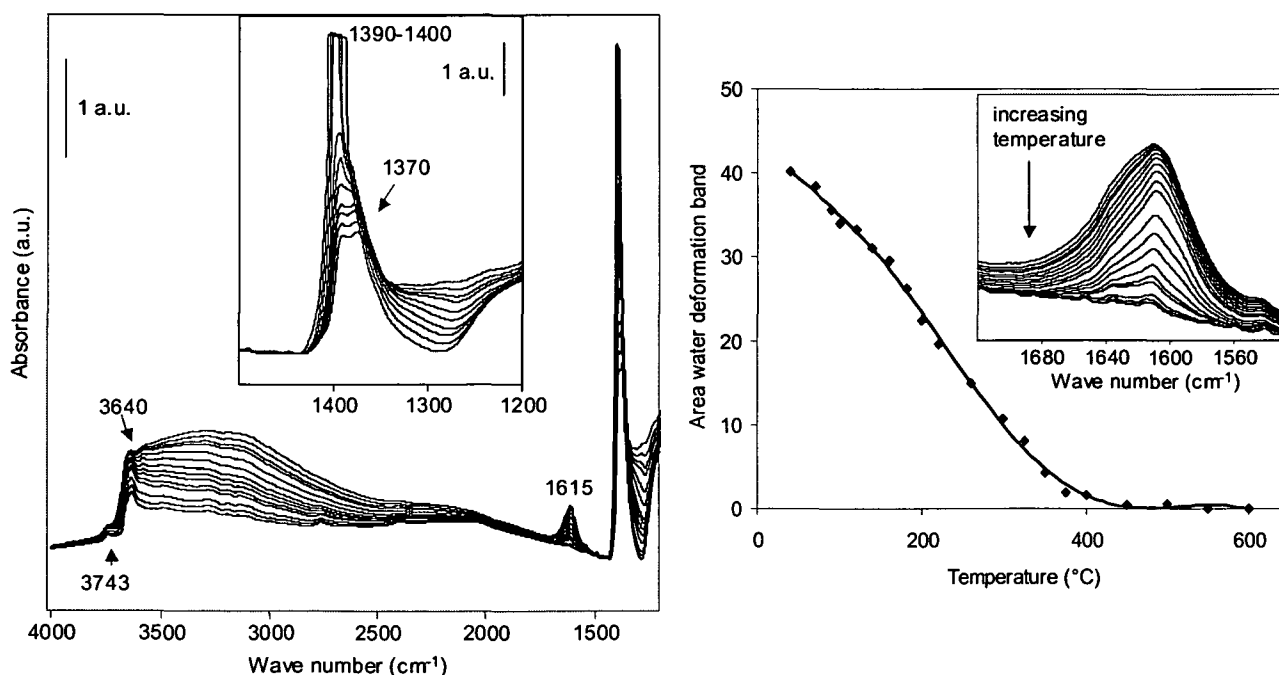


Figure 3.6: Reversible adsorption and desorption of water on SZ; decrease of the water concentration with increasing temperature when the sample is heated in vacuum

The concentration of acid sites, Lewis- and Brønsted acid sites should depend on the surface hydration/dehydration degree. According to the model of Clearfield [11] a volcano shaped curve

3. Characterization of the commercial Mel catalysts

is expected if one plots the activity vs. the amount of adsorbed water. On dehydrated surfaces mainly Lewis acidity and on hydrated surfaces Brønsted acidity occurs. The presence of some level of hydration is important for SZ to be active. The reason could be that a certain water content is crucial to develop full catalytic activity.

Since the nature of acid sites on SZ depends critically on its water content, which in turn depends on the pretreatment steps, the choice of appropriate pretreatment conditions is extremely important in controlling the activity of SZ.

For comparison the IR spectrum of an unsulfated tetragonal ZrO_2 sample is shown in Figure 3.7. In the region of the OH stretching vibrations two bands can be found at 3740 and 3675 cm^{-1} . The band at 3740 cm^{-1} is assigned to mono-coordinated terminal OH groups and the band at 3675 cm^{-1} to bridging OH groups, which are bi- or tri-coordinated to the zirconia surface. The lower wave number of the bridging OH groups in the case of the sulfated zirconia was attributed to the surface inductive effect of the sulfate group via electron withdrawal and bond polarization [18].

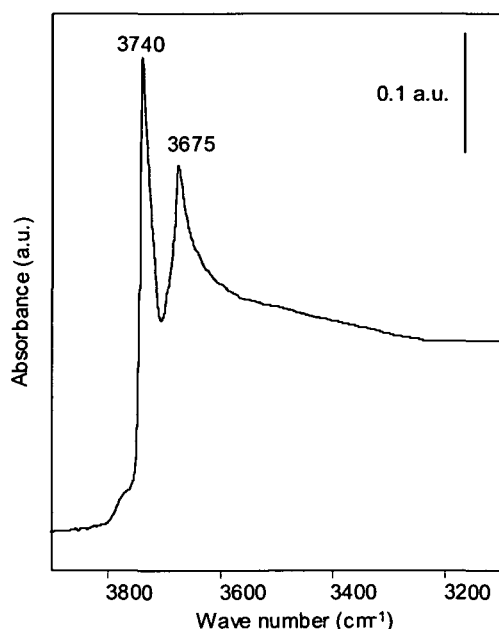


Figure 3.7: IR spectrum of tetragonal ZrO_2 after activation in vacuum at 500°C

Adsorption of benzene

Benzene is often used as a probe for the strength of Brønsted acid sites. It acts as a weak base when it is adsorbed on an acidic surface. Adsorption of benzene allows a ranking of OH groups according to their acidity [19]. The interaction of benzene with acidic hydroxyl groups leads to a

3. Characterization of the commercial Mel catalysts

shift of the band of the OH stretching vibration to lower wave numbers. This shift due to the formation of a hydrogen bond between benzene molecules and surface OH groups is a measure for the acidity [20].

The shift of the band of the bridging hydroxyl groups on SZ is shown in Table 3.2 and compared to the shift obtained on zeolite HBEA. As it can be seen the zeolite possesses significantly stronger Brønsted acid sites, which was also reported in literature [14].

Table 3.2: Shift of the acidic OH band to lower wave number after adsorption of benzene (40°C, 10^{-3} mbar)

Material	$\Delta\nu$ OH (cm^{-1})
SZ Mel 1	230
HBEA	350

Adsorption of pyridine

IR spectroscopic investigation of the adsorption of pyridine is a wide-spread method to differentiate between Lewis (LS) and Brønsted acid sites (BS). Adsorption of pyridine on Brønsted acid sites forms a pyridinium ion with IR bands at 1638, 1611, 1540 and 1486 cm^{-1} , whereas pyridine covalently bonded to Lewis acid sites gives characteristic bands at 1486 and 1445 cm^{-1} [21].

IR spectra of adsorbed pyridine on SZ and Pt/SZ were recorded after the same pretreatment conditions – activation in air at 500°C, reduction with hydrogen at 200°C, evacuation at 350°C, adsorption of 0.05 mbar pyridine, and evacuation for one hour at 120°C. In Figures 3.8 (A) and 3.8 (B) IR difference spectra of protonated (1543 cm^{-1}) and Lewis bounded (1445 cm^{-1}) pyridine can be seen. After activation both – LS and BS – are present on the surface. Impregnation with Pt leads to a higher concentration of BS in comparison to Lewis acid sites.

Adsorption of pyridine caused a shift of the S=O band from 1398 to 1336 cm^{-1} and a decrease of the water deformation band at 1615 cm^{-1} . Note that on Pt/SZ and SZ a negative band at 1594 cm^{-1} was found in the difference spectra (Fig. 3.8), indicating that pyridine can replace water from the acidic sites.

3. Characterization of the commercial Mel catalysts

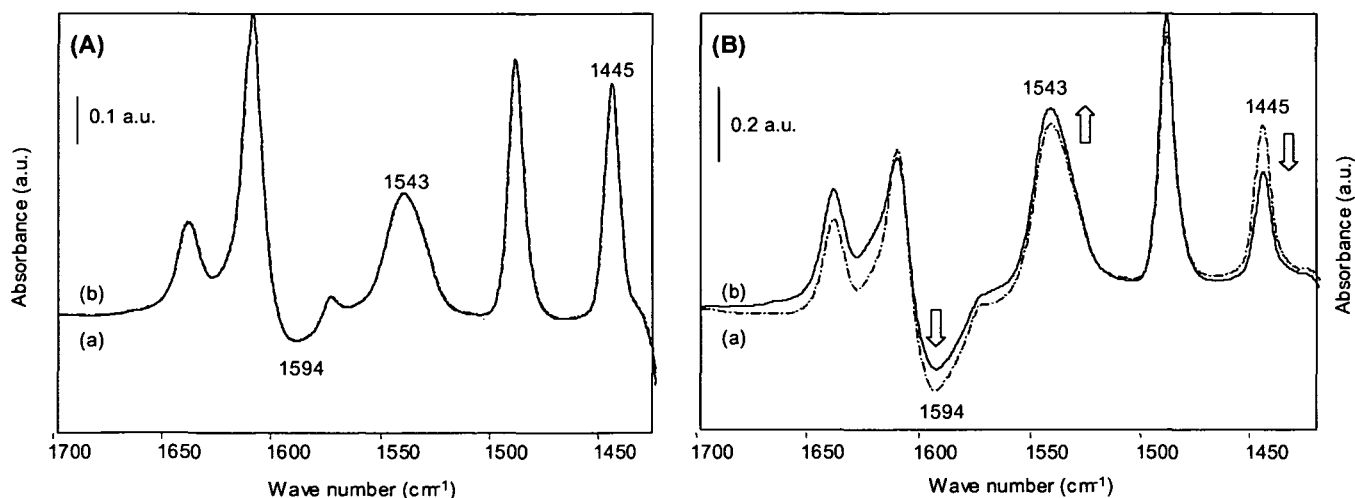


Figure 3.8: Difference spectra (obtained by subtraction of the spectrum after activation of the catalyst) after adsorption of pyridine (a) followed by treatment with hydrogen (b) at 40°C for (A) SZ and (B) Pt/SZ

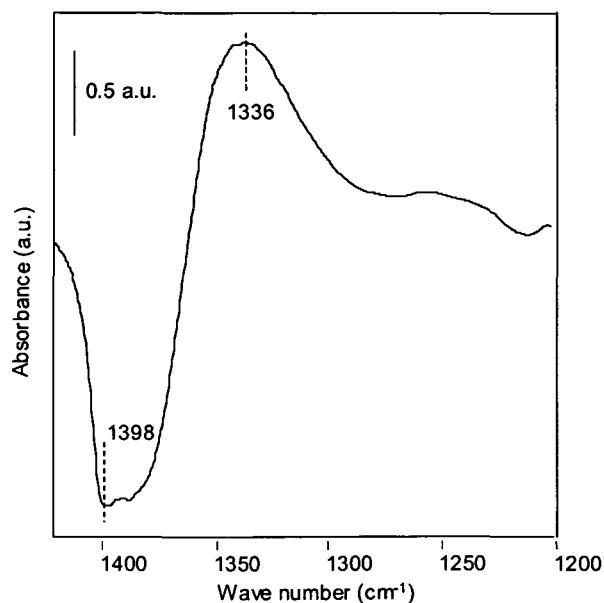


Figure 3.9: Difference spectrum of the shift of the S=O band after pyridine adsorption on Pt/SZ

The origin of the shift of the S=O band to lower wave numbers can have various reasons:

- (i) An inductive effect by the adsorption of pyridine on Lewis acidic centers (coordinatively unsaturated Zr^{4+}) while retaining the structure of the sulfates. Clearfield et al. [11] attributed this

3. Characterization of the commercial Mel catalysts

shift to a weakening of the ability of S=O to attract electrons from Zr^{4+} . The shift of the S=O band to a lower wave number corresponds to a decrease in the strength of Lewis acid sites, or

(ii) Pyridine as a strong base can displace water from Lewis acid sites, which further reacts with SO groups to transform them into more ionic forms.

Note that the pyridine – sulfate interaction shifts all components of the S=O band to lower wave numbers, which indicates that all sulfate groups are located at the surface and are influenced by or interact with pyridine.

Morterra et al. [17] studied by IR measurements the acidity of SZ samples, which were differently hydrated, by adsorption of pyridine. Under all hydration conditions acidic centers were available for interaction with pyridine. At high surface hydration they found hydrated acidic centers, which can interact with strong bases, whereas under conditions of high dehydration only few protonic centers were available.

After adsorption of pyridine, hydrogen was adsorbed at 40° and 100°C, respectively (Fig. 3.8 (A) and (B)). It can be clearly seen that on Pt/SZ the concentration of Brønsted acid sites increased whereas no change was observed on SZ (see Table 3.3), although the same pretreatment conditions were applied.

Table 3.3: Ratio of Lewis and Brønsted acid sites on Pt/SZ and SZ before and after hydrogen adsorption

Catalyst		LS/BS
Mel 1	Before H ₂ adsorption	0.73
	H ₂ 40°C	0.73
	H ₂ 100°C	0.73
Pt/Mel 1	Before H ₂ adsorption	0.55
	H ₂ 40°C	0.33
	H ₂ 100°C	0.38
Mel 2	Before H ₂ adsorption	0.80
Pt/Mel 2	Before H ₂ adsorption	0.52

The LS/BS ratio is determined by comparing the peak areas of the bands at 1445 and 1543 cm⁻¹. Extinction coefficients are difficult to determine and the values reported in literature differ

3. Characterization of the commercial Mel catalysts

widely. Therefore we did not quantitatively determine the concentration of Brønsted and Lewis acid sites. However, for qualitative investigations the ratio of the peak areas is satisfactory.

An explanation according to Ebitani [22] can be that molecular hydrogen is homolytically dissociated on Pt, the atoms are spillover to SZ where they are converted either into H^+ and H^- or $2H^+$ and 2 electrons, which affect the balance between LS and BS. Spillover hydrogen donates an electron to the LS and forms a proton, which is stabilized on the oxygen atom near the LS. The pyridine molecule that was adsorbed on the Lewis acid site moves to the protonic site to form a pyridinium ion. A second hydrogen reacts with the electron donated to the LS to form a hydride, which is consequently stabilized on the Lewis acid sites.

Heterolytic dissociation of hydrogen was also found for zirconia [23] and SZ [24], however this process is so much faster on Pt compared to pure zirconia or SZ, therefore no change in the ratio of LS/BS on sulfated zirconia was observed under our conditions.

Adsorption of deuterated acetonitrile

After adsorption of acetonitrile, a weak base, at 40°C on SZ (same activation conditions as with pyridine), the following bands were observed in the IR spectrum: 2305, 2254 and 2112 cm^{-1} (Fig. 3.10). The latter two bands belong to the asymmetric and symmetric stretching vibration of the C-D bond and are not influenced by adsorption. The band at 2305 cm^{-1} belongs to the stretching mode of the CN vibration. The OH bands at 3743 and 3640 cm^{-1} decreased and the broad band with a maximum at around 3200 cm^{-1} increased, indicating that CD_3CN has been bonded, at least partly, to OH groups. The band near 1615 cm^{-1} decreased and the sulfate region is strongly affected by the adsorption of CD_3CN , the band at 1393 cm^{-1} shifted to lower wave numbers as it was observed after pyridine adsorption.

Acetonitrile interacts with the acid sites via the nitrogen lone electron pair of the CN group. The strength of this bonding is reflected in the shift of the stretching vibration of CN (2265 cm^{-1}) to higher frequencies. According to literature data [25,26] for adsorption of acetonitrile on zeolites bands at 2320 – 2330 cm^{-1} are assigned to adsorption on strong Lewis acid sites, at 2296 - 2298 cm^{-1} to bridging OH groups and at 2310 cm^{-1} to weak Lewis acid sites. Therefore the band at 2305 cm^{-1} can be correlated to the bonding of acetonitrile to weak Lewis acid sites and/or to Brønsted acid sites. Adsorption of acetonitrile on pure tetragonal zirconia leads to an adsorption band at 2301 cm^{-1} , whereas zeolite Beta exhibits this band at 2323 cm^{-1} . Therefore one can

3. Characterization of the commercial Mel catalysts

conclude that on SZ rather weak Lewis and Brønsted acid sites were probed by adsorption of acetonitrile.

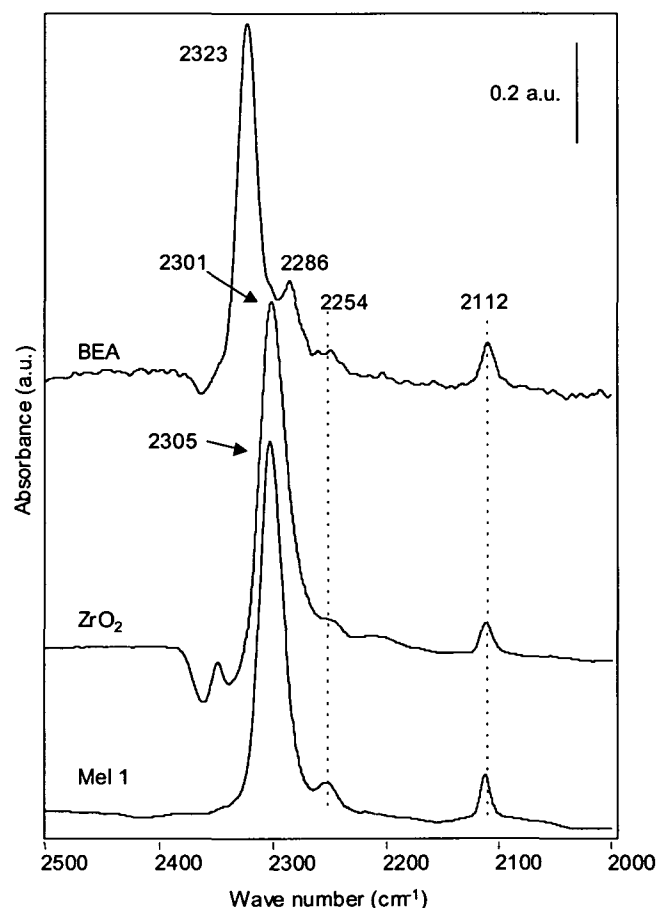


Figure 3.10: IR spectra of the adsorption of CD₃CN on Mel 1, HBEA and tetragonal ZrO₂

Adsorption of CO

Adsorption of carbon monoxide allows the characterization of the metallic sites. Intense absorption bands appear in the region of 2100 – 1700 cm⁻¹ arising from the stretching vibration of the carbon-oxygen bond. The band of gaseous carbon monoxide lies at 2143 cm⁻¹. After adsorption the molecule is linked to the metal via an electron lone pair located on the carbon, providing a metal-carbon σ -bond. Back-donation of electrons from the metal d-orbitals to antibonding orbitals in the CO strengthens the metal-carbon bond via formation of a π bond. Increased metal donation leads to a weakening of the carbon-oxygen bond, which results in a shift of the stretching frequency to lower wave numbers. The molecule can be adsorbed linearly, giving rise to bands between 2100 and 2000 cm⁻¹, or it can also exist as a bridging group between two metal atoms characterized by bands between 2000 and 1800 cm⁻¹.

3. Characterization of the commercial Mel catalysts

Via adsorption of CO it is possible to distinguish between oxidized $\text{Pt}^{\delta+}$ (2136 – 2128 cm^{-1}) and metallic Pt° (2099 – 2086 cm^{-1}) species. In Table 3.4 frequencies of adsorbed CO and in Fig. 3.11 IR spectra of CO adsorbed on differently prepared Pt/SZ are shown. The more active catalyst was prepared by impregnation of Mel 1 with Pt salts before calcination at 600°C, whereas the other sample was impregnated after calcination. Both samples were activated in air at 500°C and reduced at 200°C prior to CO adsorption. Impregnation of SZ after calcination leads to metallic Pt particles on the surface, whereas on samples impregnated before calcination Pt is partly present in an oxidized form even after reduction at 200°C. It seems that on the surface of the more active catalyst, only a small part of Pt atoms is available, although the overall concentration of Pt is the same in the two samples.

Table 3.4: CO adsorption at 20°C on different SZ samples followed by IR measurements
A: after activation in vacuum at 350°C, B: after activation in air at 500°C, C: after activation in air at 500°C followed by reduction at 200°C

Sample conditions		CO frequencies (cm^{-1})	Assignment
SZ calcined	A	2200	CO on LS
Pt/SZ impregnated – calcined	A	2204, 2145	CO on LS, $\text{Pt}^{\delta+}$
	B	2134	CO on $\text{Pt}^{\delta+}$
	C	2128, 2086	CO on $\text{Pt}^{\delta+}$, Pt°
Pt/SZ calcined - impregnated	A	2200, 2138, 2104	CO on LS, $\text{Pt}^{\delta+}$, Pt°
	B	2136, 2099	CO on $\text{Pt}^{\delta+}$, Pt°
	C	2086, 1892, 1851	CO on Pt° , bridged

Some researchers report that Pt is electron deficient or oxidized on the surface of SZ [22,27], but still dissociation of H_2 is retained which is necessary for the operation. As a reason for the positively charged Pt species the direct interaction between the acidic protons and the metal particles yielding $\text{Pt-H}^{\delta+}$ is discussed [28,29]. Paál and coworkers [30,31] postulated that SZ encapsulates Pt during calcination, which would be metallic but mostly buried in the first layers of the zirconia surface. This was confirmed by measuring XPS intensities where a dramatic loss of surface Pt was observed upon calcination. These results indicated a migration of zirconia over Pt particles, which is in agreement with the IR measurement shown in Fig. 3.11.

3. Characterization of the commercial Mel catalysts

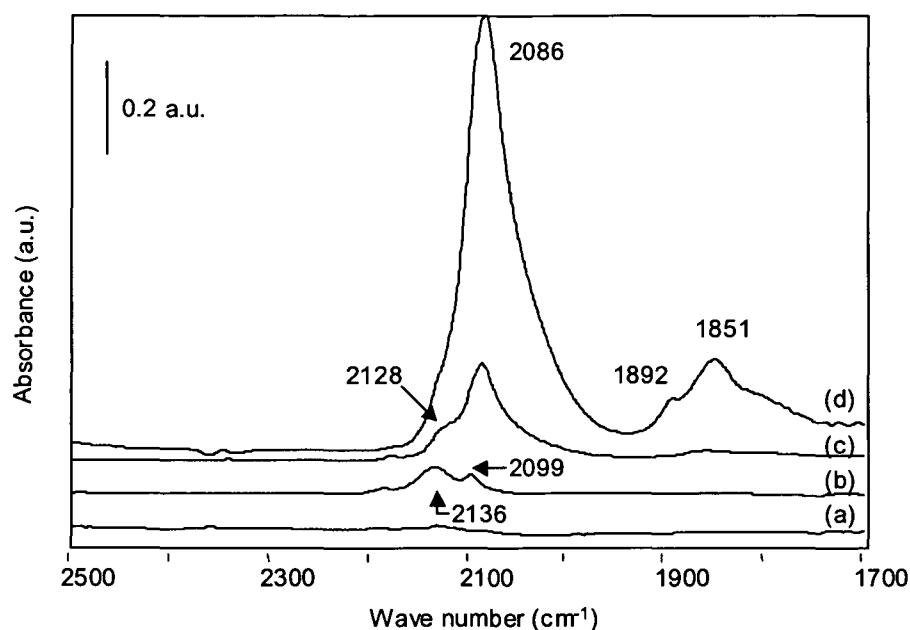


Figure 3.11: IR spectra of CO adsorption (5 mbar, 20°C) on differently prepared Pt/SZ After different activation procedures: (a) impregnated before calcination – activation in air, (b) impregnated after calcination - activation in air, (c) impregnated before calcination - activation in air and reduction at 200°C and (d) impregnated after calcination - activation in air and reduction at 200°C

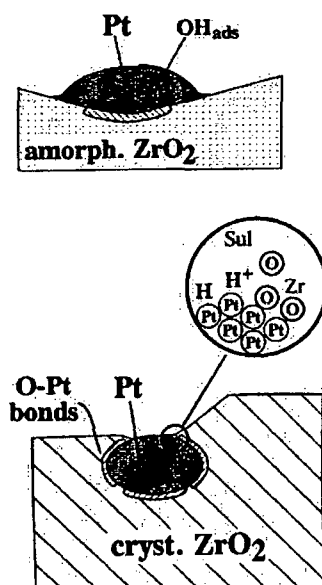


Figure 3.12: Encapsulation of Pt: proposed structure of Pt/SZ before (upper picture) and after (lower picture) calcination (taken from [31])

3. Characterization of the commercial Mel catalysts

Adsorption of n-heptane

In Figure 3.13 IR difference spectra of n-heptane adsorbed on Mel 1 at 40°C and 0.5 mbar are shown. The bands between 3000 and 2700 cm^{-1} are assigned to CH stretching vibrations, the band at around 1464 cm^{-1} comes from a CH deformation vibration.

Adsorption of n-heptane at 40°C leads to a shift of the bands of OH groups and sulfates to lower wave numbers, which means that both are affected by heptane adsorption. However, at reaction temperature (200°C) neither the OH groups nor the sulfates seem to be involved as adsorption sites for n-heptane. The shift of the band of the acidic hydroxyl groups due to the interaction with heptane amounts to 80 cm^{-1} , whereas on the zeolite HBEA the band is shifted for about 110 cm^{-1} . This indicates a weaker interaction of the surface hydroxyls of SZ with the adsorbed reactant molecules.

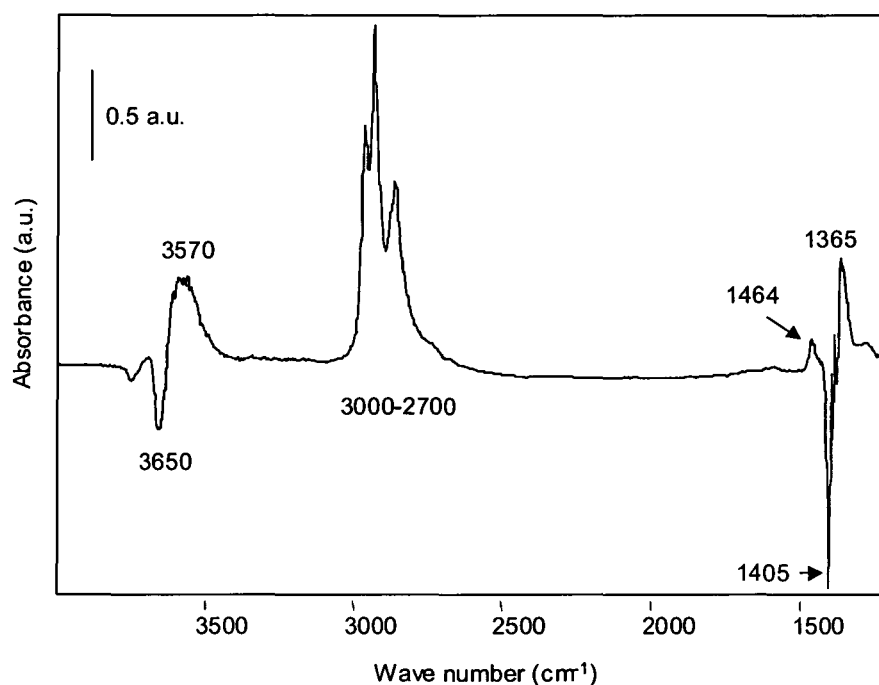


Figure 3.13: Difference spectrum of n-heptane adsorbed on Mel 1 at 40°C and 0.5 mbar

3.2.3 Diffusion measurements

Investigation of the diffusion behaviour was carried out by time resolved FTIR spectroscopy. The transport properties and as a consequence the residence time of the reactants and products on the catalyst surface can affect the selectivity, especially if there are possible consecutive reactions.

There are different approaches in order to keep the residence time of the reactants and products low and thus to improve the isomerization selectivity: an enhancement of the diffusion properties or the addition of hydride transfer agents for a fast desorption of products should lead to a significant reduction of consecutive cracking reactions. For zeolites it was reported that the fast diffusion of the branched products out of the pores is an important parameter in controlling the final catalyst selectivity [32].

When one compares data for diffusion coefficients reported in literature, differences in the order of magnitudes can be found. Therefore it seems reasonable to compare only relative diffusivities of samples measured under the same conditions.

Figure 3.14 shows the adsorption and desorption behaviour of Mel 1 and HBEA catalysts for n-heptane, and Figure 3.15 compares the fractional uptake and loss for n-hexane and n-heptane over both catalysts.

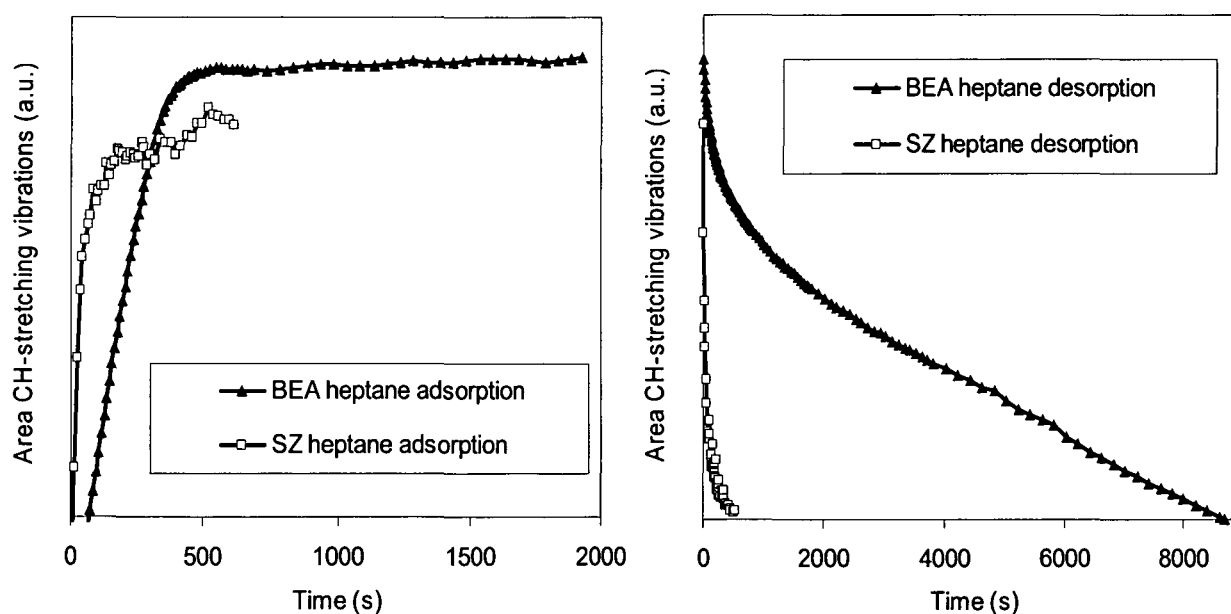


Figure 3.14: Adsorption and desorption of 0.005 mbar n-heptane at 40°C on Mel 1 and HBEA

3. Characterization of the commercial Mel catalysts

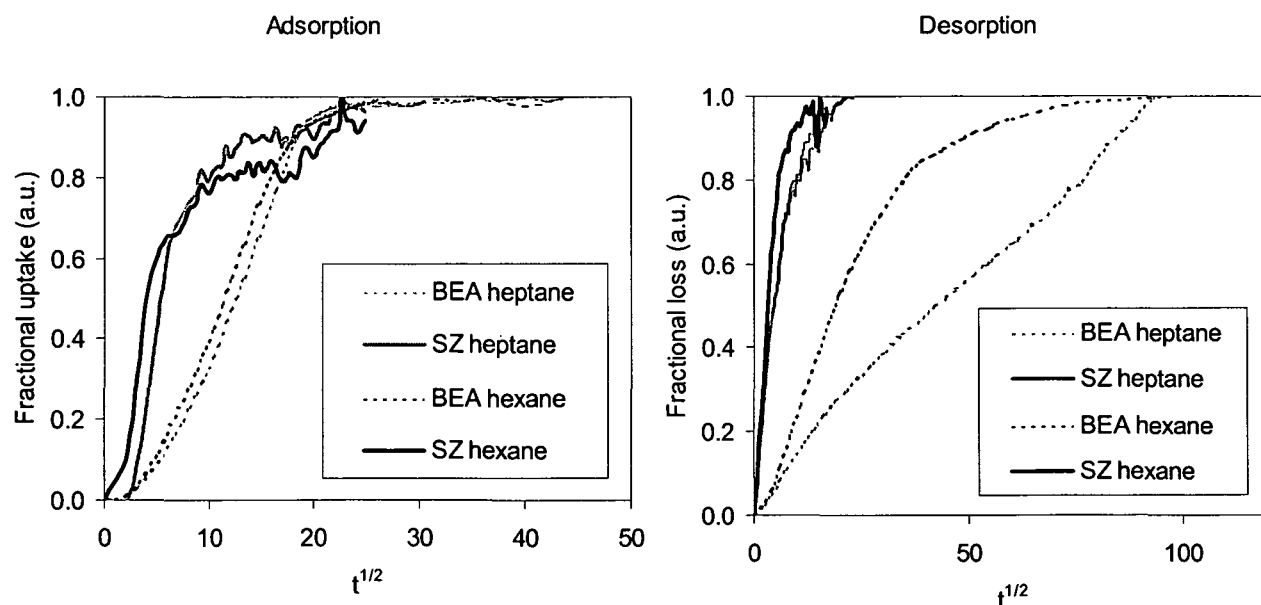


Figure 3.15: Adsorption and desorption of n-hexane and n-heptane on Mel 1 and HBEA (40°C, 0.005 mbar)

It can be seen that adsorption and desorption processes are much faster on SZ, which results in a lower residence time. Possible reasons are: (i) HBEA is a microporous material (pore diameter: 5.6 x 5.6 and 6.6 x 6.7 Å), whereas Mel 1 is a mesoporous material with an average pore diameter of 4-7 nm, therefore a slower diffusion is expected in the smaller pore system of the zeolite; (ii) the reactants are adsorbed more weakly in the case of SZ, which was also observed by DSC measurements (see next section 3.2.4).

3.2.4 Calorimetric studies

The adsorption of n-heptane on SZ was investigated in a combined TG/DSC apparatus. After activation of the sample, the n-heptane was added in small doses in a helium stream. From the observed mass change and the heat released during adsorption the differential heat of adsorption was determined at room temperature. Again the values obtained over SZ were compared to HBEA. In Table 3.5 the results are summarized. HBEA shows a higher differential heat of adsorption.

3. Characterization of the commercial Mel catalysts

Table 3.5: Heat of adsorption of n-heptane on Pt/Mel 2 and Pt/HBEA

Heat of adsorption (kJ/mol)	
Pt/Mel 2	88 +/- 8
Pt/HBEA	102 +/- 6

3.3 Conclusions and summary

Characterization of sulfated zirconia catalysts revealed medium acid strength of the acid sites. IR spectroscopy after adsorption of basic probe molecules, calorimetric studies and NH₃ TPD showed that zeolite HBEA possesses stronger acid sites than SZ. In literature controversial results were reported about acidity, but more and more researchers came to the conclusion that the acidity of SZ is weaker than zeolites [14,33].

The question remains why SZ shows such a high activity at low temperatures.

Clearfield et al. [34] suggested an explanation for the absence of strong BS on SZ. They argued that the acid strength of Brønsted acid sites depends on the presence of adjacent LS, which attract electrons and thus increase the polarity of the O-H bond. Considering this, the acid strength of a BS will be higher when the surrounding LS are empty. However, many methods for determination of the acid strength use basic probe molecules and probe the BS while LS are covered. Thus it is questionable if the results of such measurements are relevant for a catalyst operating under conditions when most sites will be empty (higher temperatures). Active sites on catalyst surfaces should therefore be studied under conditions as close as possible to the conditions during the catalytic reaction.

Characterization of the metal sites showed that Pt cannot be fully reduced and remains partly in an oxidized state, when the metal component is impregnated before calcination, which is the more active catalyst. Nevertheless the Pt is able to activate hydrogen, which was observed by hydrogen addition after adsorption of pyridine.

Investigation of the transport properties indicated a short residence time and a weaker adsorption of the reactants on SZ in comparison to HBEA.

References

-
- [1] X. Song, A. Sayari, *Catal. Rev. Sci. Eng.* 38 (1996) 329.
- [2] M. Hino, S. Kobayashi, K. Arata, *J. Am. Chem. Soc.* 101 (1979) 6439.
- [3] B.H. Davis, R.A. Keogh, R. Srinivasan, *Catal. Today* 20 (1994) 219.
- [4] N. Katada, J. Endo, K. Notsu, N. Yasunobu, N. Naito, M. Niwa, *J. Phys. Chem. B* 104 (2000) 10321.
- [5] D. Tichit, B. Coq, H. Armendariz, F. Figuéras, *Catal. Lett.* 38 (1996) 109.
- [6] V. Bolis, G. Magnacca, G. Cerrato, C. Morterra, *Topics in Catalysis* 19 (2002) 259.
- [7] J. Sommer, R. Jost, M. Hacoymy, *Catal. Today* 38 (1997) 319.
- [8] C. Morterra, G. Cerrato, M. Signoretto, *Catal. Lett.* 41 (1996) 101.
- [9] C. Morterra, G. Cerrato, G. Meligrana, M. Signoretto, F. Pinna, G. Strukul, *Catal. Lett.* 73 (2001) 113.
- [10] D.D. Yadav, J.J. Nair, *Micro. Mesoporous Mater.* 33 (1999) 1.
- [11] A. Clearfield, G.P.D. Serrette, A.H. Khazi-Syed, *Catal. Today* 20 (1994) 295.
- [12] F.R. Chen, G. Coudurier, J.F. Joly, J.C. Vedrine, *J. Catal.* 143 (1993) 616.
- [13] H. Armendariz, C. Sanchez Sierra, F. Figueras, B. Coq, C. Mirodatos, F. Levebre, D. Tichit, *J. Catal.* 171 (1997) 85.
- [14] L.M. Kustov, V.B. Kazansky, F. Figueras, D. Tichit, *J. Catal.* 150 (1994) 143.
- [15] F. Babou, G. Coudurier, J. Vedrine, *J. Catal.* 152 (1995) 341.
- [16] J.A. Moreno, G. Poncelet, *J. Catal.* 203 (2001) 453.
- [17] C. Morterra, G. Cerrato, F. Pinna, M. Signoretto, *J. Phys. Chem.* 98 (1994) 12373.
- [18] C. Morterra, G. Cerrato, G. Meligrana, M. Signoretto, F. Pinna, G. Strukul, *Catal. Lett.* 73 (2001) 113.
- [19] P.A. Jacobs, *Catal. Rev. Sci. Eng.* 24 (3) (1982) 415.
- [20] M.L. Hair, "Infrared spectroscopy in Surface Chemistry", p. 132, Marcel Dekker, N. Y. 1967.
- [21] T. Lopez, J. Navarrete, R. Gomez, O. Novaro, F. Figueras, H. Armendariz, *Appl. Catal. A* 125 (1995) 217.
- [22] K. Ebitani, J. Tsuji, H. Hattori, H. Kita, *J. Catal.* 135 (1992) 609.
- [23] S. Benfer, E. Knözinger, *J. Mater. Chem.* 9 (1999) 1203.
- [24] E. García, M.A. Volpe, M.L. Ferreira, E. Rueda, *J. Molec. Catal. A* 201 (2003) 263.
- [25] A.G. Pelemenschikov, R.A. van Santen, J. Jänchen, E. Meijer, *J. Phys. Chem.* 97 (1993) 11071.
- [26] B. Wichterlová, Z. Tvaruzková, Z. Sobalik, P. Sarv, *Micro Mesoporous Mater.* 24 (1998) 223.
- [27] X. Song, A. Sayari, *Catal. Rev.-Sci. Eng.* 38 (1996) 329.
- [28] C. Morterra, G. Cerrato, S. Di Ciero, M. Signoretto, F. Pinna, G. Strukul, *J. Catal.* 165 (1997) 172.
- [29] A.V. Ivanov, A.Yu. Stakheev, L.M. Kustov, *Stud. Surf. Sci. & Catal.* 130 (200) 263.
- [30] Z. Paál, U. Wild, M. Muhler, J.M. Manoli, C. Potvin, T. Buchholz, S. Sprenger, G. Resofszki, *Appl. Catal. A* 188 (1999) 257.
- [31] J.M. Manoli, C. Potvin, M. Muhler, U. Wild, Z. G. Resofszki, T. Buchholz, Z. Paál, *J. Catal.* 178 (1998) 338.
- [32] G. Kinger, D. Majda, H. Vinek, *Appl. Cat. A* 225 (2002) 301.
- [33] V. Adeeva, J.W. de Haan, J. Jänchen, G.D. Lei, G. Schünemann, L.J.M. van de Ven, W.M.H. Sachtler, R.A. van Santen, *J. Catal.* 151 (1995) 364.

4 N-ALKANE HYDROISOMERIZATION OVER COMMERCIAL Pt/MEL CATALYSTS

4.1 Introduction

Saturated hydrocarbons as the main components of raw oil are one of the most important sources of fuels. Since *n*-alkanes possess a low octane number isomerization to branched alkanes is necessary. In order to overcome the poor reactivity of alkanes, noble metal containing acid catalysts and/or liquid and solid strong acid catalysts are used for isomerization. Among the solid catalysts sulfated zirconia (SZ) has reached a lot of interest due to its high activity for the isomerization of light alkanes at low temperatures [1].

The deactivation of sulfated zirconia makes it unattractive for industry. The addition of Pt and the presence of hydrogen prevent deactivation. The stability of the Pt/SZ catalysts is dramatically enhanced. But the role of Pt is still controversial.

The mechanism of *n*-alkane hydroisomerization over Pt/SZ is not yet clear. According to the classical mechanism for alkane conversion over bifunctional catalysts proposed by Weisz and Swegler [2] the *n*-alkanes are dehydrogenated on the metallic sites in the first step. The formed alkenes diffuse to the acidic sites where they can be isomerized or cracked. The products finally desorb as alkenes and are hydrogenated on the metallic sites. From this point of view the distance between metal and acid sites should be as small as possible. Other authors [3] proposed a model, where hydrogen can spill over to the oxidic surface and migrate there after dissociation on the metal sites. This mobile spillover hydrogen can hydrogenate/dehydrogenate the hydrocarbons on the acid sites. Thus, the mobile species are either alkenes or spillover hydrogen. Unfortunately there is no direct spectroscopic evidence so far for spillover hydrogen. Detection of alkenes is also difficult because of the low concentration and their high reactivity.

However, it has been questioned if Pt is directly involved in the isomerization process and Pt/SZ behaves like a conventional bifunctional catalyst. Several authors reported that Pt/SZ does not exhibit common metallic properties. Iglesia et al. [4] found suppressed H₂ chemisorption over Pt/SZ. Wu et al. [5] reported that Pt on SZ exhibits a much lower benzene hydrogenation activity than Pt supported on ZrO₂ and on zeolite HBEA. They suggested that sulfur moieties poison the Pt on the SZ surface and therefore Pt/SZ may not operate as a bifunctional catalyst.

4. n-Alkane hydroisomerization over commercial Pt/Mel catalysts

In the last part of this section the activity of Pt/SZ catalysts is compared to Pt/HBEA. Both materials – zeolites and sulfated zirconia – are commercially used for n-alkane isomerization. Among the zeolites HBEA turned out to be a promising material due to its high activity and excellent isomerization selectivity. It is not yet clear why HBEA shows such a good selectivity. HBEA possesses a 3-dimensional pore system with pore diameters of 5.6 x 5.6 and 6.6 x 6.7 Å and an acid strength similar to other zeolites, such as HZSM-5.

4.2 Results and discussion

4.2.1 Activity and selectivity of bifunctional Pt/Mel

For the determination of kinetic parameters measurements with a conversion below 10% were used to make sure that the plug-flow reactor is operated in the differential mode. Since the activity and selectivity change at the beginning of the reaction (see section below), values were taken from the stable range, not the initial values.

Time dependent behaviour

In the presence of Pt and hydrogen a stable operation after an induction period was observed. At the beginning of the reaction of n-heptane at 200°C the conversion increases from 33 to 58% and the selectivity to isomerization decreases from 55 to 4%. After this induction period conversion and selectivity remain constant over days. The duration of the induction period depends on some parameters such as the temperature and pressure. With increasing reaction temperature the induction period gets shorter. Figure 4.1 shows the time on stream behaviour of Pt/Mel 2 for n-heptane isomerization at 200°C and 1 bar. For n-hexane the change in conversion is similar, whereas the selectivity changes only slightly and remains very high over the total investigated time range.

It is not yet clarified what happens during the induction period. It is discussed that either the active sites have to be built up or reactive intermediates are formed. Falco et al. [6] assumed that the acidity of Pt/SZ is generated under reaction conditions by the simultaneous presence of Pt, hydrogen and SZ. An induction period of several hours was reported [7] for the reaction of n-butane over unpromoted SZ at low temperatures. After reaching the maximum activity a gradual deactivation was observed. Sayari et al. [8] suggested that carbenium-type intermediates formed by protonation of butenes accumulate on the surface in the induction period.

4. *n*-Alkane hydroisomerization over commercial Pt/Mel catalysts

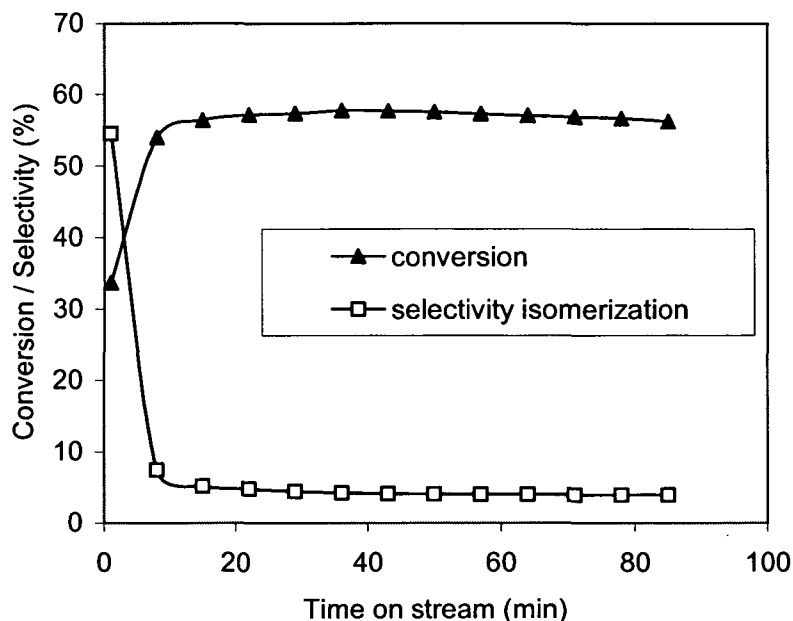


Figure 4.1: Reaction of *n*-heptane on Pt/Mel 2 (2.5% Pt) at 200°C and 1 bar in hydrogen flow (40 ml/min): conversion and isomerization selectivity vs. time on stream

Influence of the reactant: selectivity and product distribution

n-Heptane and *n*-hexane were used as reactants. With hexane higher reaction temperatures were necessary, but the isomerization selectivity was excellent (above 90 %). Mainly monomethyl-isomers were formed during the reaction.

When *n*-heptane was used as reactant, lower reaction temperatures of around 50°C less were sufficient to reach the same conversion than with hexane. But the isomerization selectivity was very low, mainly cracking to propane and iso-butane took place. Among the C₇ isomers monomethyl-isomers were the predominant reaction products. Propane and iso-butane were produced in nearly equimolar amounts. The product distribution indicates acidic cracking. If hydrogenolysis at the metal sites occurred, then mainly *n*-butane would be formed. However, hydrogenolysis products (methane, ethane, linear alkanes) were not observed, the main cracking products were propane and iso-butane. No unsaturated or cyclic compounds were detected under the applied reaction conditions.

4. *n*-Alkane hydroisomerization over commercial Pt/Mel catalysts

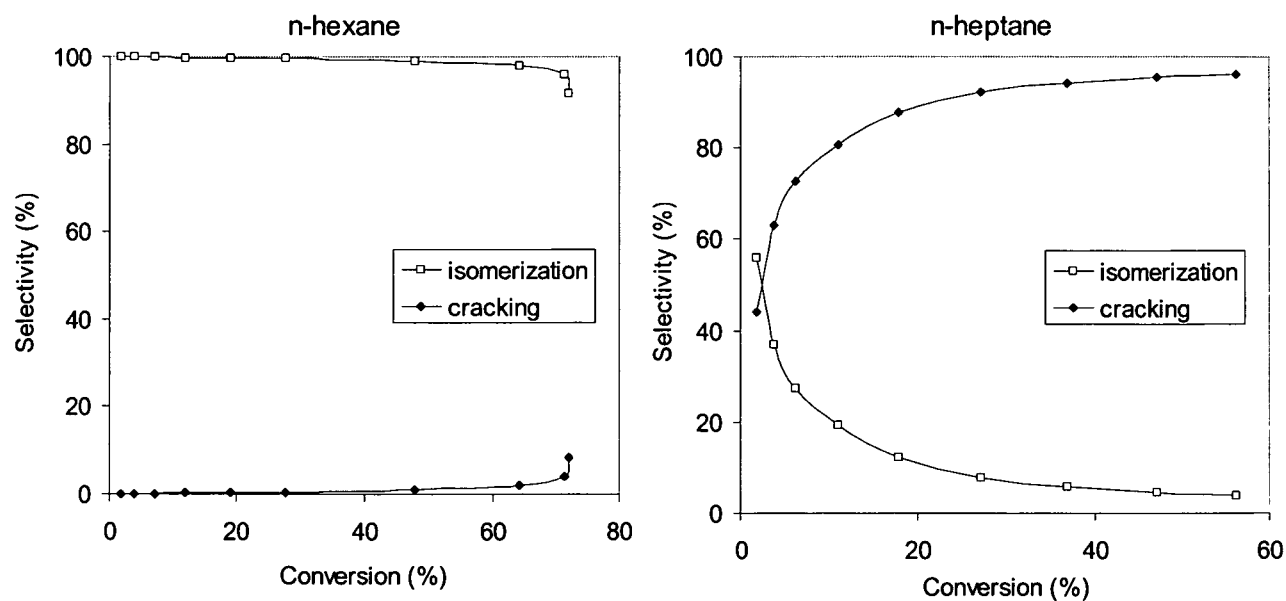


Figure 4.2: Selectivity to isomerization and cracking versus conversion obtained over Pt/Mel 2 (2.5% Pt) at different temperatures in hydrogen

Table 4.1: Activity and product selectivities (in %) for *n*-hexane isomerization over Pt/Mel 2 (2.5% Pt) at different temperatures in hydrogen

Temperature (°C)	Conversion (%)	Rate ($\mu\text{mol}/(\text{g}\cdot\text{s})$)	ΣiC_6	Mono- branched	Multi- branched	$\text{C}_1 + \text{C}_2$	C_3	iC_4	nC_4	C_5	Σcrack	Mo/ Mu
280	72.1	80.7	91.7	86.6	5.1	0.4	6.5	0.4	0.5	0.5	8.3	17
260	71.4	80.0	96.1	90.4	5.7	0.2	2.7	0.2	0.3	0.4	3.9	16
240	64.2	71.9	98.1	93.5	4.6	0.2	1.2	0.1	0.2	0.2	1.9	20
220	48.0	53.7	99.1	96.3	2.8	0.1	0.5	0.1	0.1	0.1	0.9	35
200	27.6	31.0	99.7	98.0	1.7	0	0.3	0	0	0	0.3	58
190	18.9	21.2	99.7	98.3	1.4	0	0.3	0	0	0	0.3	70
180	11.9	13.3	99.7	98.4	1.3	0	0.3	0	0	0	0.3	78
170	7.1	7.9	100	98.8	1.2	0	0	0	0	0	0	82
160	3.8	4.2	100	99.0	1.0	0	0	0	0	0	0	100
150	1.9	2.1	100	99.3	0.7	0	0	0	0	0	0	147

Mo/Mu: ratio of mono- to multibranched isomers

4. *n*-Alkane hydroisomerization over commercial Pt/Mel catalysts

Table 4.2: Activity and product selectivities (in %) for *n*-heptane isomerization over Pt/Mel 2 (2.5% Pt) at different temperatures in hydrogen

Temperature (°C)	Conversion (%)	Rate ($\mu\text{mol}/(\text{g}\cdot\text{s})$)	ΣiC_7	Mono- branched	Multi- branched	C ₃	iC ₄	nC ₄	Σcrack	Mo/ Mu
200	56.3	16.0	3.9	2.6	1.4	46.4	48.4	1.2	96.1	1.9
190	47.1	13.4	4.5	2.9	1.6	46.2	48.4	0.8	95.5	1.8
180	36.8	10.5	5.7	3.7	2.0	45.7	47.8	0.7	94.3	1.9
170	27.2	7.7	7.8	5.1	2.7	44.8	47.2	0.1	92.2	1.9
160	17.9	5.1	12.3	8.1	4.1	42.5	45.3	0	87.7	2.0
150	11.1	3.2	19.3	12.8	6.4	39.0	41.8	0	80.7	2.0
140	6.3	1.8	27.2	19.1	8.1	35.4	37.3	0	72.8	2.4
130	3.8	1.1	37.1	25.4	11.7	30.9	32.1	0	62.9	2.2
120	1.9	0.5	55.9	38.2	17.7	21.3	22.9	0	44.1	2.2

Mo/Mu: ratio of mono- to multibranched isomers

Hydroisomerization of *n*-alkanes with more than 6 carbon atoms is difficult due to their pronounced tendency to cracking, which was already recognized by Weitkamp et al. [9] in the early eighties. Whereas a highly selective isomerization reaction is possible for C₅ and C₆ alkanes, extensive cracking takes place using heptane as feed. This can be explained by considering the stability of the involved carbenium ions (see section 1.2.2). Cracking proceeds via formation of a carbenium ion as intermediate, which undergoes a β -scission. The heat of formation of carbenium ions decreases with the degree of branching on the positively charged carbon atom. Thus, the cracking reaction proceeds much faster if secondary and tertiary carbenium ions are involved.

Influence of the temperature

The change of activity and selectivity with temperature is shown in Figure 4.3. With increasing reaction temperature the conversion increases. However, at higher conversion the isomerization selectivity decreases, strongly with *n*-heptane as reactant and only slightly in the case of *n*-hexane.

4. *n*-Alkane hydroisomerization over commercial Pt/Mel catalysts

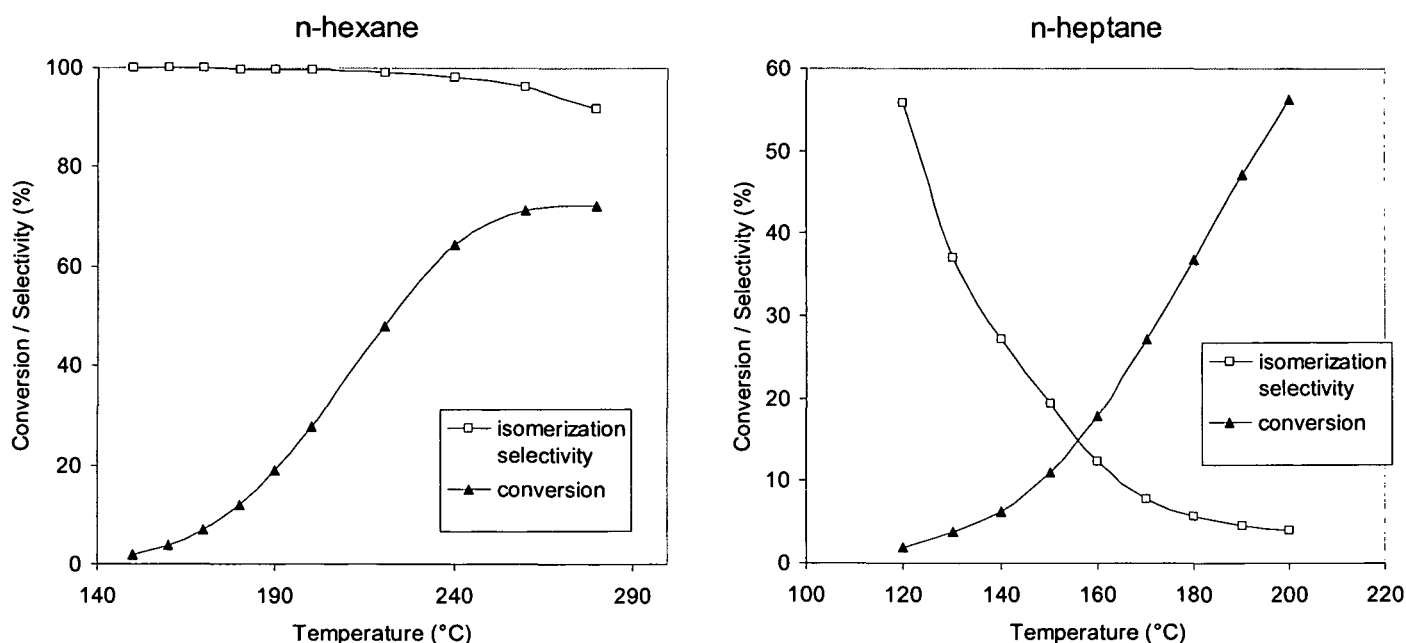


Figure 4.3: Dependence of activity and isomerization selectivity on the temperature for *n*-hexane and *n*-heptane isomerization over Pt/Mel 2 in hydrogen

From the temperature dependence of the rate the apparent activation energy E_a can be determined according to the equation of Arrhenius:

$$k = A \cdot e^{-\frac{E_a}{RT}}$$

In this equation k is the rate constant, A the pre-exponential factor, R is the gas constant and T the temperature (in K). The apparent activation energy values can be determined by plotting $\ln(r)$ versus $1/T$. The apparent activation energy is usually lower than the true activation energy because the former value includes the heat of adsorption.

$$E_{a,true} = E_{a,app} + \Delta H_{ads}$$

At higher temperatures the influence of the diffusion on the reaction increases. A change of the apparent activation energy can indicate diffusion limitation, which can be observed by a change of the slope in the plot of $\ln(k)$ versus $1/T$. A deviation from the linear curve indicates a transition from the region of kinetic control to the diffusion-controlled region. Above around 25–30% conversion, which corresponds to a reaction temperature of 200°C for *n*-hexane and 175°C for *n*-heptane under the present reaction conditions, an influence of the diffusion can be observed. The limitation is less pronounced for cracking than for the isomerization reaction. Characterization of the transport properties (see chapter 3.2.3) showed that the diffusion

4. *n*-Alkane hydroisomerization over commercial Pt/Mel catalysts

limitation on Pt/SZ should be attributed rather to a very fast reaction and high turn over frequency at the acid sites with limited supply of reactants than to geometric diffusion effects due to the pore system.

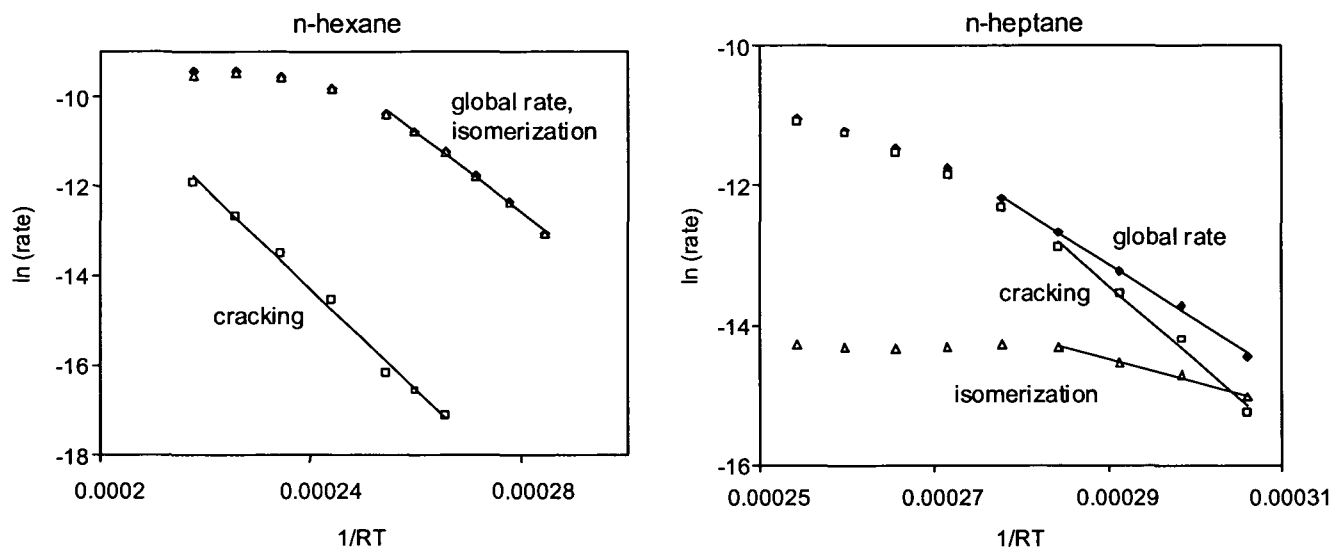


Figure 4.4: Determination of apparent activation energy values obtained over Pt/Mel 2 (2.5% Pt)

The global apparent activation energies and the apparent activation energy values for isomerization and cracking are summarized in Table 4.3.

Table 4.3: Global apparent activation energies E_a and the apparent activation energy values for isomerization and cracking obtained over Pt/Mel 2 (2.5% Pt)

Reactant	Global E_a (kJ/mol)	E_a isomerization (kJ/mol)	E_a cracking (kJ/mol)
n-hexane	89	89	112
n-heptane	79	33	108

Influence of the hydrogen partial pressure

The following power rate law was used for the calculation of reaction orders:

$$r = k \cdot p_{H_2}^m \cdot p_{n-alkane}^n$$

4. *n*-Alkane hydroisomerization over commercial Pt/Mel catalysts

In this equation r is the reaction rate, k is the rate constant, p the partial pressure of the corresponding component and n and m are the reaction orders in hydrogen and the reacting hydrocarbon.

Different hydrogen partial pressures were obtained by dilution with helium keeping the total pressure and overall flow rate constant. From the observed changes in conversion and reaction rates the order in H_2 was determined. It was found to be negative with a value of -0.25 .

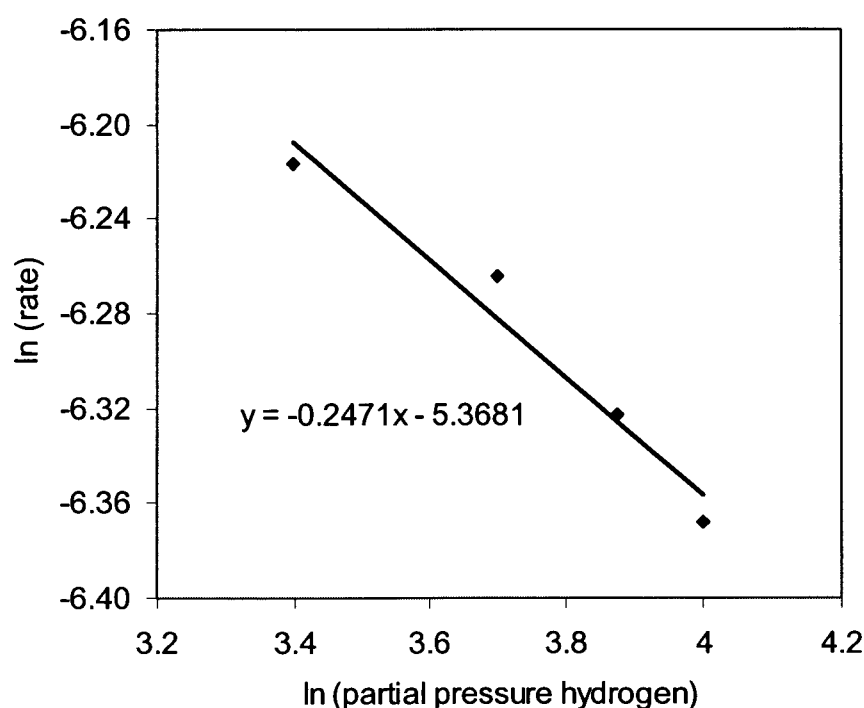


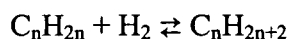
Figure 4.5: Determination of the order in hydrogen over Pt/Mel 2 (reaction conditions: 200°C, 40 ml/min total flow, 1 bar total pressure, 15 mbar *n*-heptane)

Controversial results were reported in literature concerning the reaction order in hydrogen. Positive H_2 orders were observed for *n*-heptane isomerization over Pt/SZ by Iglesia and coworkers [4] and for *n*-hexane isomerization by Comelli et al. [10]. This would suggest that the catalyst operates by a monofunctional acid mechanism with the Pt removing coke precursors and thus preventing deactivation. Iglesia et al. [4] proposed a reaction mechanism where the rate-determining step is the alkane desorption via hydride transfer, which would explain the positive order. Garin et al. [11] studied the effect of hydrogen in two pressure ranges for *n*-heptane conversion: low pressure (190-760 Torr) and high pressure (900-3000 Torr). They observed a negative hydrogen reaction order for low hydrogen pressures, but a positive effect on the reaction

4. n-Alkane hydroisomerization over commercial Pt/Mel catalysts

rate at higher H₂ pressures. Negative reaction orders in hydrogen were observed by Liu et al. [12]. Nascimento and coworkers [13] found an inhibiting effect of hydrogen for n-butane and practically no effect for n-hexane.

Over bifunctional catalysts molecular hydrogen can be regarded as inhibitor at high partial pressure by shifting the hydrogenation/dehydrogenation equilibrium from alkene to alkane and by competitive adsorption on active sites.



This equilibrium is regarded as the initial step of the reaction over bifunctional catalysts (see chapter 1.2). The equilibrium concentration of alkenes is very low and can be influenced by the temperature and the hydrogen pressure.

Influence of the n-alkane partial pressure

Variation of the n-alkane partial pressure was done with a syringe pump, where the amount of alkane injected into the gas stream per time unit can be adjusted. The n-alkane partial pressure was varied between 15 and 175 mbar. Figure 4.6 shows the influence on the rate of n-heptane and n-hexane conversion and product formation. The rate increases with n-alkane pressure. The orders in n-hexane and n-heptane are derived from the slope of ln (rate) vs. ln (p alkane). The reaction orders in n-hexane and in n-heptane were found to be 0.6 and 0.8, respectively.

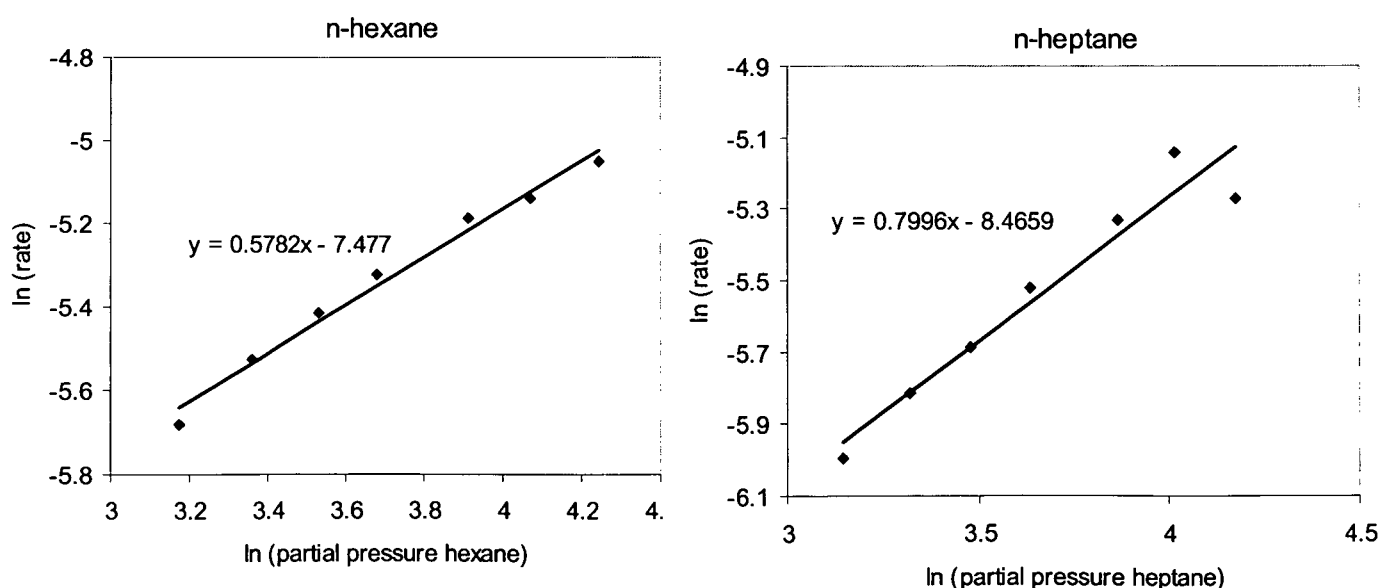


Figure 4.6: Determination of the order in hydrocarbon (Pt/Mel 2, reaction at 1 bar and 150°C for n-heptane and 170°C for n-hexane in hydrogen)

4. *n*-Alkane hydroisomerization over commercial Pt/Mel catalysts

For a mono- or intramolecular mechanism the reaction order in the hydrocarbon is expected to be between 0 and 1. If the reaction would proceed via a bi- or intermolecular mechanism, the order in alkane would be between 0 and 2, as it was found in the case of *n*-butane isomerization [12]. Generally the intra-molecular mechanism is accepted for hydrocarbons having more than 5 carbon atoms [4,14,15].

Influence of the pretreatment conditions

A variation of the calcination temperature between 550 and 700°C was carried out. The commercial $\text{Zr}(\text{OH})_4$ precursor material Mel 1 from MEL Chemicals was calcined at different temperatures after impregnation with 2.5 wt% Pt. In Figure 4.7 the activity for *n*-heptane conversion and the isomerization selectivity are displayed. Maximum activity was found for samples calcined at 600 and 650°C.

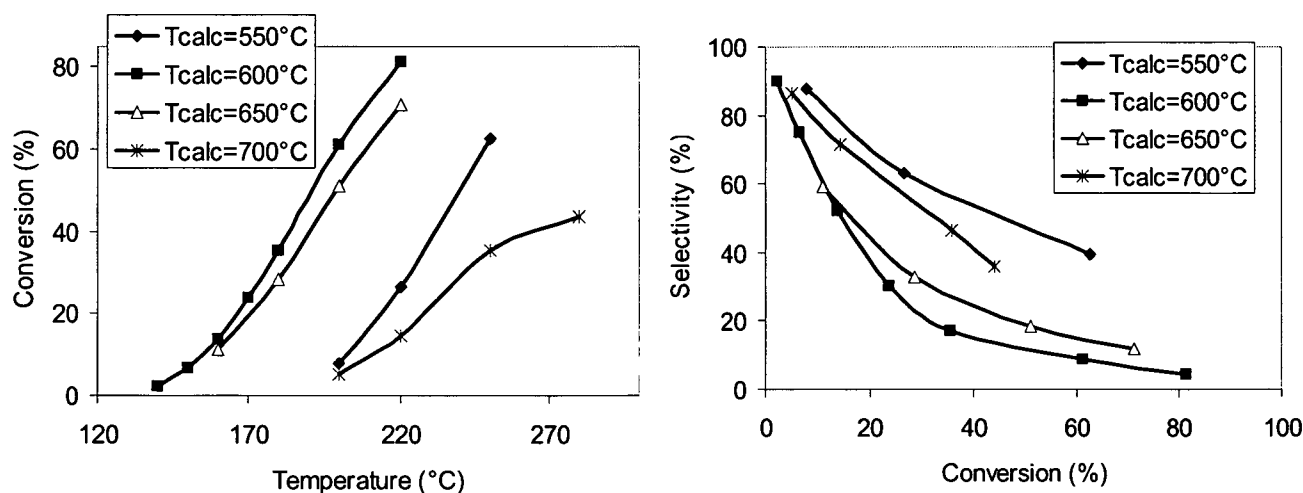


Figure 4.7: Activity and *n*-heptane isomerization selectivity over Pt/Mel 1 catalysts calcined at different temperatures (reaction conditions: 5 bar total pressure, 15 mbar *n*-heptane, 40 ml/min hydrogen flow)

In Figure 4.8 IR spectra after pyridine adsorption on samples calcined at different temperatures are shown. The band at 1543 cm^{-1} comes from pyridine adsorbed on BS and the band at 1445 cm^{-1} is assigned to pyridine coordinatively bonded to LS. The calcination temperature influences the concentration of LS and BS, as it can be seen in Figure 4.8 and Table 4.4. The specific surface area and the sulfate content are summarized in Table 4.4.

4. *n*-Alkane hydroisomerization over commercial Pt/Mel catalysts

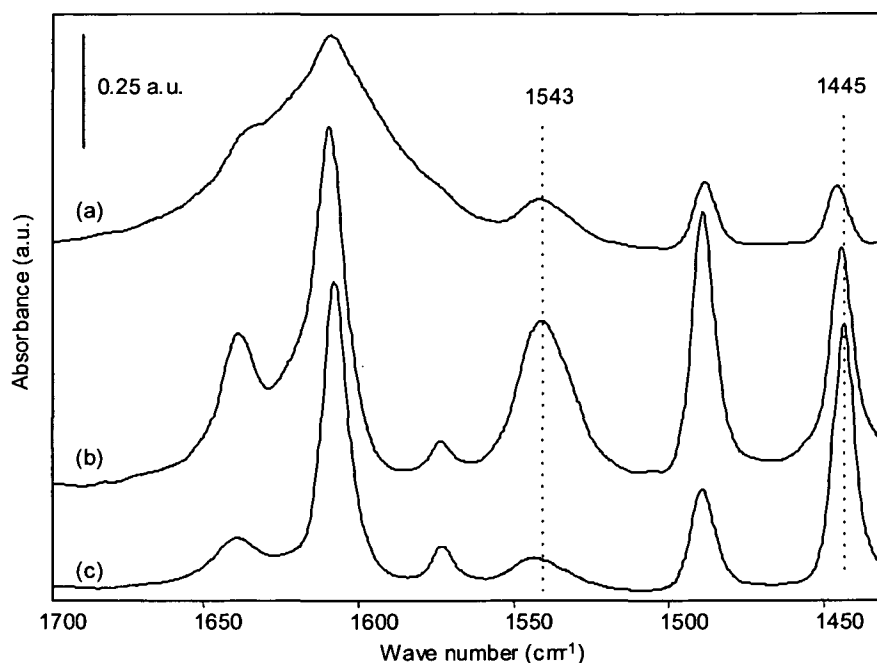


Figure 4.8: IR spectra after pyridine adsorption on Mel 1 catalysts calcined at different temperatures: (a) $T_{\text{calc}} = 550^{\circ}\text{C}$, (b) $T_{\text{calc}} = 600^{\circ}\text{C}$ and (c) $T_{\text{calc}} = 700^{\circ}\text{C}$ (activation in vacuum at 350°C , 0.05 mbar pyridine, removal of physisorbed species by evacuation at 120°C 1h)

Table 4.4: Ratio of Lewis to Brønsted acid sites, specific surface area and sulfate content of Pt/Mel 1 samples calcined at different temperatures

Calcination temperature ($^{\circ}\text{C}$)	Specific surface area (m^2/g)	wt % SO_4^{2-}	LS/BS
550	130	6.9	0.51
600	111	5.0	0.73
650	108	3.3	
700	79	2.1	2.06

The sample calcined at 700°C shows a significantly smaller activity, a lower amount of sulfate groups and predominantly Lewis acid sites.

Variation of the activation temperature prior to the kinetic measurement revealed maximum activity after activation at 500°C in synthetic air. The reason could be an optimum hydration/dehydration degree after this pretreatment and as a consequence an optimum LS/BS ratio.

4. *n*-Alkane hydroisomerization over commercial Pt/Mel catalysts

The metal component – Pt

The role of Pt is still largely unknown. Pt is very suitable as metal component. It exhibits an excellent activity for hydrogen activation, a noble character and a lower activity for unwanted hydrogenolysis reactions as for example Ni.

Two differently prepared catalysts were compared in this work. Impregnation with Pt was done before and after calcination, this means either on the hydroxide or on the already crystalline oxide. CO adsorption showed that in the case of impregnation before calcination Pt could not be fully reduced (see chapter 3.2.2.2). Paal et al. [16] suggested that the Pt is somehow encapsulated during the calcination process. However, this catalyst shows a significantly higher activity than the one impregnated with Pt after calcination, where Pt was fully in the metal state.

The influence of the distance metal – acid site was tested via comparison with a so-called hybriide catalyst, a mechanical mixture of pure sulfated zirconia and Pt supported on an inert carrier material such as SiO₂. Mechanical mixtures of Pt/SiO₂ and sulfated zirconia exhibit a lower conversion and a worse isomerization selectivity than Pt-promoted SZ (see Fig. 4.9) due to the larger distance between the acid and metallic functions. From this it can be concluded that a certain vicinity should exist between metal and acid sites.

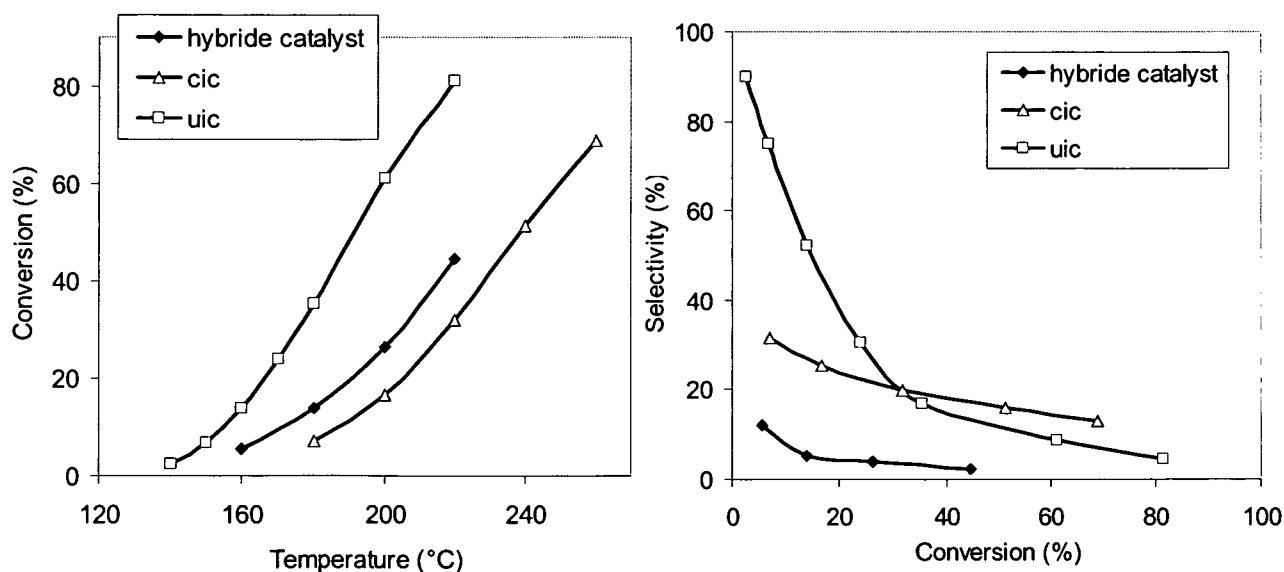


Figure 4.9: *n*-Heptane conversion and selectivity over Mel 1 impregnated with 2.5% Pt before and after calcination (cic = calcined – impregnated – calcined; uic = uncalcined – impregnated – calcined) and over a hybriide catalyst (a mechanical mixture of Mel 1 and Pt/SiO₂)

4. *n*-Alkane hydroisomerization over commercial Pt/Mel catalysts

It was also observed by Ebitani et al. [17] that Pt remains mostly in an oxidized state. Combined metal-acid sites, $(\text{Pt}_n\text{-H})^+$ adducts, were proposed by Sachtler et al. [18] as active sites. On these sites H_2 is dissociated on the metal and can be converted on adjacent acidic sites to protons and electrons or to hydride ions, the first can act as active sites for isomerization, whereas the hydrides can support the hydrogenation of the isomerized carbenium ions and hence the desorption of iso-alkanes. This model would explain why the close vicinity of metal and acid sites is essential.

After reduction at 200°C part of the Pt remains in an oxidized state. However, the reduction temperature is limited, because above approximately 260°C H_2S formation starts due to the reduction of sulfate groups in the presence of Pt (see Figure 4.10). Without Pt H_2S formation starts at about 560°C .

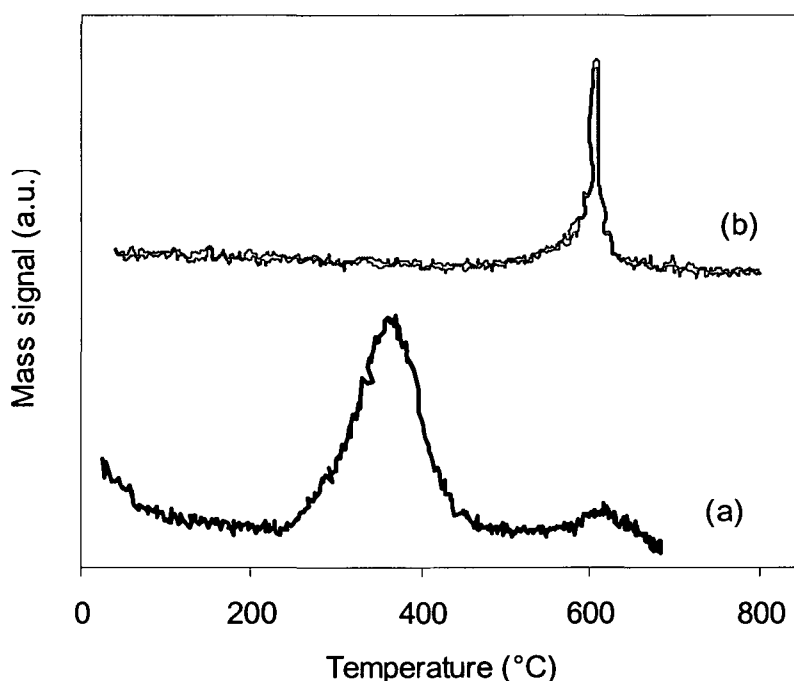


Figure 4.10: TPR (temperature programmed reduction): mass signal of H_2S (a) on Pt/Mel 2 (2.5% Pt) and (b) unpromoted Mel 2. Reduction in a flow of 10vol% H_2 in He, heating rate $10^\circ/\text{min}$

Additionally, the influence of the metal content was investigated (Fig. 4.11). With increasing metal loading the activity first increases and then decreases again. Higher metal loading leads to

4. *n*-Alkane hydroisomerization over commercial Pt/Mel catalysts

an improvement of the isomerization selectivity. Usually the Pt content is in the range of 0.1 to 0.5 wt%. Arata et al. [19] found the highest activity of SZ with 3 wt% Pt for the catalyst prepared by double calcination, while the highest activity was observed with 7.5 wt% Pt in the case of the single calcination.

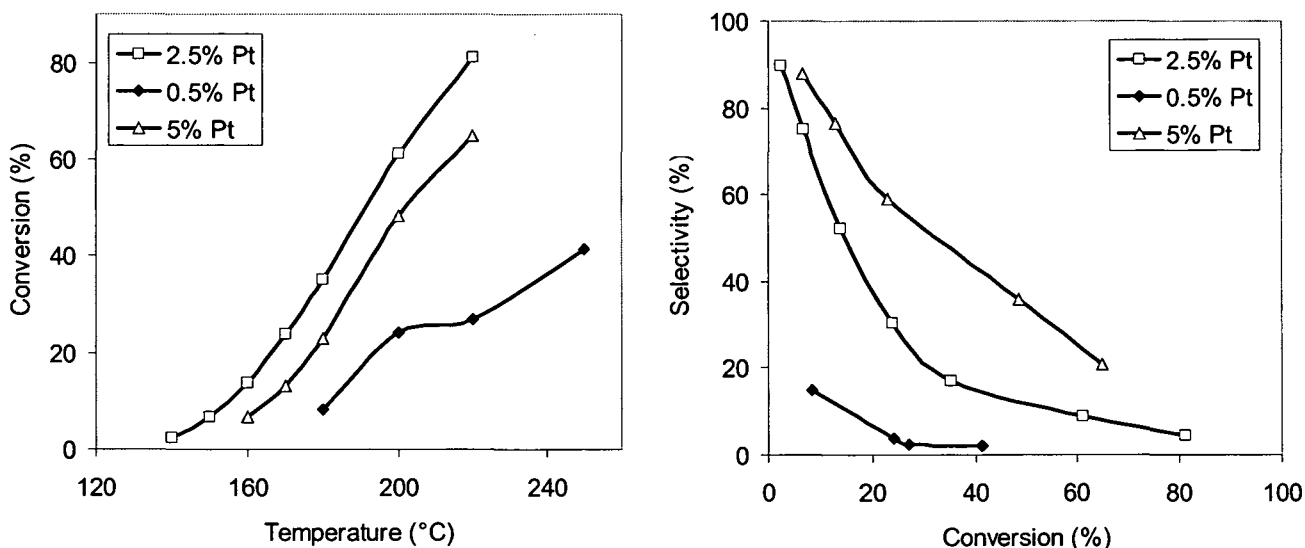


Figure 4.11: Influence of the metal loading on the *n*-heptane conversion and selectivity

Obviously, there is a pronounced influence of the metal function on the selectivity to isomerization. The catalyst which contains only 0.5% Pt as well as the hybriide catalyst show a significantly lower isomerization selectivity, even at low conversion. The reason could be that the supply with hydride ions necessary for the desorption of the isomerized hydrocarbons is reduced and thus they remain longer at the catalyst surface, which leads to an increased cracking probability.

4.2.2 Comparison of sulfated zirconia and zeolite HBEA

A commercial zeolite HBEA obtained from Degussa was used for the comparative measurements. The properties are summarized in Table 4.5.

Table 4.5: Properties of HBEA

Number of acid sites (mmol/g)	Si/Al ratio	Specific surface area (m ² /g)	Pore size
0.61	24	529	5.6 x 5.6 Å
			6.6 x 6.7 Å

4. *n*-Alkane hydroisomerization over commercial Pt/Mel catalysts

Comparison of the acidity

Characterization of the acidic properties of SZ and HBEA revealed weaker acid sites on SZ. This was observed by benzene adsorption, adsorption of CD₃CN and calorimetric determination of the heat of *n*-heptane adsorption (see chapter 3).

Comparison of the catalytic activity

Activity and isomerization selectivity of Pt/SZ and Pt/HBEA catalysts were compared under the same reaction conditions. In Figure 4.12 it can be seen that SZ exhibits a significantly higher activity. The same level of conversion could be reached at about 80°C lower reaction temperature. However, the zeolite showed an excellent isomerization selectivity for *n*-heptane up to 75% conversion, whereas over Pt/SZ cracking was the main reaction in this case.

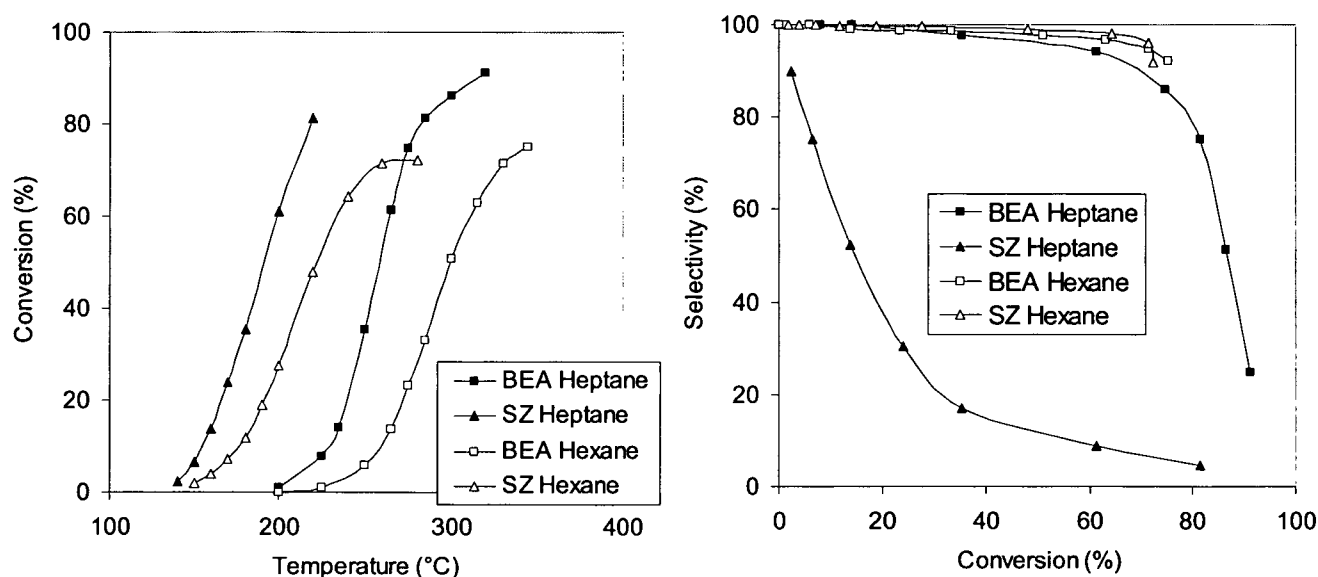


Figure 4.12: Conversion and selectivity of *n*-hexane and *n*-heptane isomerization over Pt/Mel 1 (2.5% Pt) and Pt/HBEA (0.8% Pt) in 40 ml/min hydrogen at 5 bar

Comparison of the transport properties

An investigation of the diffusion behaviour was carried out by time resolved FTIR spectroscopy. The results were presented in section 3.2.3 and are only shortly summarized here. The transport properties and as a consequence the residence time of the reactants and products on the catalyst surface can affect the selectivity, especially if there are possible consecutive reactions. Shorter residence time of the reactants on the catalytic surface is expected to yield mainly mono-branched isomers, whereas a longer residence time should lead mainly to the formation of multi-branched

4. *n*-Alkane hydroisomerization over commercial Pt/Mel catalysts

isomers and/or cracking products. Normally branched hydrocarbons crack more easily than linear isomers, because secondary and tertiary carbenium ions are involved, which are much more stable. Therefore, consecutive cracking reactions are faster in the case of branched hydrocarbons. Over SZ a much faster adsorption and desorption and a significantly shorter residence time was observed than in the pore system of the zeolite.

4.3 **Conclusions and summary**

The conventional bifunctional metal-acid mechanism is characterized by specific kinetic data: (i) apparent activation energies between 84 and 126 kJ/mol, (ii) hydrocarbon reaction orders near +1, and (iii) hydrogen reaction orders between -1 and 0 [20,21]. The kinetic studies presented in this chapter show clearly that the commercial Pt/SZ catalyst fulfils all these conditions.

An excellent selectivity to branched isomers was observed for *n*-hexane hydroisomerization over Pt/SZ. However, this catalyst is not appropriate for *n*-heptane isomerization, because mainly acidic cracking to propane and iso-butane occurred.

The zeolite HBEA shows a much better performance with a good selectivity to heptane isomerization up to 75% conversion, although the reaction temperature is shifted for about 80°C to higher values to reach the same conversion. Since the activation energy for cracking reactions is higher than for isomerization, cracking reactions are usually favoured at higher temperatures. Additionally, the stronger acid sites and the longer residence time of the reactants in the pore system of the zeolite would favour cracking of the reactants. Therefore a better selectivity was expected for the SZ catalyst than for the zeolite. However, the opposite behaviour was observed. So far we could not find an explanation for this result.

A close vicinity of the metal and acidic sites leads to a better performance of the catalyst. Mechanical mixtures of SZ and Pt supported on an inert carrier material as well as impregnation of the metal component on an already calcined oxide results in less active catalysts due to the larger distance between the sites. Ensembles containing metallic and acidic sites – so-called collapsed bifunctional sites $(Pt_n-H)^+$ – were proposed as active sites in literature [18] together with hydride ions necessary for the desorption of the products. Our results support this assumption.

References

-
- [1] X. Song, A. Sayari, *Catal. Rev. Sci. Eng.* 38 (1996) 329.
 - [2] P.B. Weisz, E.W. Swegler, *Science* 126 (1957) 31.
 - [3] A. Zhang, I. Nakamura, K. Aimoto, K. Fujimoto, *Ind. Eng. Chem. Res.* 34 (1995) 1074.
 - [4] E. Iglesia, S.L. Soled, G.H. Kramer, *J. Catal.* 144 (1993) 238.
 - [5] H. Wu, L. Leu, C. Naccache, K. Chao, *J. Mol. Cat. A* 127 (1997) 143.
 - [6] M.G. Falco, J.M. Grau, N.S. Figoli, *Appl. Catal. A* 264 (2004) 183.
 - [7] X. Li, K. Nagaoka, L.J. Simon, J.A. Lercher, *J. Catal.* 227 (2004) 130.
 - [8] A. Sayari, Y. Yang, X. Song, *J. Catal.* 167 (1997) 346.
 - [9] J. Weitkamp, *Ind. Eng. Chem. Prod. Res. Dev.* 21 (1982) 550.
 - [10] R.A. Comelli, Z.R. Finelli, S.R. Vaudagna, N.S. Figoli, *Cat. Lett.* 45 (1997) 227.
 - [11] Ü.B. Demirci, F. Garin, *J. Mol. Catal. A* 188 (2002) 233.
 - [12] H. Liu, V. Adeeva, G.D. Lei, W.M.H. Sachtler, *J. Mol. Catal.* 100 (1995) 35.
 - [13] M.T. Tran, N.S. Gnep, M. Guisnet, P. Nascimento, *Catal. Lett.* 47 (1997) 57.
 - [14] H. Liu, G.D. Lei, W.M.H. Sachtler, *Appl. Cat. A* 146 (1996) 165.
 - [15] A. Sassi, J. Sommer, *Appl. Cat. A* 188 (1999) 155.
 - [16] J.M. Manoli, C. Potvin, M. Muhler, U. Wild, Z.G. Resofszki, T. Buchholz, Z. Paál, *J. Catal.* 178 (1998) 338.
 - [17] K. Ebitani, H. Konno, T. Tanaka, H. Hattori, *J. Catal.* 135 (1992) 60.
 - [18] T.J. McCarthy, G.D. Lei, W.M.H. Sachtler, *J. Catal.* 159 (1996) 90.
 - [19] K. Arata, H. Matsushashi, M. Hino, H. Nakamura, *Catal. Today* 81 (2003) 17.
 - [20] J.H. Sinfelt, *Adv. Chem. Eng.* 5 (1964) 37.
 - [21] M. Belloum, C. Travers, J.P. Burnonville, *Rev. Inst. Fr. Pet.* 46 (1991) 89.

5 IN SITU IR INVESTIGATION OF n-HEXANE ISOMERIZATION OVER SULFATED ZIRCONIA AND Pt CONTAINING SULFATED ZIRCONIA – INFLUENCE OF THE CARRIER GAS

5.1 Introduction

Sulfated zirconia (SZ) has attracted a lot of interest due to its high activity for the isomerization of light alkanes at low temperatures. However, a very fast deactivation was found when hydrocarbons react on sulfated zirconia. The nature of this deactivation is still under discussion. Deactivation was attributed to (i) carbon accumulation [1,2], (ii) to surface reduction of Zr^{4+} to Zr^{3+} during the reaction of hydrocarbons, (iii) reduction of S^{6+} to lower oxidation states with possible removal of sulfur entities in case of reduction to volatile species such as H_2S , (iv) to sulfur migration into the bulk of the oxide or (v) to changes in the surface phase from tetragonal to monoclinic [3].

Isomerization of hydrocarbons over Pt/SZ operating under a partial pressure of hydrogen allows a more stable operation [4]. It was found that the simultaneous presence of hydrogen and Pt is essential to obtain a stable active catalyst [5]. Tanaka et al. [6] concluded from XANES studies that Pt on SZ is electron deficient after activation by hydrogen treatment, and their EXAFS studies indicate the presence of Pt-O and Pt-Pt pairs as in PtO_2 and Pt metal, respectively. According to Ebitani et al. [7] Pt on SZ remains mostly in an oxidized state, even after hydrogen reduction at 673 K. Ebitani [8] proposed that Brønsted acid sites were developed from dissociative adsorption of H_2 on Pt, spillover of the H atoms onto the SZ and then electron transfer from the H atoms to Lewis acid sites leaving protons on the surface. Sachtler et al. [9] proposed $[Pt_nH]^+$ adducts, „collapsed bifunctional sites”, which can act as active sites.

Until now a discussion exists about the nature of the active sites on Pt/SZ. Moreover, other factors than the strength of the acid sites are discussed to be the cause of the high activity. The optimum residence time of surface species was assumed to be an important factor in isomerization activity [2]. Liu et al. [10] proposed that an extremely active catalyst for an acid catalyzed reaction need not to be an extremely strong acid. Instead, the reaction can proceed via a less energy intensive bimolecular mechanism for small alkanes.

The aim of this chapter is to investigate the isomerization of *n*-hexane over Pt/SZ and SZ by in situ IR measurements and to determine which factors influence the deactivation.

5.2 *In situ* IR measurements

In situ characterization methods are of great importance in catalysis. IR spectroscopy under reaction conditions offers the possibility to study processes occurring at the surface during the reaction, to identify reaction intermediates and the sites participating in the reaction. This information can be correlated to the corresponding activity and selectivity. Thus, the big advantage of in situ IR spectroscopic measurements is the simultaneous investigation of the catalytic activity and the processes occurring at the surface and involving the surface sites.

The catalyst is pressed to a self-supporting wafer and placed inside a heatable IR cell, where transmission spectra are recorded during the reaction. The carrier gas saturated with the *n*-alkane passes by the sample and the hydrocarbons react on the catalytic surface. Finally the reaction products are analyzed by gas chromatography.

The IR reaction cell shows different characteristics than the plug flow reactor, approximating a continuously stirred tank reactor. The residence time is about ten times longer than the residence time of the reactants in the catalyst bed of the plug flow reactor, when the same total flow is applied. Additionally, the reactant flow passes by the catalyst, whereas in the plug flow reactor the reactants stream through the catalyst bed. This is illustrated in Figure 5.1 for the IR cell.

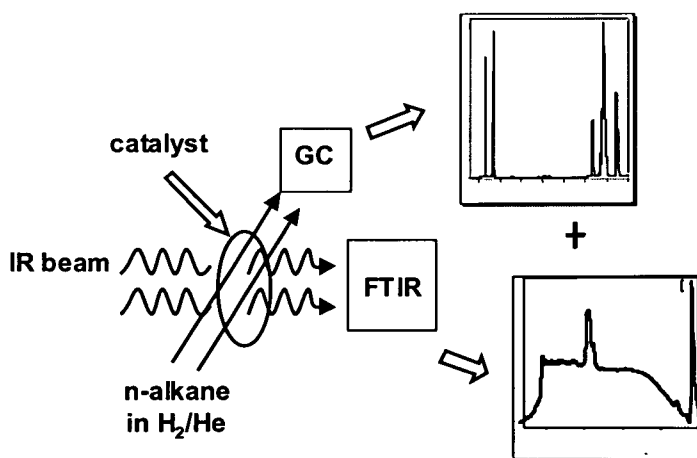


Figure 5.1: Scheme of the in situ IR measurements

Therefore, the achieved reaction rates cannot be directly compared to the ones obtained in the plug flow reactor. The conversion is limited, because a part of the reactants can by-pass the catalyst, and the selectivity to cracking is higher at comparable conversion levels due to the longer residence time. However, the observed trends are the same.

5.3 Results and discussion

5.3.1 In situ IR measurements of the *n*-hexane isomerization over Pt/SZ and SZ

In situ IR measurements of *n*-hexane conversion in hydrogen over Pt/SZ as a function of time on stream (TOS) are shown in Fig 5.2. In the range of 3000 to 2800 cm^{-1} bands of C-H stretching vibrations and at 1460 cm^{-1} a C-H deformation vibration band of *n*-hexane are observed. The band near 1615 cm^{-1} and 1390 cm^{-1} , assigned to adsorbed water and to S=O vibrations respectively, showed only subtle changes in comparison to the spectrum after activation. The intensity of both bands decreased slightly. Under these conditions the catalyst was stable and the conversion and selectivity were found to be nearly constant (Table 5.1). The selectivity to hexane isomers was higher than 90% with 83% monobranched and 10% dibranched compounds.

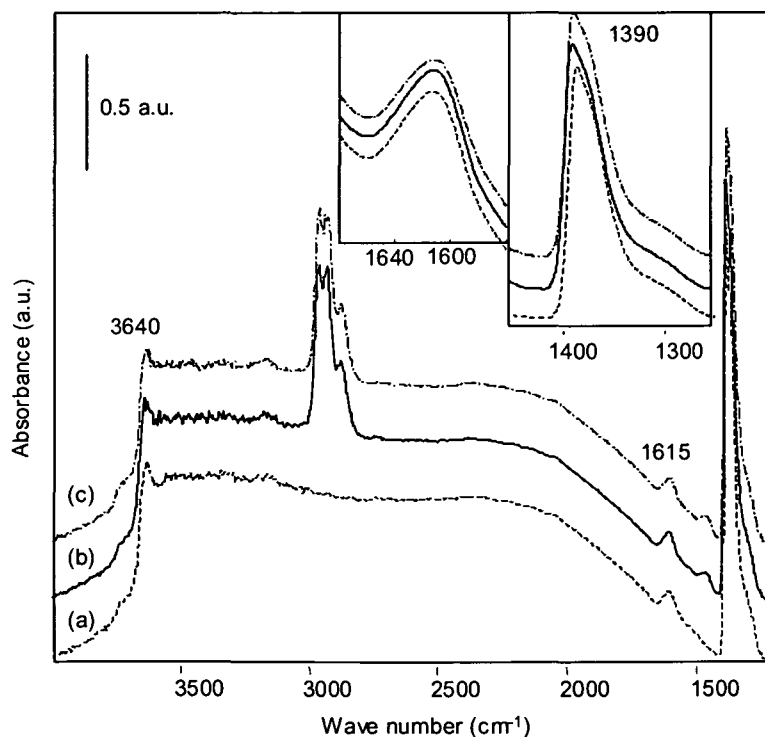


Figure 5.2: In situ IR spectra of *n*-hexane isomerization at 250°C in hydrogen over Pt/SZ: (a) after activation, (b) after 1 min and (c) 67 min time on stream

5. In situ IR investigation of *n*-hexane isomerization over SZ and Pt/SZ

Table 5.1: *n*-Hexane conversion at 250°C in hydrogen or He over Pt/Mel 1

Time on stream (min)	Conversion (%)	Selectivity i-C6 (%)	Selectivity monobranched isomers (%)	Selectivity dibranched isomers (%)
(A): Hydrogen over Pt/SZ				
1	9.7	91.3	80.9	10.4
7	8.5	92.5	82.0	10.5
31	8.5	93.9	83.7	10.2
61	8.6	94.2	84.3	9.9
103	8.6	93.2	83.8	9.4
(B): He over Pt/SZ				
1	6.8	76.3	66.6	9.7
7	0			

If isomerization is carried out in He instead of H₂ the IR spectrum is quite different. In Fig. 5.3 IR spectra of Pt/SZ after activation, 1 min and 63 min TOS in hexane are depicted. After the start of the reaction a huge band in the OH region developed, the band near 1615 cm⁻¹ increased and then decreased again whereas a small band near 1670 cm⁻¹ and a broad band between 1540 and 1580 cm⁻¹ were built up. The catalyst was only active at the very beginning of TOS (Table 5.1), afterwards no conversion was found.

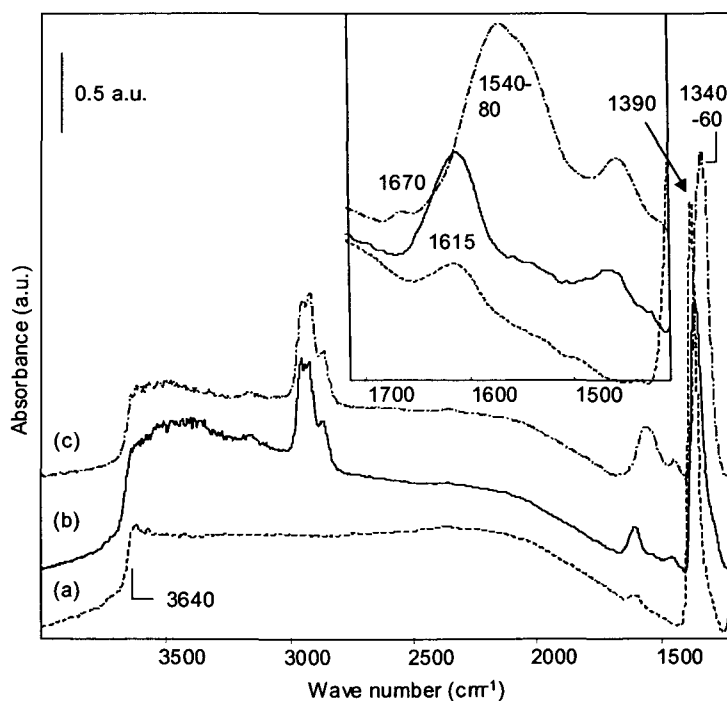


Figure 5.3: In situ IR spectra of *n*-hexane isomerization at 250°C in He over Pt/SZ: (a) after activation, (b) after 1 min and (c) 63 min time on stream

5. In situ IR investigation of n-hexane isomerization over SZ and Pt/SZ

In Figure 5.4 in situ IR spectra of the region between 1700 and 1400 cm^{-1} , where bands of water and coke are located, are shown of a Pt/Mel 1 sample after activation in air, then carrying out the n-hexane isomerization reaction in helium, flushing the sample in pure helium and then in hydrogen in each case for one hour at 250°C and finally reactivating the catalyst in synthetic air at 500°C. The behaviour of the S=O bands at 1395 and 1350 cm^{-1} as well as the conversion during this procedure are shown in Figure 5.5.

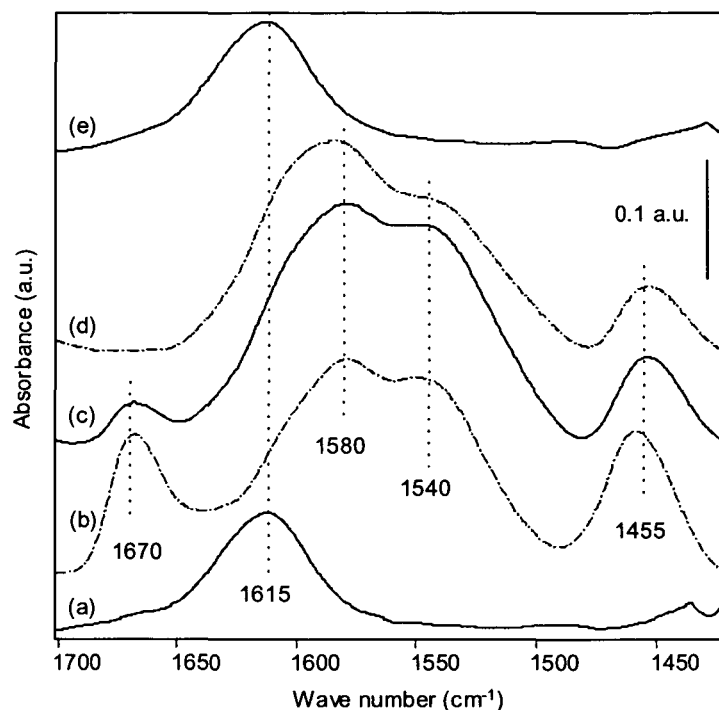


Figure 5.4: IR spectra (range of water and coke bands) obtained on a Pt/Mel 1 catalyst during the following procedure: (a) activation in air at 500°C, (b) reaction of n-hexane in helium at 250°C (spectrum after 1h TOS), (c) flushing in helium for one hour at 250°C, (d) flushing in hydrogen for 1h at 250°C and (e) reactivation in synthetic air at 500°C

Flushing in He or hydrogen cannot restore the activity; the broad band around 1540 – 1580 cm^{-1} assigned to coke and coke precursors did not decrease. The band near 1670 cm^{-1} decreased only partly in helium, whereas it disappeared completely in hydrogen. After flushing the deactivated catalyst in hydrogen a small activity was observed during the reaction in hydrogen, but the product distribution indicates hydrogenolysis on the metal sites. Only activation in air and then starting the reaction in hydrogen led back to the initial activity. The activity seems to be connected to the band at 1395 cm^{-1} . Coke deposition and water formation can lead to a shift of the

5. In situ IR investigation of *n*-hexane isomerization over SZ and Pt/SZ

S=O band to lower wave numbers. Restoration of the initial state via removal of the coke leads to an active catalyst.

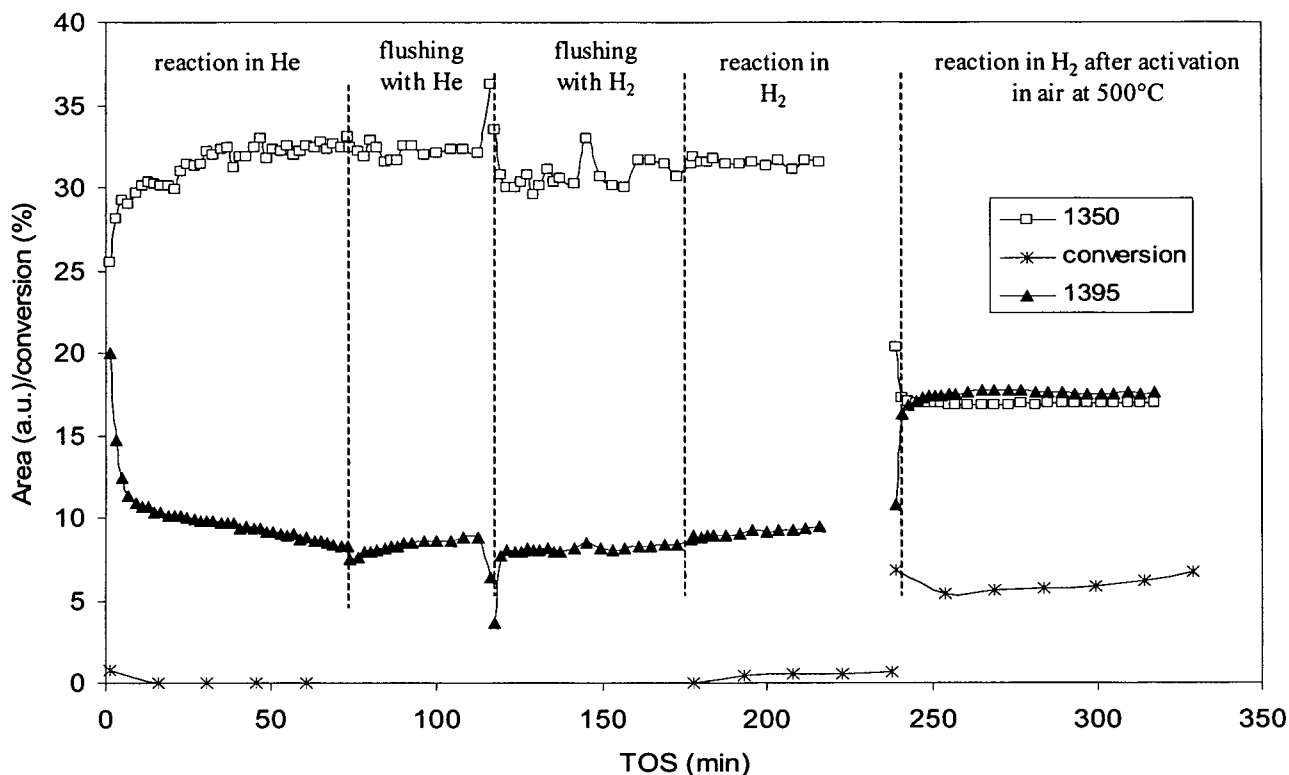


Figure 5.5: Integrated area of the S=O bands at 1395 and 1350 cm^{-1} and conversion versus time during the procedure described in Figure 5.4

The isomerization of *n*-hexane in He over SZ corresponds to that over Pt/SZ. In Fig. 5.6 the IR spectrum of SZ after activation in air at 500°C and the spectra after 1 and 61 min TOS in *n*-hexane under He are shown. At the beginning of the reaction water is formed indicated by the broad band between 3500 and 3100 cm^{-1} and by the increase of the band at 1615 cm^{-1} . An additional band near 1670 cm^{-1} was built up with TOS and a broad band around 1540 cm^{-1} was found like on Pt/SZ. The catalyst deactivated very rapidly. After flushing with He the band near 1670 cm^{-1} decreased only slightly, whereas with hydrogen a stronger decrease was observed, the intensity of the band at 1540 cm^{-1} did not change.

5. In situ IR investigation of *n*-hexane isomerization over SZ and Pt/SZ

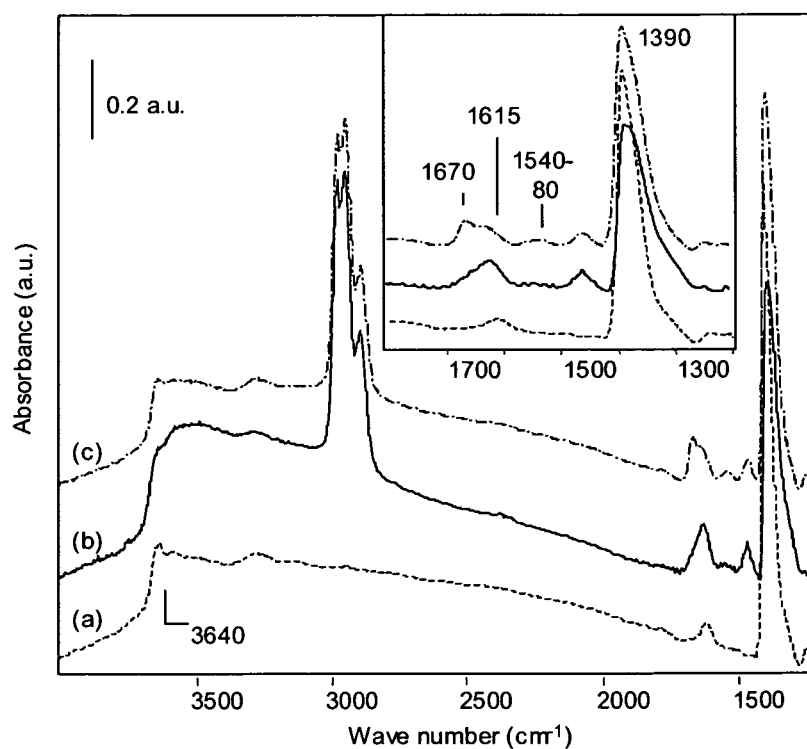


Figure 5.6: In situ IR spectra of *n*-hexane isomerization at 250°C in He over SZ: (a) after activation, (b) after 1 min and (c) 61 min time on stream

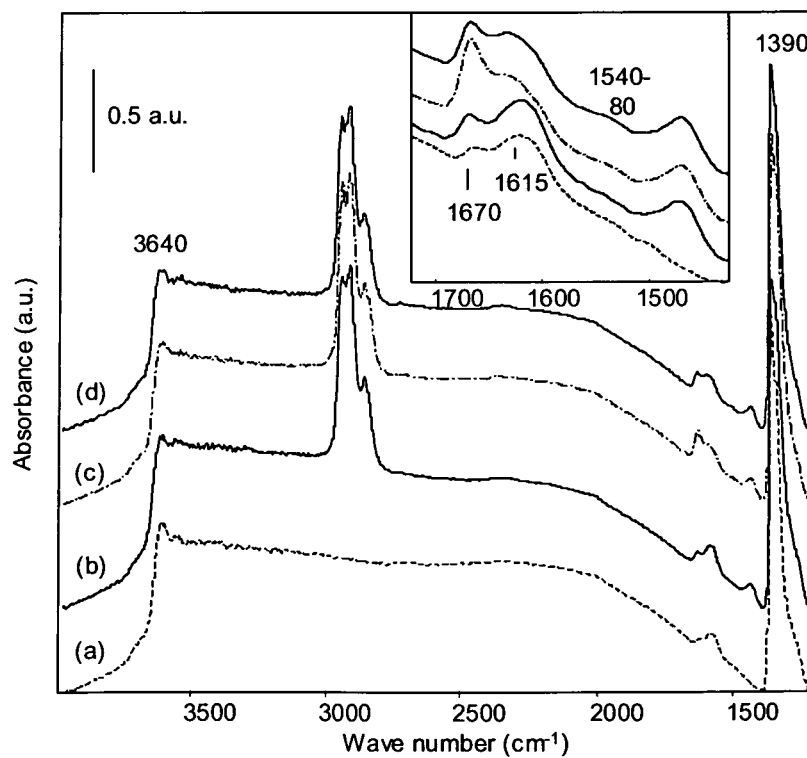


Figure 5.7: In situ IR spectra of *n*-hexane isomerization at 250°C in hydrogen over SZ: (a) after activation, (b) after 1 min, (c) 19 min and (d) 63 min time on stream

5. *In situ* IR investigation of *n*-hexane isomerization over SZ and Pt/SZ

If the reaction was carried out in hydrogen (Fig. 5.7), formation of water was not pronounced, the band near 1615 cm^{-1} vanished and the band near 1670 cm^{-1} increased, passed through a maximum and weak bands at $1540 - 1580\text{ cm}^{-1}$ developed. In this state the catalyst showed a constant conversion of less than 1% with 20% selectivity to isomerization, which remained constant over the investigated period.

From the IR data one can conclude that *n*-hexane is converted via two different reaction mechanisms over Pt/SZ in hydrogen and Pt/SZ or SZ in He. Only Pt/SZ in the presence of hydrogen was found to be an active and stable catalyst. In the other cases, using He as carrier gas, only an initial activity was observed followed by a rapid deactivation.

Vaudagna et al. [11] found that Pt/SZ under H_2 showed a good activity and hexane isomerization selectivity with TOS. But using Pt/SZ under nitrogen or SZ under H_2 or N_2 they observed only a good initial activity with a poor selectivity for isomerization. After a short TOS the activity drops rapidly and the catalysts are almost completely deactivated after 9 min-on-stream.

Duchet et al. [12] found that hexane isomerization was not observed over Pt/SZ without hydrogen owing to rapid deactivation. They proposed a mechanism involving Lewis acid sites in which hydride abstraction from *n*-hexane on coordinatively unsaturated Zr atoms creates carbenium ions which adsorb on Lewis basic sites i.e. bridged oxygen atoms. Also, Manoli et al. [13] observed that Pt improves the stability of SZ and hydrogen was indispensable for a sustainable hexane isomerization.

As active sites Brønsted acid sites, such as $\text{OH}/\text{H}_2\text{O}$ attached to sulfate groups, and coordinatively unsaturated Zr ions acting as Lewis acid sites are discussed [14,15]. Sachtler et al. [16] identified the combined metal-acid sites – small Pt particles anchored to the support by a proton as active sites. Paál et al. [17] used the name “compressed bifunctional sites” for the metal acid sites adduct. These sites are composed by sulfate sites and neighboring Pt atoms.

The experimental results point to Pt-proton adducts nearby sulfate groups and hydride ions connected to Lewis acid sites as the active sites, which is in agreement with Sachtler [16] and Paál [17]. Spillover hydrogen produced on Pt can be converted on SZ to protons and electrons or to hydride ions. The first can act as active sites for isomerization, whereas the hydrides can support the hydrogenation of the isomerized carbenium ions and hence the desorption of iso-alkanes. Therefore the catalytically active sites are created from hydrogen (and reactants) and the catalyst during the reaction. These sites are only available under reaction conditions, therefore probing the real strength of these sites should be very difficult.

5. *In situ* IR investigation of *n*-hexane isomerization over SZ and Pt/SZ

Paál et al. [18] discussed alkane adsorption in an ionic form on acid sites as start of alkane isomerization, rather than by the traditional bifunctional mechanism. Hydride ions react with intermediate surface carbenium ions forming the isomeric hexanes and also promote their desorption, which is essential for this isomerization route. The proton obtained together with the hydride ion would regenerate the Brønsted acid site.

If the reaction is carried out in He, water is produced at the beginning. This can be explained by an alternative initiation step of alkane activation, which is the oxidative dehydrogenation: in this case sulfur in the oxidation state of 6+ could be reduced to S^{4+} together with the formation of water and oxidized hydrocarbon species. From XPS data Song and Sayari [19] revealed that the oxidation state of sulfur in catalysts showing high activity was 6+, but catalysts containing S in a lower oxidation state were inactive. Furthermore, it was found that unpromoted SZ oxidizes saturated hydrocarbons just at 60°C [20]. Also Paál and coworkers [17] observed in XPS spectra reduced sulfur and oxidized carbon entities, C-O structures, as well as COOH groups and they related deactivation to the appearance of a minor S^{4+} peak. The authors found only a relative small loss of sulfur, but if we take into account that not all sulfate groups were active in isomerization it can be obvious that the few, highly active sulfate groups, were most affected by this reduction. The oxidative dehydrogenation is then a stoichiometric surface reaction and ceases once the active surface sulfates are consumed. In this respect SZ is not a catalyst but a reagent.

When spillover hydrogen is not present, i.e. in He the carbenium ions built up by the oxidative dehydrogenation remain on the surface, where they are oligomerized, cracked or polymerized into coke precursors or coke characterized by the bands at 1540 – 1580 cm^{-1} . Carrying out isomerization of *n*-hexane over SZ in hydrogen, a very small but stable conversion was obtained. It was shown that pure ZrO_2 can catalyze the hydrogenation of olefins [21], therefore it can activate hydrogen, but only to a minor extent compared to Pt. Since SZ based catalysts possess oxidation ability, an oxidation step cannot be excluded.

On the deactivated catalyst a band near 1670 cm^{-1} was observed. Babou et al. [22] assigned a band near 1680 cm^{-1} to adsorbed H_3O^+ . From adsorption and desorption of water on SZ followed by IR, no band near 1670 cm^{-1} was found. Therefore this band is assigned rather to oxidized hydrocarbons formed on the surface. This is in agreement with Davydov [23] who assigned bands located in the 1620 – 1670 cm^{-1} range to the stretching frequency of bridged carbonates. With TOS the intensity of this band decreased and bands in the region around 1540 - 1580 cm^{-1} developed, which were ascribed to coke or coke precursors. This band near 1670 cm^{-1} vanished

when the catalyst was flushed with hydrogen (see Figure 5.4), immediately when Pt was present and more slowly without Pt. The bands near $1540 - 1580\text{ cm}^{-1}$ are stable in hydrogen and vanished only after an oxidative treatment.

It is proposed that the deactivation of SZ is due to the deposition of carbonaceous deposits [2,24]. An additional cause of deactivation could be the reduction of sulfur.

5.3.2 Characterization of the coked catalysts

Quantitative analysis of the amount of coke deposited during the reaction of hydrocarbons in helium as carrier gas was done by thermogravimetric analysis (TG). Carbon deposits were removed by heating in synthetic air and thus burning off the coke. The samples were first exposed to the hydrocarbons in helium flow at 200°C reaction temperature in the reactor and then transferred to the TG apparatus. Assignment of the mass steps was done by comparison with TPD-MS measurements carried out under the same conditions.

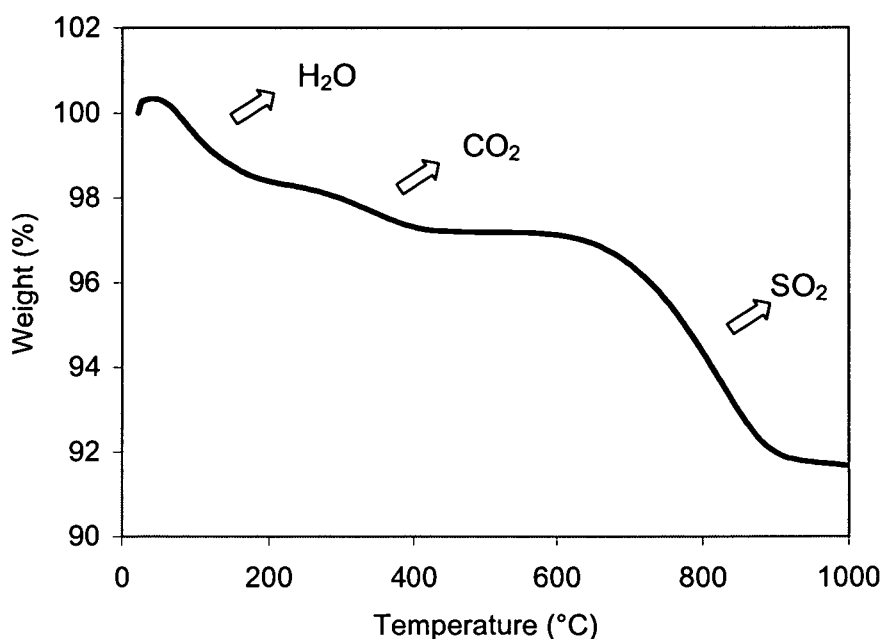


Figure 5.8: Determination of the amount of coke deposited on a Pt/Mel 2 catalyst after 2h reaction of *n*-heptane in helium by TG analysis in flowing synthetic air, heating rate $10^{\circ}/\text{min}$

Table 5.2 shows the amount of coke formed on Mel 2 catalysts with and without Pt after different reaction times. Practically no difference was observed for samples after 15 min and after 2h time

5. *In situ IR investigation of n-hexane isomerization over SZ and Pt/SZ*

on stream. Therefore, coking occurs in the first minutes of the reaction and afterwards the amount of coke stays the same. It was already observed in kinetic and in situ IR measurements that coking is very fast and catalysts have lost all activity after the first minutes of reaction time (see also Table 5.1). On Pt containing SZ more coke is formed than on unpromoted SZ. Carbonaceous deposits are burnt off between 250 and 400°C on Pt/SZ and between 400 and 550°C on SZ, since Pt is able to activate oxygen.

Table 5.2: Amount of coke formed during the reaction of n-heptane over SZ and Pt/SZ at 200°C in helium; determined by TG analysis

	Reaction time	wt% coke
Mel 2	15 min	0.59
Mel 2	2 h	0.45
Pt/Mel 2 (2.5% Pt)	15 min	0.83
Pt/Mel 2 (2.5% Pt)	2 h	0.90

The amount of coke, which leads to a total loss of the catalytic activity, is remarkably small. Less than 1 wt% of coke leads to a complete deactivation, therefore only a small fraction of the acid sites would be occupied by the coke molecules. This observation supports an assumption proposed by some authors [25,26,27]: they suggested that only a small number of extremely active sites are responsible for the catalytic activity. In HRTEM studies Benaissa et al. [25] found a small number of zirconia crystallites containing high Miller-index surfaces, and they proposed that the presence of sulfate groups near or on these particles could give rise to a small number of highly acidic sites of SZ. Kim et al. [26] found that about 20% of the sulfate groups are involved as reversible butane adsorption sites. Via determination of the differential heat of NH₃ adsorption Fogash and coworkers [27] observed that about 20% of the acid sites are of strong or intermediate acid strength, and they suggested that these sites are responsible for the isomerization activity.

TG and XRD measurements revealed no loss of sulfate groups during the reaction of n-alkanes in helium and no changes of the crystal structure of a coked catalyst.

The concentration of acid sites was studied by pyridine adsorption on a coked Pt/SZ catalyst. The ratio of LS/BS was found to be 1.76, which suggests that mainly BS would be blocked by the carbon deposits.

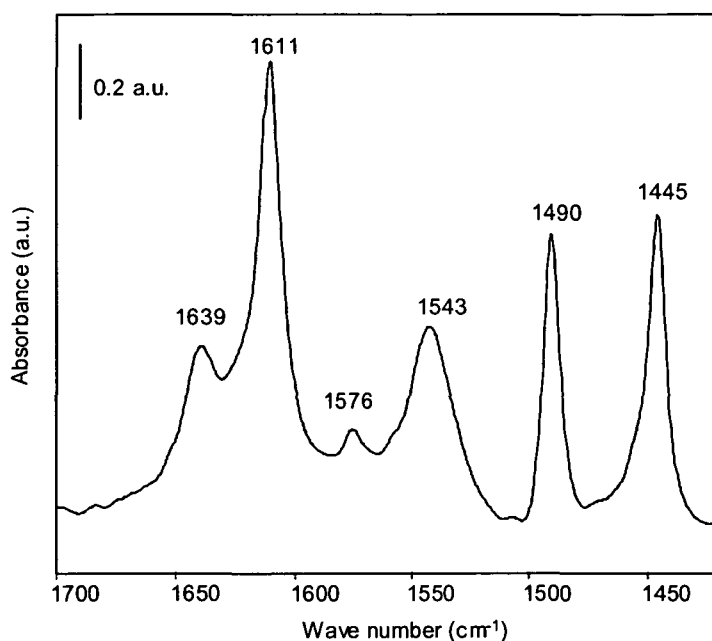


Figure 5.9: Adsorption of pyridine on a coked Pt/Mel 2 sample (after reaction of *n*-heptane in helium at 200°C for 15 min); prior to adsorption activation in vacuum at 200°C; difference spectrum (related to spectrum after activation)

5.4 Conclusions and summary

Ensembles containing metallic and acidic sites – $(Pt_n H)^+$ - nearby sulfate groups are assumed to be the active sites together with hydride ions necessary for hydrogenation and desorption of iso-alkanes.

The initiation step of hexane isomerization is different over Pt/SZ in hydrogen and over Pt/SZ and SZ in He. In the first case it is a real catalytic reaction whereas otherwise a surface reaction took place. The last reaction is interpreted as an oxidative dehydrogenation characterized by water formation, by a band near 1670 cm^{-1} , assigned to oxidized carbon species, which are transformed into coke precursors or coke.

Deactivated SZ contains a small amount of coke and reduced sites probably sulfur in the oxidation state of 4+. Reactivation of deactivated catalysts could only be done by oxidation in air.

References

-
- [1] R.A. Keogh, D.E. Sparks, B.H. Davis, *Stud. Surf. Sci. Catal.*, Vol. 88, Elsevier, Amsterdam, 1994, 647.
 - [2] G. Resofszki, M. Muhler, S. Sprenger, U. Wild, Z. Paál, *Appl. Catal. A* 240 (2003) 71.
 - [3] R. Ahmad, J. Melsheimer, F.C. Jentoft, R. Schlögl, *J. Catal.* 218 (2003) 365.
 - [4] B.H. Davis, R.A. Keog, S. Alerasool, D.J. Zalweski, D.E. Day, P.K. Doolin, *J. Catal.* 183 (1999) 45.
 - [5] Ü.B. Demirci, F. Garin, *J. Mol. Catal.* 188 (2002) 233.
 - [6] T. Tanak, T. Shishido, H. Hattori, K. Ebitani, S. Yoshida, *Physica B* 208-209 (1995) 649.
 - [7] K. Ebitani, H. Konno, T. Tanaka, H. Hattori, *J. Catal.* 135 (1992) 60.
 - [8] K. Ebitani, J. Konishi, H. Hattori, *J. Catal.* 130 (1991) 257.
 - [9] T.J. McCarthy, G.D. Lei, W.M.H. Sachtler, *J. Catal.* 159 (1996) 90.
 - [10] H. Liu, V. Adeeva, G.D. Lei, W.M.H. Sachtler, *J. Mol. Catal. A* 146 (1996) 165.
 - [11] S.R. Vaudagna, R.A. Comelli, N.S. Figoli, *Catal. Lett.* 47 (1997) 259.
 - [12] J.C. Duchet, D. Guillaume, A. Monnier, C. Dujardin, J.P. Gilson, J. van Gestel, G. Szabo, P. Nascimento, *J. Catal.* 198 (2001) 328.
 - [13] J.M. Manoli, C. Potvin, M. Muhler, U. Wild, Z. G. Resofszki, T. Buchholz, Z. Paál, *J. Catal.* 178 (1998) 338.
 - [14] M.-T. Tran, N.S. Gnep, G. Szabo, M. Guisnet, *Appl. Catal. A* 171 (1998) 153.
 - [15] K. Shimidzu, N. Kounami, H. Wada, T. Shishido, H. Hattori, *Catal. Lett.* 54 (1998) 153.
 - [16] H. Liu, H. Lei, W.M.H. Sachtler, *Appl. Catal. A* 137 (1996) 167.
 - [17] T. Buchholz, U. Wild, M. Muhler, G. Resofszki, Z. Paál, *Appl. Catal.* 189 (1999) 225.
 - [18] Z. Paál, U. Wild, M. Muhler, J.M. Manoli, C. Potvin, T. Buchholz, S. Sprenger, G. Resofszki, *Appl. Catal. A* 188 (1999) 257.
 - [19] X. Song, A. Sayari, *Catal. Rev. Sci. Eng.* 38 (1996) 329.
 - [20] A. Ghenciu, D. Farcasiu, *Catal. Lett.* 44 (1997) 29.
 - [21] K. Domen, J. Kondo, K. Maruya, T. Onishi, *Catal. Lett.* 12 (1992) 127.
 - [22] F. Babou, G. Coudurier, J. Viedrine, *J. Catal.* 152 (1995) 341.
 - [23] A.A. Davydov, *Infrared Spectroscopy of Adsorbed species on the Surface of Transition Metal Oxides*, Wiley, New York 1990, Chapter 1, p. 38.
 - [24] R.A. Comelli, C.R. Vera, J.M. Parera, *J. Catal.* 151 (1994) 464.
 - [25] M. Benaissa, J.G. Santiesteban, G. Díaz, C.D. Chang, M.J. Yacamán, *J. Catal.* 161 (1996) 694.
 - [26] S.Y. Kim, J.G. Goodwin Jr., D. Galloway, *Catal. Today* 63 (2000) 21.
 - [27] K.B. Fogash, G. Yularis, M.R. Gonzalez, P. Ouraipryvan, D.A. Ward, E.I. Ko, J.A. Dumesic, *Catal. Lett.* 32 (1995) 241.

6 DEACTIVATION AND REGENERATION OF Pt CONTAINING SULFATED ZIRCONIA AND SULFATED ZIRCONIA

6.1 Introduction

High-octane gasoline, which is free of aromatics and sulfur containing compounds, can be produced either by isomerization of n-alkanes or by alkylation of iso-butane with $C_3 - C_5$ alkenes. For alkylation sulfuric and hydrofluoric acid, for isomerization Pt on chlorided alumina and Pt containing mordenite are commercially used. To find stable solid acid catalysts as compensation for liquid acids and for chlorided alumina is highly desirable.

Sulfated zirconia (SZ) is one of the benign alternatives for the substitution of liquid acids answering the demand for clean technologies [1]. Much work has been devoted to sulfated zirconia, which is compiled in several reviews [2-4]. SZ is able to catalyze the following reactions: alkane isomerization, alkane cracking, iso-alkane alkylation and acylation of aromatics [2,5]. Sulfated zirconia (SZ) has reached a lot of interest due to its high activity for the isomerization of light alkanes at low temperatures [4].

The industrial use of SZ is currently restricted to the isomerization of C_5 - C_6 paraffinic cuts for enhancing the octane number of gasoline [6]. In contact with hydrocarbons SZ alone deactivated quickly. To set up a stable process addition of Pt and working under hydrogen is necessary to prevent SZ from deactivation [7,8].

The catalytic properties of SZ significantly depend upon the preparation method and the activating treatment [9]. It is reported that the calcination step, which selectively eliminates sulfates from some specific terminations of the zirconia crystallites belonging to the high symmetry crystal phases [10], is crucial for activity.

Until now a discussion exists about the nature of the active sites on Pt/SZ, as well as the mechanism through which the catalytic sites are formed [11]. Moreover, other factors than the strength of the acid sites are discussed to be the cause of the high activity. Liu et al. [12] proposed that an extremely active catalyst for an acid catalyzed reaction need not to be an extremely strong acid. Instead, the reaction can proceed via a less energy intensive bimolecular mechanism for

6. Deactivation and regeneration of Pt/SZ and SZ

small alkanes. Falco et al. [13] meant that the acidity of Pt/SZ and Pt/WZ is generated under reaction conditions by the simultaneous presence of Pt, hydrogen and SZ (WZ).

Beside the acid sites also the role of the Pt sites is discussed. Normally the Pt content is in the range of 0.1 to 0.5 wt%. Arata et al. [14] found the highest activity of SZ with 3 wt% Pt for the catalyst prepared by double calcination, while the highest activity was observed with 7.5 wt% Pt in the case of a single calcination.

According to Ebitani et al. [15] Pt on SZ remains mostly in an oxidized state, even after hydrogen reduction at 673 K. Ebitani [16] proposed that Brønsted acid sites were developed from dissociative adsorption of hydrogen on Pt, spillover of the H atoms onto the SZ and then electron transfer from the H atoms to Lewis acid sites left protons on the surface. Sachtler et al. [17] proposed $[\text{Pt}_n\text{H}]^+$ adducts, „collapsed bifunctional sites” which can act as active sites.

Dijs et al. [18] observed that water free SZ was not active; only after addition of water catalytic activity was exhibited. The main conclusion of this research was that the catalytic activity of SZ originates from supported sulfuric acid containing water.

A very fast deactivation was found when hydrocarbons react on sulfated zirconia. A deactivation process was observed over all SZ systems, cubic, tetragonal and monoclinic during the isomerization of n-butane at 423 K [19]. This process is not irreversible and the activity can be completely restored by reactivating the various catalysts in dry air at 673 K. The nature of this deactivation is still under discussion. Deactivation was attributed to carbon accumulation [20,21], to surface reduction of Zr^{4+} to Zr^{3+} during the reaction of hydrocarbons, to a loss of sulfur entities, to reduction of sulfate groups and H_2S formation or to a change in the surface phase from tetragonal to monoclinic [1].

If sulfur is reduced to lower oxidation states irreversible deactivation could take place. García et al. [22] found that only 10% of the active sites in SZ, probably SOHZr , are the most active.

The aim of this chapter is to investigate the nature of active sites, to determine which factors influence the deactivation and to study regeneration processes.

6.2 Results and discussion

6.2.1 Deactivation and regeneration of SZ and Pt/SZ studied by TG, TPD and in situ IR spectroscopy

Hydroisomerization of n-heptane uses Pt, Pd or Ni supported on zeolites. With Beta as zeolite support the isomerization selectivity was always high, even when n-octane and n-nonane were used as reactants [23,24]. But when SZ is used as acidic component a high selectivity to cracking products is observed. The isomerization selectivity of n-octane was found to be very low over Pt/SZ, cracking was the preferred reaction path [25]. That is a reason why industrial isomerization is limited in practice only to C₄, C₅ and C₆ alkanes [26].

The surface properties of sulfated zirconia change concomitantly with temperature, pressure and the presence of water vapor [18]. SZ is a very hygroscopic material and rehydration occurs easily after calcination at 600°C and storage at room temperature. For this reason, reactivation prior to reaction is necessary. Since the catalytic activity of SZ and Pt/SZ is strongly dependent on the activation process different activation and regeneration procedures were followed by TG, TPD and IR measurements.

Activation of the Pt/SZ catalyst in synthetic air or N₂, then cooling down to 200°C and reduction at this temperature leads to an active material. Reactivation in air restores the initial activity.

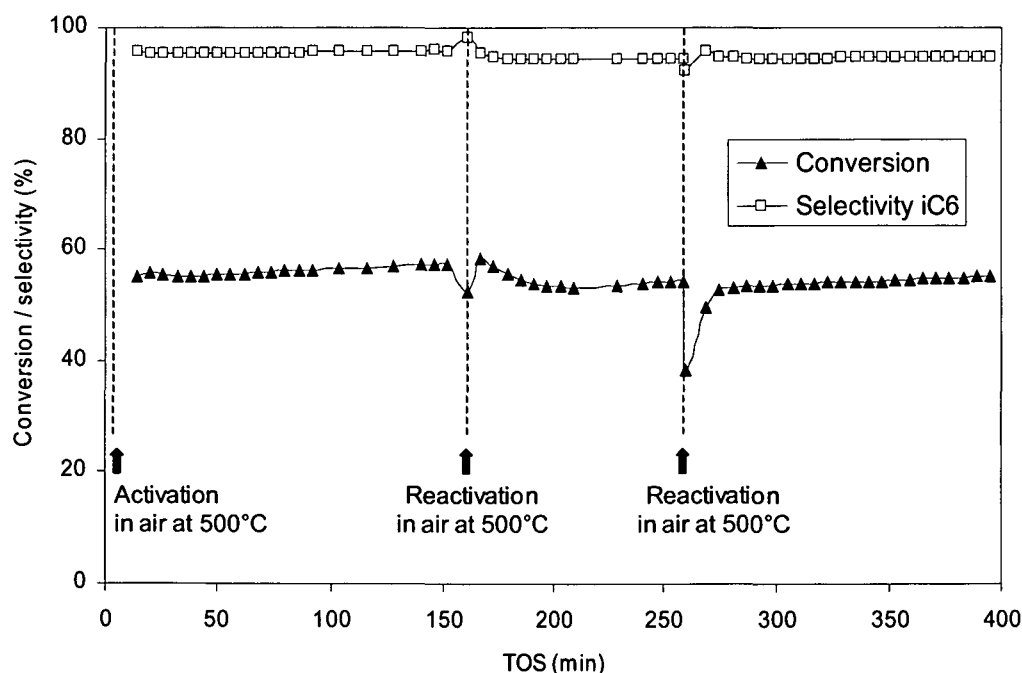


Figure 6.1: n-Hexane isomerization at 250°C and 5 bar in hydrogen over Pt/Mel 2

6. Deactivation and regeneration of Pt/SZ and SZ

In Figure 6.2 – 6.4 different activation procedures followed by TG and TPD measurements are shown. Pt/Mel 2 and Mel 2 were activated in He or in air (or He/O₂ mixture respectively) with a rate of 10 K/min up to 500°C and kept at this temperature for 1 hour, then the samples were cooled down to 200°C and reduced in hydrogen for 15 min. Afterwards the sample was heated either in air (He/O₂) or in He until 900°C.

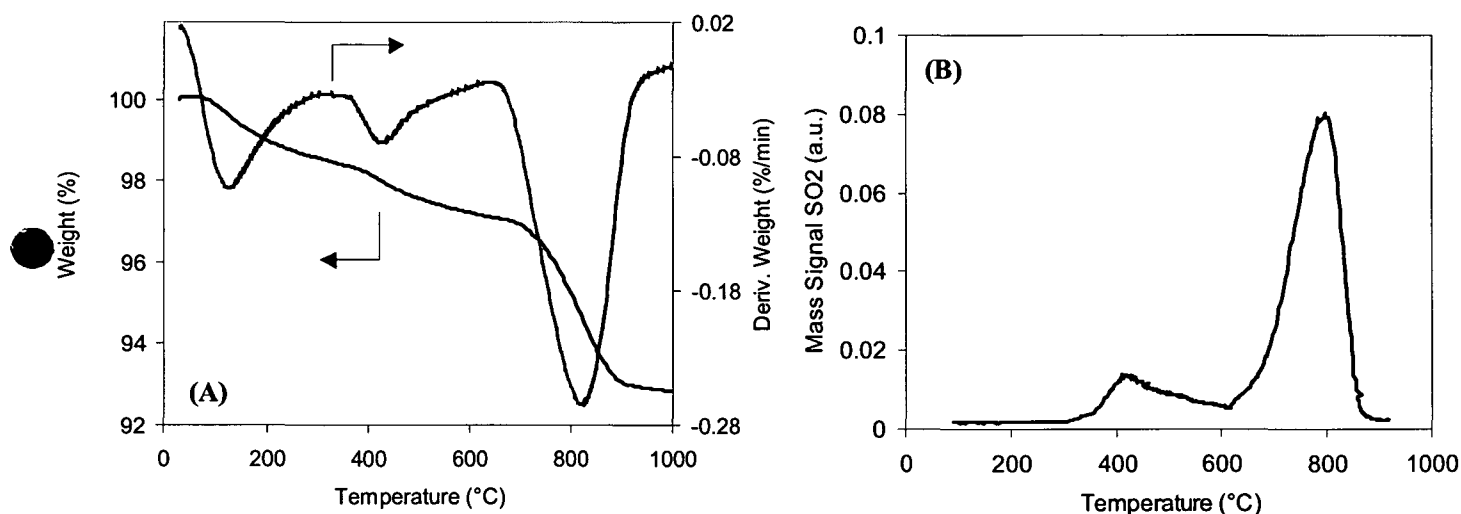


Figure 6.2: TG (A) and TPD (B) measurements of Pt/SZ in He flow after activation in synthetic air or He at 500°C followed by reduction at 200°C

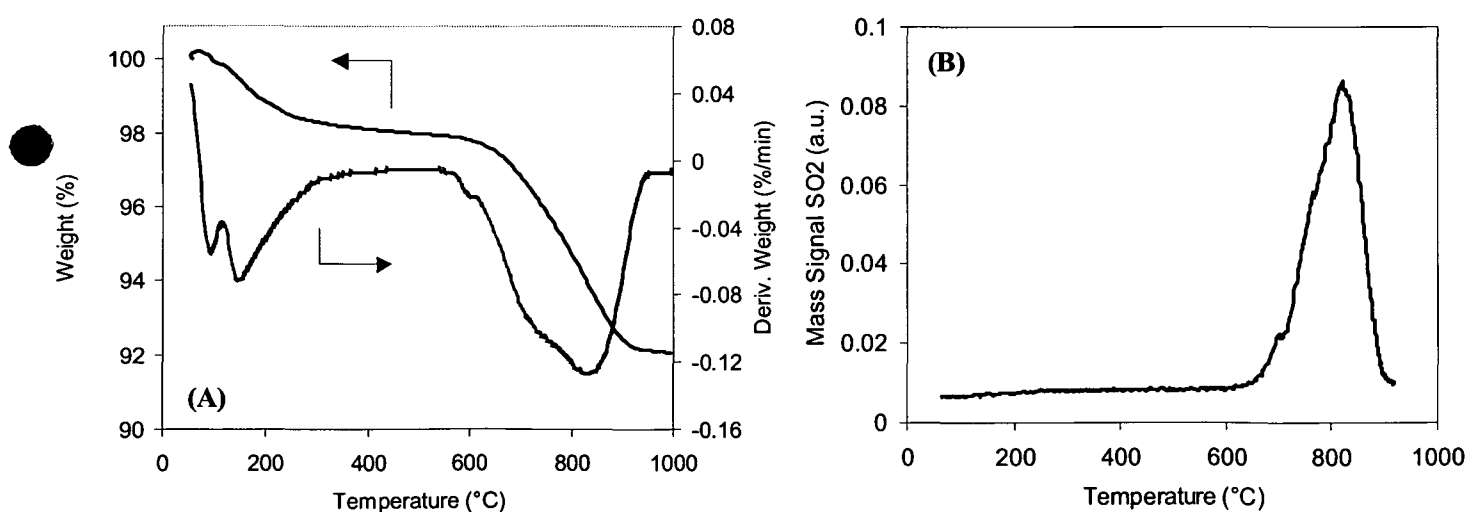


Figure 6.3: TG (A) and TPD (B) measurements of Pt/SZ in air after activation in He at 500°C followed by reduction at 200°C

6. Deactivation and regeneration of Pt/SZ and SZ

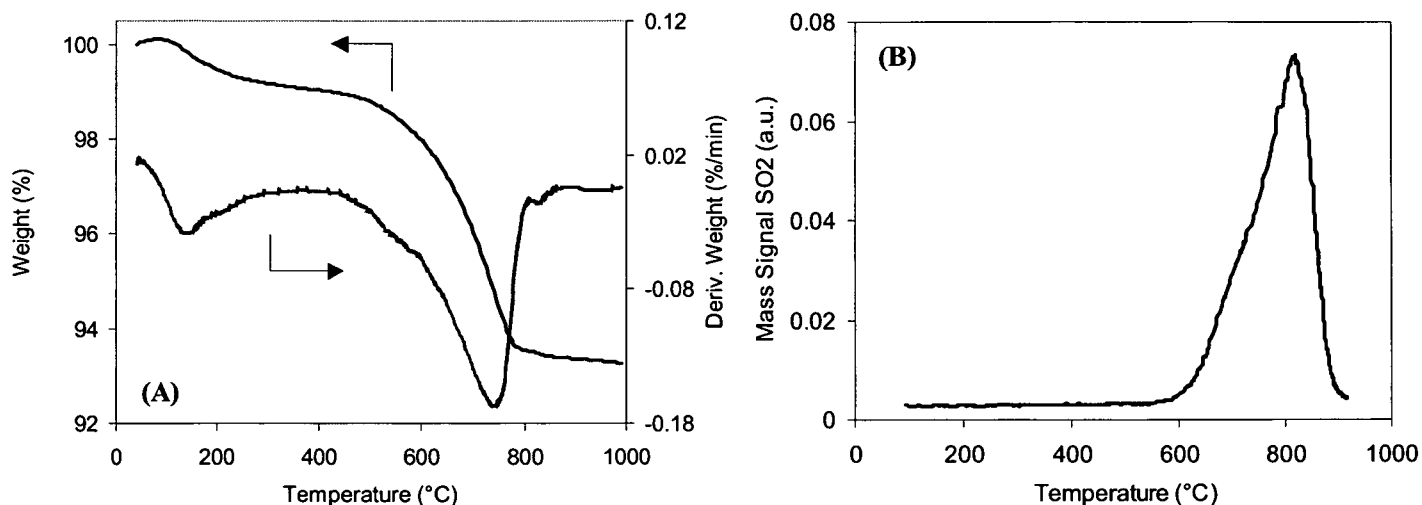


Figure 6.4: TG (A) and TPD (B) measurements of SZ in He flow after activation in synthetic air or He at 500°C followed by reduction at 200°C

Only from Pt/SZ, which was reduced before heating in an inert gas stream, a part of the sulfate groups was lost as SO₂ in the temperature interval between 350 and 550°C, and the other part was released above 600°C. When the sample was heated in air after reduction, SO₂ was evolved only at the higher temperature. The same was found when heating the Pt/SZ sample twice in inert gas without carrying out a reduction in between. Kinetic measurements showed that Pt/SZ was inactive for isomerization when heated in He or N₂ to 500°C after a reduction step, whereas it stays active when it is treated under oxidizing conditions after reduction.

SZ showed the evolution of SO₂ always only between 600 and 850°C whatever the activation procedure.

The amount of SO₂ evolved at lower temperatures depends on the reduction conditions. For the TPD and TG measurements described above the obtained values are shown in Table 6.1.

Beside the reduction in hydrogen, also the reaction with hydrocarbons can be regarded as reductive step. Thus, regeneration in inert gas at 500°C after reaction of n-alkanes in helium resulted in a loss of part of the sulfates at lower temperatures. In the same temperature range, carbonaceous deposits were removed as CO₂. Regeneration in air removes only the coke at temperatures below 600°C.

6. Deactivation and regeneration of Pt/SZ and SZ

Table 6.1: TG and TPD measurements of (Pt)/Mel 2 after different pretreatment steps

	Activation procedure	TG/TPD in	SO ₃ ^{LT} (wt%) *	SO ₃ ^{HT} (wt%) *	ΣSO ₃ (wt%) *	Ratio SO ₃ ^{HT} / SO ₃ ^{LT} *	Ratio of HT/LT SO ₂ peak areas calculated from TPD
Pt/SZ	He 500°C, Red. 200°C	He	0.74	4.16	4.90	5.7	3.9
Pt/SZ	Air 500°C, Red. 200°C	He	0.74	4.06	4.80	5.5	3.7
Pt/SZ	He 500°C, Red. 200°C	Air	-	5.87	5.87	-	-
SZ	He 500°C, Red. 200°C	He	-	5.15	5.15	-	-

LT: low temperature (< 600°C) HT: high temperature (> 600°C) * from TG measurements

Li and Gonzalez [27,28] found that regeneration of SZ in N₂ at 550°C resulted in a complete loss of catalytic activity, while regeneration in O₂ at 450°C essentially restored the catalytic activity to that of a fresh catalyst. From the fresh catalyst SO₂ evolved at 800°C, whereas for a deactivated catalyst CO₂ and part of SO₂ are released around 600°C. In both cases sulfur was evolved as SO₂. The sulfate species evolved at the lower temperature amounted to 10 – 14% of the total sulfate content.

With Pt/SZ it is sufficient to carry out heating in an inert gas stream after a reduction step to lose a certain amount of SO₂ at lower temperature, i.e. 500°C. With SZ, SO₂ is lost only between 600 and 800°C even with a reduction step before a TPD measurement. It was shown that in the case of SZ a reaction with hydrocarbons is necessary to detect SO₂ at lower temperature [27]. Li and Gonzalez observed two SO₂ desorption maxima from deactivated SZ. The low temperature maximum corresponds to the release of SO₂ and CO₂ and the other one to SO₂ alone. CO₂ can be burned off under air and the catalyst was active again, whereas under N₂ both components were released from the surface and the catalyst was irreversibly deactivated. The amount of coke deposited on SZ, which is capable of poisoning the active sites, was found to be unusually small. From HRTEM studies the presence of a small number of zirconia crystallites containing high Miller-index surfaces is revealed [29] and it was proposed that the presence of sulfate groups near

6. Deactivation and regeneration of Pt/SZ and SZ

or on these particles could give rise to the highly acidic sites of SZ. The number of such sites would therefore be small.

Hydrogen, which is activated on Pt and spilt over to the ZrO_2 surface, is able to reduce the bond between the sulfate groups or between the sulfates and the oxidic surface and SO_2 is evolved at lower temperature. If an oxidizing step is carried out after the reduction, the initial situation is reestablished and no SO_2 is lost at lower temperatures (below 600°C).

Different activation procedures and the reaction of n-heptane were followed by in situ IR measurements using a flow cell. All measurements were done on the same Pt/SZ sample. Pt/SZ was first activated at 500°C in a nitrogen flow for one hour and an IR spectrum was measured (Figure 6.5). In the OH region several bands were observed: a very small band at around 3740 cm^{-1} , a band at 3640 , a small band at 3578 cm^{-1} and a very broad band with a maximum at around 3200 cm^{-1} . In the literature [30,31], the first two bands are described as isolated ZrOH groups and as hydroxyls groups bridging between 2 or 3 Zr atoms respectively, the low frequency band at 3578 cm^{-1} was attributed to non-specified hydroxyl groups present on sulfated zirconia. The broad band around 3200 cm^{-1} has been attributed to terminal Zr-OH groups where the protons are substituted by HSO_4^- anions creating a new type of Brønsted acid sites, presumably protons forming multicenter bonds with sulfate anions, or to OH groups strongly interacting with each other or with the surface through hydrogen bonding [32]. The deformation vibration of adsorbed water was observed at 1605 cm^{-1} , even after activation at 500°C .

In the SO region a very intense band at 1400 cm^{-1} was observed, other bands below 1200 cm^{-1} could not be detected due to our instrumental setup. The intense band at $1400 - 1380\text{ cm}^{-1}$ can be ascribed to the stretching vibration of S=O [33,34]. Bands at lower wave numbers are assigned to adsorbed forms of sulfuric acid. Li and Gonzalez [28] assigned bands at 1272 , 1154 , 1022 and 999 cm^{-1} to a bidentate sulfate ion coordinated to Zr^{4+} .

After the first activation step in nitrogen the catalyst was reduced at 200°C for 15 min and then n-heptane reacted on the surface. Reduction in hydrogen led to a pronounced increase of the OH bands. A shift of the SO band to 1386 cm^{-1} and a shoulder at about 1300 cm^{-1} were observed after 11 min TOS in n-heptane. The catalyst was active with an isomerization selectivity of 44%, the cracked products were propane and iso-butane with only a small amount of n-butane (Table 6.2).

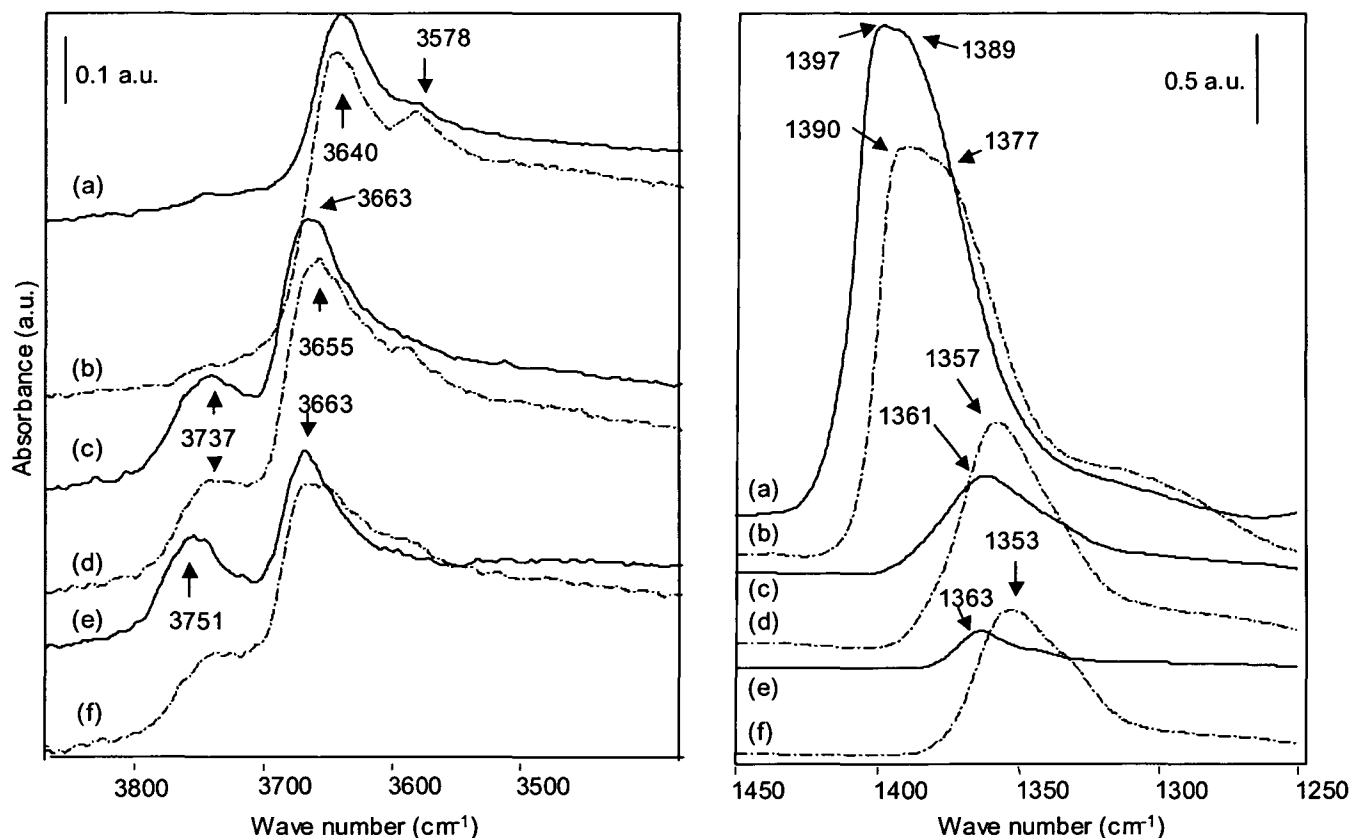


Figure 6.5: In situ IR spectra of Pt/SZ after different activation procedures carried out consecutively on the same sample; every activation step is followed by reduction at 200°C and n-heptane isomerization at 200°C in H₂ (spectra not shown here, only spectra directly after activation are displayed): (a) after activation in N₂, (b) in air, (c) in N₂, (d) in air, (e) in N₂ and (f) in air at 500°C

The sample was reactivated in air and then the same procedure as described above was applied. The intensity of the bands in the OH and SO region did not change during this treatment and the catalyst was active and the selectivity was approximately the same as before.

The next activation was done in nitrogen at 500°C. The OH band at 3740 cm⁻¹ increased strongly in intensity, the band at 3640 shifted to 3663 cm⁻¹ and the band at 3578 cm⁻¹ was absent. The SO band shifted to 1361 cm⁻¹ and the intensity was drastically reduced to 22% of its initial value and the catalyst was practically inactive, only 0.1% conversion with 100% selectivity to monobranched isomers was found. These results together with results from TG and TPD measurements demonstrate that sulfate groups evolved as SO₂ were lost from the surface. Morterra et al. [35] found that the $\nu_{S=O}$ shifts from 1400 cm⁻¹ to 1360 cm⁻¹ with decreasing

6. Deactivation and regeneration of Pt/SZ and SZ

concentration of sulfates on the surface. An additional hint is the formation of terminal Zr-OH groups at 3740 cm^{-1} and the shift from 3640 to 3663 cm^{-1} . The bands at 3640 and 3578 cm^{-1} are assigned to OH groups on SZ, whereas the bands at 3740 and 3663 cm^{-1} belong to OH groups on pure zirconia [34].

Reactivation in air at 500°C and reduction at 200°C led to n-heptane conversion of 1.0% with an isomerization selectivity of 13.3%. Note the cracking products were now propane and n-butane in approximately the same amounts. Bands belonging to Zr-OH at 3740 and 3655 cm^{-1} were observed and additionally a small band at 3578 cm^{-1} , which is characteristic for sulfated zirconia. The band in the SO region at $1357\text{-}1353\text{ cm}^{-1}$ increased in intensity to 46% of its initial value. After repeating this cycle in nitrogen the catalyst is totally inactive. Only bands for Zr-OH groups were detected and the intensity of the SO band at 1363 cm^{-1} decreased to 6%.

After reactivation in air the conversion was only 1.0% with a low selectivity of 5.7% to isomerization. The cracking products were again propane and n-butane. The S=O band at 1353 cm^{-1} increased in intensity to 30% of its initial value.

These changes of the area of the SO band between 1350 and 1400 cm^{-1} after the different activation steps are summarized in Table 6.2, but since we cannot detect the sulfate species in the range below 1200 cm^{-1} , these values have to be treated with caution.

Table 6.2: Isomerization of n-heptane at 200°C in H_2 over Pt/SZ after different activation procedures (carried out consecutively on the same sample)

Activation procedure	TOS (min)	Conversion (%)	Selectivity (%)				Area SO (%) ⁽ⁱ⁾
			iC ₇	C ₃	iC ₄	nC ₄	
N ₂ 500°C , Red. 200°C	8	23.9	43.6	27.6	26.8	1.0	100
Air 500°C , Red 200°C	8	30.8	27.0	36.4	35.1	1.1	102
N ₂ 500°C , Red. 200°C	8	0.1	100	0.0	0.0	0.0	22
Air 500°C , Red 200°C	8	1.0	13.3	20.6	0.0	20.8	46
N ₂ 500°C , Red. 200°C	8	0.0	-	-	-	-	6
Air 500°C , Red 200°C	8	1.0	5.7	17.0	0.0	15.6	30

TOS = Time on stream

iC₇: sum of all branched heptane isomers; C₃: propane; iC₄: iso-butane; nC₄: n-butane

⁽ⁱ⁾: integrated area of SO band between 1350 and 1400 cm^{-1} related to the area after the first pretreatment step

6. Deactivation and regeneration of Pt/SZ and SZ

A loss of sulfate species from Pt/SZ was observed when the sample was activated in an inert gas stream, then reduced and a second treatment at 500°C in He or N₂ followed, after these procedures Pt/SZ could not be reactivated by thermal treatment. The catalyst lost its acid properties and the rest of activity comes rather from the metal sites on which isomerization and hydrogenolysis of n-heptane to propane and n-butane can take place.

During the reduction treatment, hydrogen can dissociate to form H atoms on Pt followed by spillover to the zirconia support. Spillover hydrogen seems to be able to reduce sulfur species to a lower oxidation state. During heating in He or N₂ at temperatures above 400°C water and a part of sulfur species desorb as SO₂ and the catalyst loses its activity. Heating in air or oxygen restores the original oxidation state of sulfur and the sample stays active.

SZ was treated under the same conditions as Pt/SZ (Figure 6.6). The intensity of the bands in the OH and SO region did not change during these treatments.

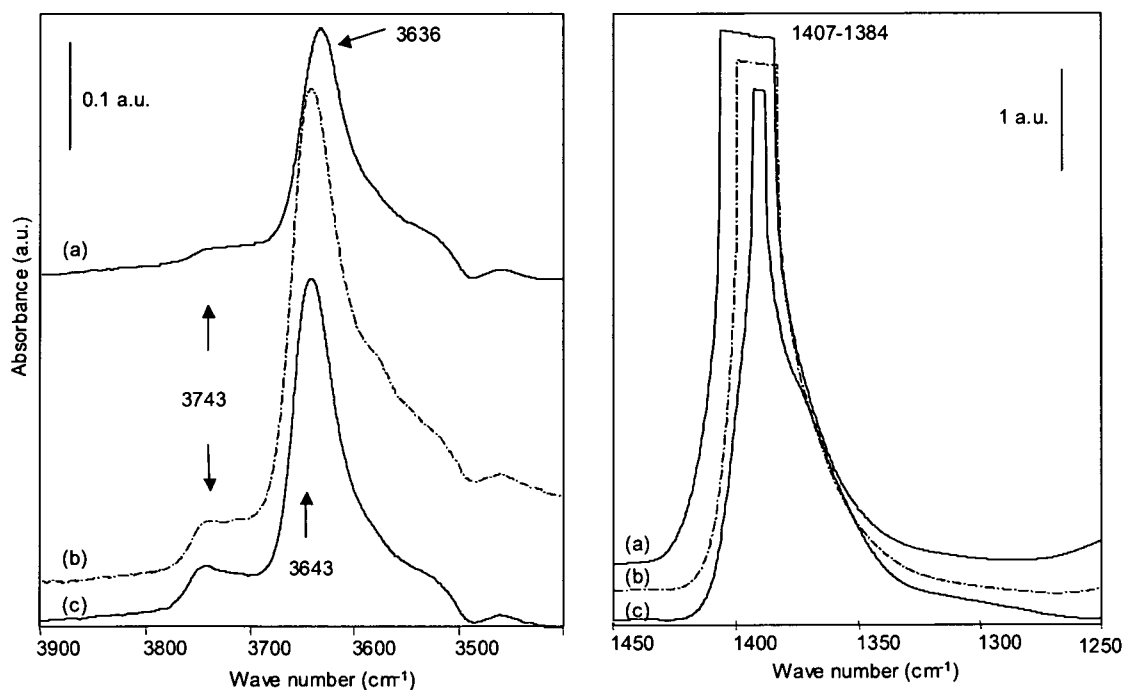


Figure 6.6: In situ IR spectra of SZ after different activation procedures carried out consecutively on the same sample; every activation step is followed by reduction at 200°C and n-heptane isomerization at 200°C in H₂ (spectra not shown here, only spectra directly after activation are displayed): (a) after activation in N₂, (b) in N₂ and (c) in air at 500°C

6. Deactivation and regeneration of Pt/SZ and SZ

SZ without Pt is hardly active for n-heptane conversion and deactivates very quickly. Only a very small amount of isomerized products was detected, the main part were cracked products, i.e. propane and mainly iso-butane. It could be shown [36] that a plausible initiation step of alkane activation over SZ is the oxidative dehydrogenation. In an inert atmosphere coke precursors or coke were built up.

Li and Gonzalez [28] using SZ for the isomerization of n-butane found that a deactivated catalyst could be completely restored by burning off the coke in the presence of oxygen or air. If, however, SZ is regenerated in nitrogen a loss of the surface sulfur species was observed and SZ was irreversibly deactivated. Also Resofszki et al. [21] observed that the activity of SZ can be fully regenerated by oxidation in air burning off carbon impurities.

Since the catalytic activity of SZ is very low addition of Pt is necessary to promote activity and selectivity to isomerization of n-alkanes. Vaudagna et al. [37,38] found that SZ is active only with Pt and under hydrogen for n-hexane isomerization. They compared SZ and Pt/SZ under nitrogen and hydrogen atmosphere. Only Pt/SZ under hydrogen showed a good activity and stability with a high selectivity to C₆ isomers, the other three samples showed a high initial activity and selectivity to cracking products, but they were almost completely deactivated after 9 min TOS.

On SZ the dissociation of hydrogen is not favored and the carbenium ions, which are formed and isomerized on the acid sites, remain long time at the surface where they are either oligomerized and then cracked or polymerized into coke. On Pt/SZ hydrogen can be easily activated and can form protons as a source of Brønsted acid sites and hydride ions, which can interact with carbenium ions forming isomerized alkanes. Therefore Pt is not directly involved in the isomerization process; it is more likely involved in the generation of active reaction sites on the surface. Metallic and acidic sites show a concerted action rather than acidic sites isomerizing alkenes formed on metallic sites.

When Pt/SZ becomes inactive, i.e. after regeneration in an inert atmosphere, sulfate groups were lost. With decreasing concentration of sulfate groups the activity of n-heptane conversion decreases and the catalyst cannot be regenerated by thermal treatment. But the in situ IR measurements showed that already after the first treatment at 500°C in an inert gas after reduction the activity was completely lost and a further decrease of the SO band did not have any effect on the activity. Li and Gonzalez found that the loss of a small part of the sulfate groups is enough to deactivate the catalyst totally [28]. Kim et al. [39] determined the fraction of sulfate species

possibly utilized as reversible adsorption sites to be only 20% or even less of the sulfate species available on the surface.

6.2.2 Characterization of the inactive catalyst

The exact amount of SO₂ evolved at lower temperatures depends on the reduction conditions. During the TG and TPD measurements shown above about 15% (TG) and 20% (TPD) of the sulfate groups were removed below 500°C (see Table 6.1). Consequently the coverage of the surface with sulfate groups is reduced from 58% to 49% and 46%, respectively.

The loss of the active sulfate groups leads to a partial change of the crystal phase (see Figure 6.7). A small amount (approximately 5%) of the monoclinic phase was detected in the XRD pattern of an inactive catalyst. The surface area decreased slightly from 155 to 138 m²/g.

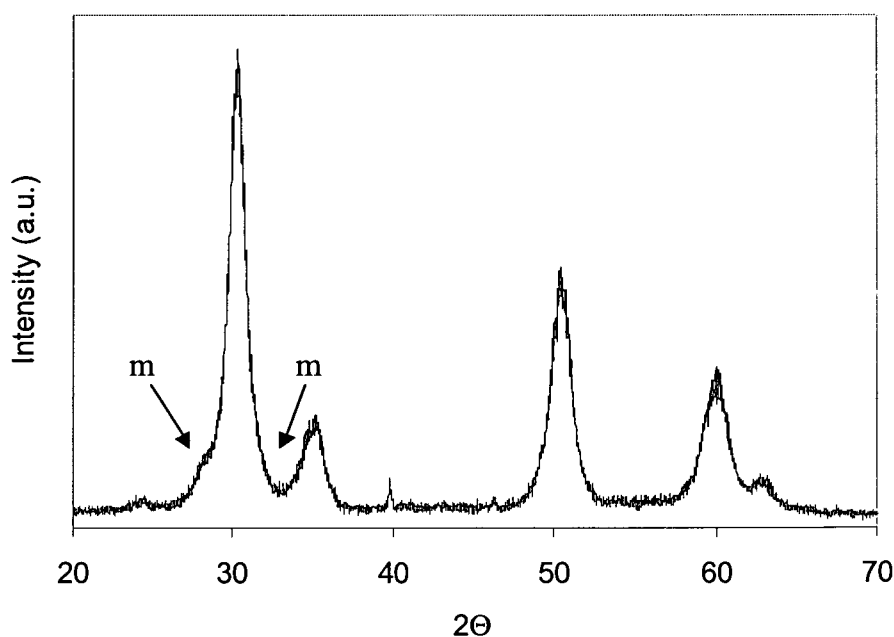


Figure 6.7: XRD pattern of an inactive Pt/Mel 2 catalyst

FTIR measurements after pyridine adsorption showed only Lewis acid sites on an inactive Pt/Mel 2 catalyst. No Brønsted acid sites were observed. From this it can be concluded that Brønsted acid sites play a crucial role in the n-alkane conversion over Pt/SZ catalysts.

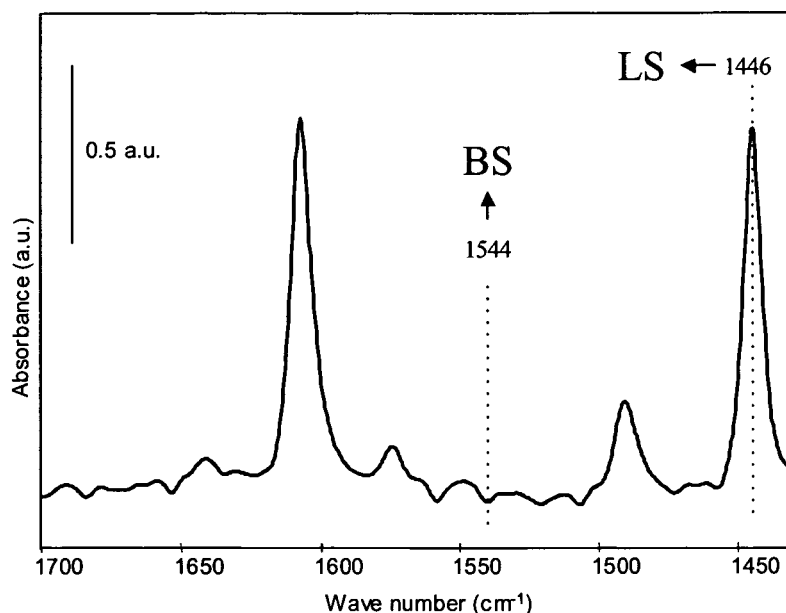


Figure 6.8: FTIR spectra after adsorption of pyridine (5 mbar, 20°C) on an inactive Pt/Mel 2 catalyst (which had lost a part of the sulfate groups during regeneration in helium at 500°C after the reaction of n-heptane in hydrogen at 200°C)

6.2.3 Reactivation of an inactive catalyst

The activity of an inactive Pt/Mel 2 catalyst, which had lost the active sulfate species after regeneration in inert gas, could not be restored by thermal treatment. However, it was possible to recover the catalytic activity of such an inactive material via resulfation.

Resulfation was carried out by impregnation of the inactive sample with 1 N H₂SO₄ under stirring. Then the material was dried at 100°C.

Table 6.3 shows the n-heptane conversion and isomerization selectivity at 200°C in hydrogen, the sulfate content and the ratio of LS/BS, which was determined by IR measurements of pyridine adsorption, in comparison to an active and an inactive Pt/Mel 2 catalyst. Increasing the sulfate content results in an active material. However, it was not possible to reach the same catalytic activity as before. BS were now present on the surface. Investigation of the crystal structure by XRD showed that the small reflexes of the monoclinic phase remain.

6. Deactivation and regeneration of Pt/SZ and SZ

Table 6.3: Sulfate content, activity for n-heptane conversion at 200°C in hydrogen and ratio of LS/BS of an active, an inactive and a resulfated Pt/Mel 2 catalyst

Catalyst	wt% SO ₄ ²⁻	Surface coverage (%)	Conversion (%)	Selectivity iC ₇ (%)	Rate (μmol/(g's))	LS/BS
active	5.7	58	56.3	4	16.0	0.52
inactive		approx. 40-50	0	-	0	LS
resulfated	6.9	78	16.2	14	4.7	0.39

6.3 Conclusions

The first activation of Pt/SZ can be done in air or in an inert atmosphere, followed by reduction at 200°C. Then Pt/SZ is active in the conversion of hydrocarbons independent of the activation atmosphere. The activity and selectivity in the isomerization of n-alkanes in hydrogen atmosphere is nearly the same. Regeneration in air restored the catalytic activity and selectivity of Pt/SZ completely.

If, however, regeneration of Pt/SZ is done in He or N₂ a remarkable loss of SO₂ was observed and the catalyst was irreversibly inactive. The loss of SO₂ was detected by TG and TPD measurements and was observed by the decreasing intensity of the SO band and the increasing Zr-OH bands in the IR spectrum.

From this it can be concluded that there are at least two different sulfate species present on the surface of sulfated zirconia. The sulfate species, which are more weakly bonded to the surface after a reductive step and are therefore evolved at lower temperatures (between 300 and 500°C) in inert gas, are essential for catalytic activity, whereas the sulfate groups, which are removed at higher temperatures above 600°C, are inactive for n-alkane conversion.

When the reaction was carried out in He or N₂ after activation or regeneration in air, Pt/SZ deactivated quickly and bands correlated to coke precursors or coke were found in the IR spectrum. Regeneration in air burned off the coke, no loss of sulfates was observed and the catalyst was active, whereas regeneration in an inert gas atmosphere is connected with decreasing amount of sulfates and leads to an inactive catalyst.

n-Heptane is converted to mono-methyl-, di-methyl-isomers and to propane and iso-butane over the active Pt/SZ, whereas over the inactive form only hydrogenolysis to propane and n-butane take place.

6. Deactivation and regeneration of Pt/SZ and SZ

Independent of the activation and reaction atmosphere, H₂ or N₂, SZ without Pt deactivates very quickly due to coke formation. No loss of sulfate groups was observed and regeneration could restore the initial activity.

The loss of the active sulfate species during regeneration of Pt/SZ in inert gas leads to an inactive catalyst, which possesses only LS and exhibits a small amount of monoclinic ZrO₂. It is possible to re-activate this material via resulfation. Increasing the sulfate content leads again to an active catalyst, where BS are present on the surface. The changes of the crystal structure remain.

References

-
- [1] R. Ahmad, J. Melsheimer, F.C. Jentoft, R. Schlögl, *J. Catal.* 218 (2003) 365.
 - [2] K. Arata, *Adv. Catal.* 61 (1990) 165.
 - [3] A. Corma, *Chem. Rev.* 95 (1995) 559.
 - [4] X. Song, A. Sayari, *Catal. Rev. Sci. Eng.* 38 (1996) 329.
 - [5] M. Misino, T. Okuhara, *Chemtech* (1993) 23.
 - [6] P.G. Blommel, Ch.D. Gosling, S.A. Wilcher, US Patent 5,763,713 (1998).
 - [7] C.R. Vera, J.C. Yori, C.L. Pieck, S. Irusta, J.M. Parera, *Appl. Catal. A* 240 (2003) 161.
 - [8] Ü.B. Demirci, F. Garin, *J. Mol. Catal.* 188 (2002) 233.
 - [9] G.D. Yadav, J.J. Nair, *Micro. Meso. Mat.* 33 (1999) 1.
 - [10] C. Morterra, G. Cerrato, M. Signoretto, *Catal. Lett.* 41, 1996, 101.
 - [11] V. Bolis, G. Magnacca, G. Cerrato, C. Morterra, *Topics in Catalysis* 19 (2002) 259.
 - [12] H. Liu, V. Adeeva, G.D. Lei, W.M.H. Sachtler, *J. Mol. Catal. A* 146 (1996) 165.
 - [13] M.G. Falco, J.M. Grau, N.S. Figoli, *Appl. Catal. A* 264 (2004) 183.
 - [14] K. Arata, H. Matsushashi, M. Hino, H. Nakamura, *Catal. Today* 81 (2003) 17.
 - [15] K. Ebitani, H. Konno, T. Tanaka, H. Hattori, *J. Catal.* 135 (1992) 60.
 - [16] K. Ebitani, J. Konishi, H. Hattori, *J. Catal.* 130 (1991) 257.
 - [17] T.J. McCarthy, G.D. Lei, W.M.H. Sachtler, *J. Catal.* 159 (1996) 90.
 - [18] I.J. Dijs, J.W. Geus, L.W. Jenneskens, *J. Phys. Chem. B* 107 (2003) 13403.
 - [19] C. Morterra, G. Cerrato, G. Meligrana, M. Signoretto, F. Pinna, G. Strukul, *Catal. Lett.* 73 (2001) 113.
 - [20] R.A. Keogh, D.E. Sparks, B.H. Davis, *Stud. Surf. Sci. Catal.*, Vol. 88, Elsevier, Amsterdam, 1994, 647.
 - [21] G. Resofszki, M. Muhler, S. Sprenger, U. Wild, Z. Paál, *Appl. Catal. A* 240 (2003) 71.
 - [22] E. García, M.A. Volpe, M.L. Ferreira, E. Rueda, *J. Mol. Catal. A* 201 (2003) 263.
 - [23] A. Lugstein, A. Jentys, H. Vinek, *Appl. Catal. A* 176 (1999) 119.
 - [24] G. King, A. Lugstein, R. Swagera, M. Ebel, A. Jentys, H. Vinek, *Micro. Meso. Mat.* 39 (2000) 307.
 - [25] J.M. Grau, C. R. Vera, J.M. Parera, *Appl. Catal. A* 172 (1998) 311.
 - [26] N. Bouchenafa-Saib, R. Issaadi, P. Grange, *Appl. Catal. A* 259 (2004) 9.
 - [27] B. Li, R.D. Gonzalez, *Appl. Catal. A* 165 (1997) 291.
 - [28] B. Li, R.D. Gonzalez, *Catal. Today* 46 (1998) 55.

- [29] M. Benaissa, J.G. Santiesteban, G. Díaz, C.D. Chang, M.J. Yacamán, *J. Catal.* 161 (1996) 694.
- [30] H. Armendariz, C. Sanchez Sierra, F. Figueras, B. Coq, C. Mirodatos, F. Levebre, D. Tichit, *J. Catal.* 171 (1997) 85.
- [31] L.M. Kustov, V.B. Kazansky, F. Figueras, D. Tichit, *J. Catal.* 150 (1994) 143.
- [32] J.A. Moreno, G. Poncelet *J. Catal.* 203 (2001) 453.
- [33] C. Morterra, G. Cerrato, F. Pinna, M. Signoretto, *J. Phys. Chem.* 98 (1994) 12373.
- [34] F. Babou, G. Coudurier, J. Vedrine, *J. Catal.* 152 (1995) 341.
- [35] C. Morterra, G. Cerrato, C. Emanuel, V. Bolis, *J. Catal.* 142 (1993) 349.
- [36] K. Föttinger, G. Kinger and H. Vinek, *Appl. Catal. A* 266 (2004) 195.
- [37] S.R. Vaudagna, R.A. Comelli, S.A. Canavese, N.S. Figoli, *J. Catal.* 169 (1997) 389.
- [38] S.R. Vaudagna, R.A. Comelli, N.S. Figoli, *Catal. Lett.* 47 (1997) 259.
- [39] S.Y. Kim, J.G. Goodwin Jr., D. Galloway, *Catal. Today* 63 (2000) 21.

7 INFLUENCE OF THE SULFATE CONTENT ON THE ACTIVITY OF Pt CONTAINING SULFATED ZIRCONIA

7.1 Introduction

The skeletal isomerization of n-alkanes to iso-alkanes over solid acid catalysts is an important technology for improvement of the octane number in oil refining. The importance continues to increase as environmental regulations on gasoline composition continue to grow [1].

Sulfate doped zirconia (SZ), as solid catalyst for low temperature alkane isomerization and for other acid catalyzed reactions too, has been the object of great interest [2,3]. Improving the robustness and decreasing the operation temperature of SZ catalysts appears to be a major focus of current research. To improve the stability of SZ Pt as promotor and hydrogen as carrier gas are used. Pt/SZ acts then as a bifunctional metal-acid catalyst with Pt as the metallic function and the acid function is generated by the interaction of hydrogen dissociated on the metal with sulfate species, as discussed by Hattori [4] and by Ebitani et al. [5].

The convenient procedure to have an efficient SZ system is to load the precursor with more than a statistical monolayer of sulfates (in order to generate protonic centres otherwise absent on plain zirconia) and then to calcine the sulfated precursor, in order to induce the selective elimination of sulfates from crystal defects.

Several kinds of sulfate groups, such as monosulfates and pyrosulfates, could be present on the surface of sulfated zirconia as demonstrated by IR spectroscopy [6] and by calculations based on density-functional theory [7,8].

The surface of SZ contains Brønsted (BS) and Lewis acid sites (LS) and much work has been carried out in attempts to better understand the structure, number and strength of these sites. Undoubtedly the acidity is generated by the sulfate anions and involves Brønsted and Lewis acid sites. Zhang et al. [9] investigated the relationship of Brønsted to Lewis acid sites by NMR studies of adsorbed pyridine and trimethylphosphine. They did not find any connection between the sulfur content and the number of BS in the sample. It was questioned if the acid strength is the most important factor in isomerization activity; instead, the optimum residence time of surface species was discussed [10].

7. Influence of the sulfate content on the activity of Pt containing sulfated zirconia

The BS/LS acidity ratio depends at least on the surface hydration/dehydration degree and the calcination temperature. SZ in a very high hydration state possesses a high amount of Brønsted acid sites, but the activity in alkane conversion was rather low [11].

The aim of this chapter is to investigate the influence of the sulfate concentration on the activity and selectivity in n-heptane isomerization.

7.2 Results and discussion

Four samples with different amounts of sulfates should be synthesized. Based on the surface area of Zr(OH)_4 of $55 \text{ m}^2/\text{g}$ after calcination at 600°C , which was used as precursor material, the samples should contain 1/3, 2/3, one and two monolayers of sulfates. In Table 7.1 the surface areas, the sulfate content measured by TG, the starting decomposition temperature of sulfate loss and the sulfate coverages are presented.

Table 7.1: Properties of different sulfated zirconia samples

Catalysts	Surface area (m^2/g)	SO_4 (wt%) measured	Starting decomposition temp. ($^\circ\text{C}$)	Experimental monolayers	Theoretical monolayers
SZ 1	48	1.4	770	0.46	0.33
SZ 2	66	2.4	700	0.57	0.66
SZ 3	77	3.1	650	0.63	1.00
SZ 4	81	3.0	625	0.59	2.00
Mel 2	155	5.7	650	0.58	

For all samples the water content was in the range of 2 – 3 wt% and water desorption is finished at 300°C .

The amount of sulfur retained is smaller than the amount impregnated as sulfuric acid. Assuming a surface area of 0.25 nm^2 for a sulfate group [12] the experimentally determined coverage varied between 46 and 63% of a monolayer. The onset temperature for sulfate decomposition decreased from 770 to 625°C with increasing sulfate content. This suggests that at least two different types of sulfate groups exist on the surface, one more strongly bonded than the other.

7. Influence of the sulfate content on the activity of Pt containing sulfated zirconia

Figure 7.1 shows the powder XRD patterns of Mel 2, SZ 1, 2 and 3. All samples show pure tetragonal structure, except for SZ 1 with a sulfate coverage less than half a monolayer a small amount of monoclinic ZrO_2 phase was detected. However, XRD is a bulk technique, therefore it is not possible to rule out structure changes which may occur on the surface.

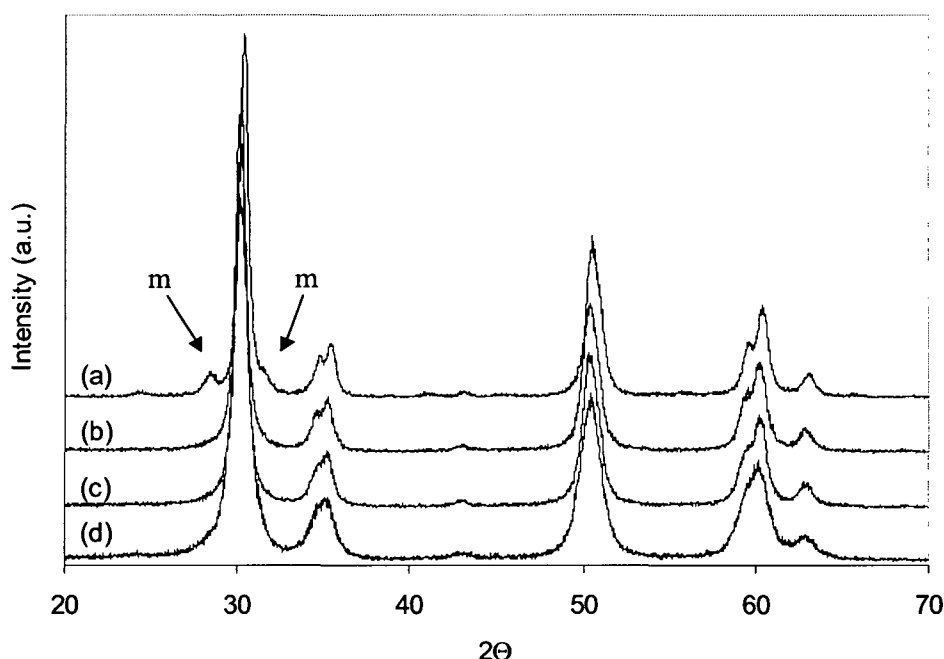


Figure 7.1: XRD patterns of (a) SZ 1, (b) SZ 2, (c) SZ 3 and (d) Mel 2
(m = reflexes of monoclinic phase)

NH_3 TPD spectra are shown in Figure 7.2. All catalysts are characterized by similar broad desorption peaks with a maximum below 200°C spanning in the range of $100 - 400^\circ\text{C}$ and asymmetric on the high temperature side. Note, that the area of ammonia signal is much bigger for the Mel catalyst, but taking into account the higher surface area, the concentration of acid sites is similar for Mel 2, SZ 3 and SZ 4.

Ammonia TPD for determining acidity of SZ catalysts is certainly not suitable, because ammonia decomposes sulfate at higher temperatures. However, for qualitative investigation of the strength of the acid sites this process is straightforward. Following the decomposition of sulfates two desorption maxima are observed when ammonia was adsorbed before. Without ammonia only one maximum at the higher temperature due to the loss of sulfate groups was detected when SZ is heated up to 1000°C . When SZ is regenerated after an alkane isomerization in an inert atmosphere a loss of a part of sulfate groups at lower temperature was observed [13] and the

7. Influence of the sulfate content on the activity of Pt containing sulfated zirconia

catalyst was inactive and could not be reactivated by thermal treatment. However, when the regeneration of SZ was done in an oxidizing atmosphere the catalyst was active and sulfate loss was detected only at the higher temperature. Therefore, it can be assumed that ammonia adsorption-desorption or alkane conversion induce a (partial) reduction of sulfates.

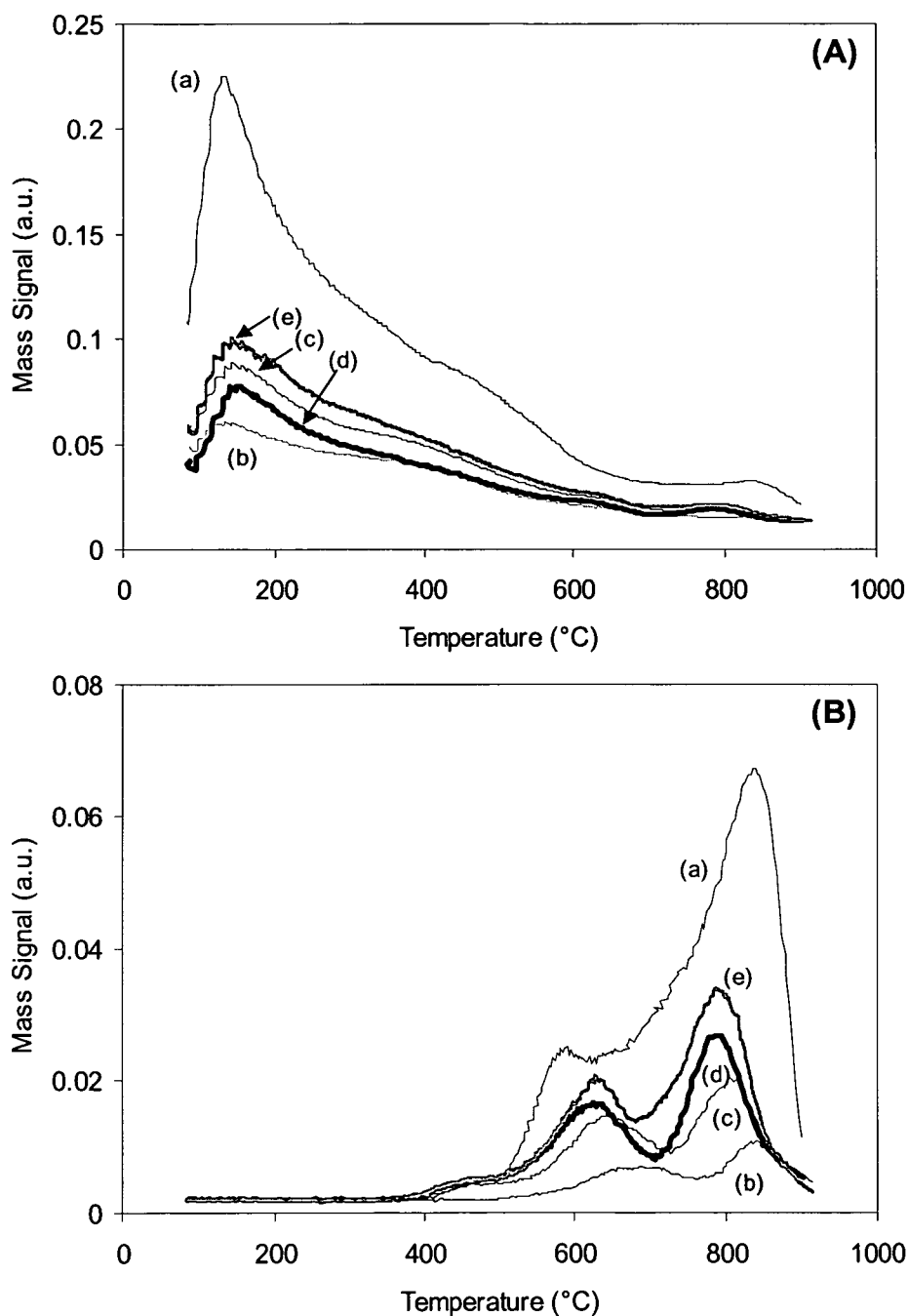


Figure 7.2: NH₃ TPD of (a) Mel 2, (b) SZ 1, (c) SZ 2, (d) SZ 3 and (e) SZ 4 in He flow: mass signal of (A) ammonia and (B) SO₂

7. Influence of the sulfate content on the activity of Pt containing sulfated zirconia

Adsorption of CO

Via adsorption of CO followed by IR spectroscopy it is possible to distinguish between oxidized $\text{Pt}^{\delta+}$ ($2136 - 2128 \text{ cm}^{-1}$) and metallic Pt^0 ($2099 - 2086 \text{ cm}^{-1}$) species. In Table 7.2 frequencies of adsorbed CO and in Figure 7.3 IR spectra of CO adsorbed on Pt/SZ samples are shown. All samples were activated in air at 500°C and reduced at 200°C prior to CO adsorption.

Table 7.2: CO adsorption on different Pt/SZ samples followed by IR measurements

Sample	CO frequencies (cm^{-1})	Assignment
Pt/ Mel 2 impregnated – calcined	2128, 2086	CO on $\text{Pt}^{\delta+}$, Pt^0
Pt/Mel 2 calcined – impregnated	2086, 1860	CO on Pt^0 mono-, bidentate
Pt/SZ 1	2049, 1802	CO on Pt^0 mono-, bidentate
Pt/SZ 2	2053, 1817	CO on Pt^0 mono-, bidentate
Pt/SZ 3	2080	CO on Pt^0 monodentate
Pt/SZ 4	2095	CO on Pt^0 monodentate

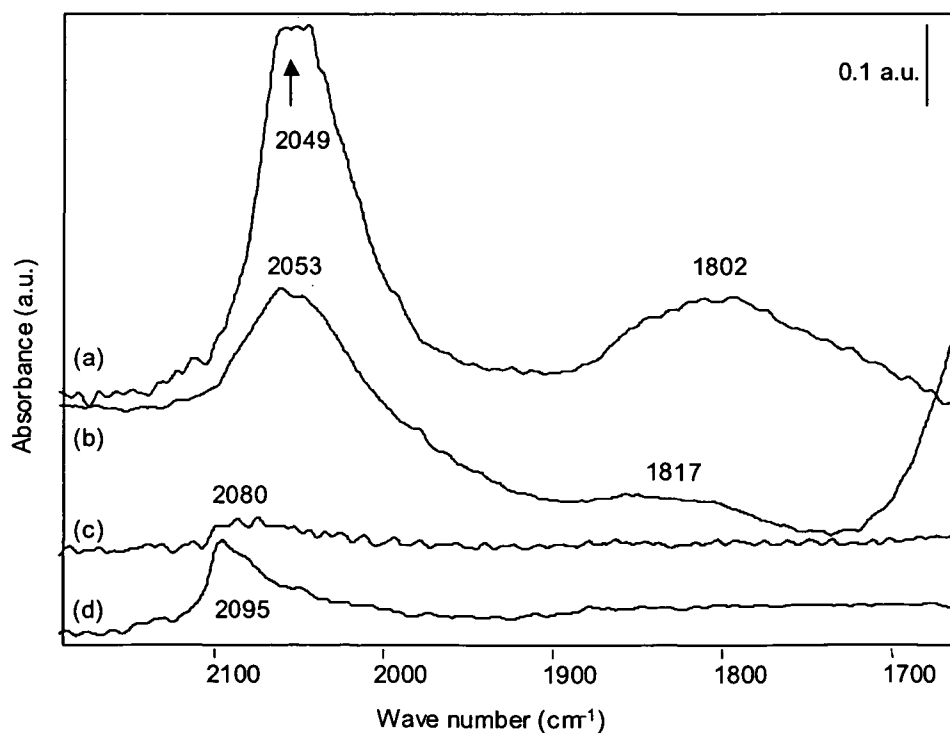


Figure 7.3: IR spectra of CO adsorption (5 mbar, 20°C) on different Pt/SZ samples after activation in air at 500°C and reduction at 200°C : (a) Pt/SZ 1, (b) Pt/SZ 2, (c) Pt/SZ 3 and (d) Pt/SZ 4

7. Influence of the sulfate content on the activity of Pt containing sulfated zirconia

Many researchers report that Pt is electron deficient or oxidized on the surface of SZ [14,15], but still dissociation of H_2 is retained which is necessary for the catalyst stability. As a reason for the positively charged Pt species the direct interaction between the acidic protons and the metal particles yielding $Pt-H^{\delta+}$ is discussed [6,16]. Paál and coworkers [17,18] postulated that SZ encapsulates Pt during calcination, which would be metallic but mostly buried in the first layers of the zirconia surface.

On the surface of Mel 2 Pt is present in a partially oxidized form, when Pt was impregnated on uncalcined sulfated zirconium hydroxide [19]. Impregnation of calcined Mel led to metallic Pt only. With the self-prepared SZ samples impregnation was always done before calcination. Pt was found in the metallic state. Note, that the frequency of CO linearly bonded to Pt shifted from 2049 cm^{-1} for SZ 1 to 2095 cm^{-1} for SZ 4. Sachtler and Zhang [20] observed the stretching frequency of adsorbed CO on reduced Pt/NaHY at 2090 cm^{-1} , which is shifted to 2068 cm^{-1} by neutralization with NaOH. This shift was interpreted as a weakening of the metal-CO bond with increasing acidity. Under the assumption that the acidity increased with increasing sulfate content Pt became partially oxidized or a $Pt-H^{\delta+}$ ensemble is present. On SZ 1 and SZ 2, the samples with the lowest sulfate content, CO is found linearly and bridged bonded to Pt. The wave numbers of the bridged bonded samples are rather low. Anderson et al. [21] found CO bridged bonded on Pt at 1845 cm^{-1} , own measurements on Pt/SiO₂ showed 1835 cm^{-1} for bridged and 2069 cm^{-1} for linearly bonded CO.

Adsorption of pyridine:

The type of acid sites present was studied with FTIR spectroscopy of chemisorbed pyridine. IR spectra of adsorbed pyridine on the different Pt/SZ samples were recorded after the same pretreatment conditions – activation in air at 500°C , reduction with hydrogen at 200°C , evacuation at 350°C , adsorption of 5 mbar pyridine and evacuation for one hour at 120°C . For comparison pyridine adsorption was measured on an inactive and on a coked Pt/Mel sample. The inactive sample was obtained by regeneration in inert gas at 500°C after the reaction in hydrogen. Sulfate loss was observed after this treatment, this is described in more detail in [13] and in chapter 6. Coking was found when the alkane reaction was carried out in He (see chapter 5).

Adsorption of pyridine on Brønsted acid sites forms a pyridinium ion with IR bands at 1638 , 1611 , 1540 and 1486 cm^{-1} , whereas pyridine covalently bonded to Lewis acid sites gives characteristic bands at 1486 and 1445 cm^{-1} [22].

7. Influence of the sulfate content on the activity of Pt containing sulfated zirconia

In Table 7.3 the ratio of Lewis to Brønsted acid sites after pumping off physically adsorbed pyridine at 120°C is shown. The ratio LS/BS was calculated from the band area at 1540 and 1445 cm⁻¹, respectively. Furthermore the S=O frequency before adsorption and the shift of the S=O band after pyridine adsorption are indicated.

Table 7.3: Ratio of Brønsted and Lewis acid sites and shift of the S=O band after pyridine adsorption on different (Pt)/SZ samples followed by IR measurements

Catalysts	LS/BS	ν S=O (cm ⁻¹)	$\Delta\nu$ S=O (cm ⁻¹)
Mel 2	0.8	1398	66
Pt/Mel 2	0.52	1398	62
Pt/Mel 2 inactive	Only LS	1369	49
Pt/Mel 2 resulfated	0.39	1401	69
Pt/Mel 2 coked	1.76	1390	53
Pt/SZ 1	Only LS	1352	41
Pt/SZ 2	1.6	1378	50
Pt/SZ 3	1.06	1402	70
Pt/SZ 4	1.1	1402	80

In Figures 7.4 and 7.5 IR difference spectra of protonated and Lewis bonded pyridine and the changes in the S=O region can be seen.

With increasing sulfate content the wave number of the S=O band changed from 1352 for Pt/SZ 1 to 1402 cm⁻¹ for Pt/SZ 3 and 4. The bands at lower wave numbers are assigned to isolated surface (SO₄)²⁻ groups, whereas the band around 1400 cm⁻¹ is tentatively attributed to a S₂O₇²⁻ species [23]. All of the sulfate species present are mainly (if not totally) on the surface, since the S=O band was observed to shift to lower wave numbers upon adsorption of CO or pyridine.

The origin of the shift of the S=O band can have various reasons: (i) Pyridine as a strong base can displace water from Lewis acid sites, which further reacts with SO groups to transform them into more ionic forms; or (ii) Clearfield et al. [24] attributed this shift to a weakening of the ability of S=O to attract electrons from Zr⁴⁺. The shift of the S=O band to a lower wave number corresponds to a decrease in the strength of Lewis acid sites.

7. Influence of the sulfate content on the activity of Pt containing sulfated zirconia

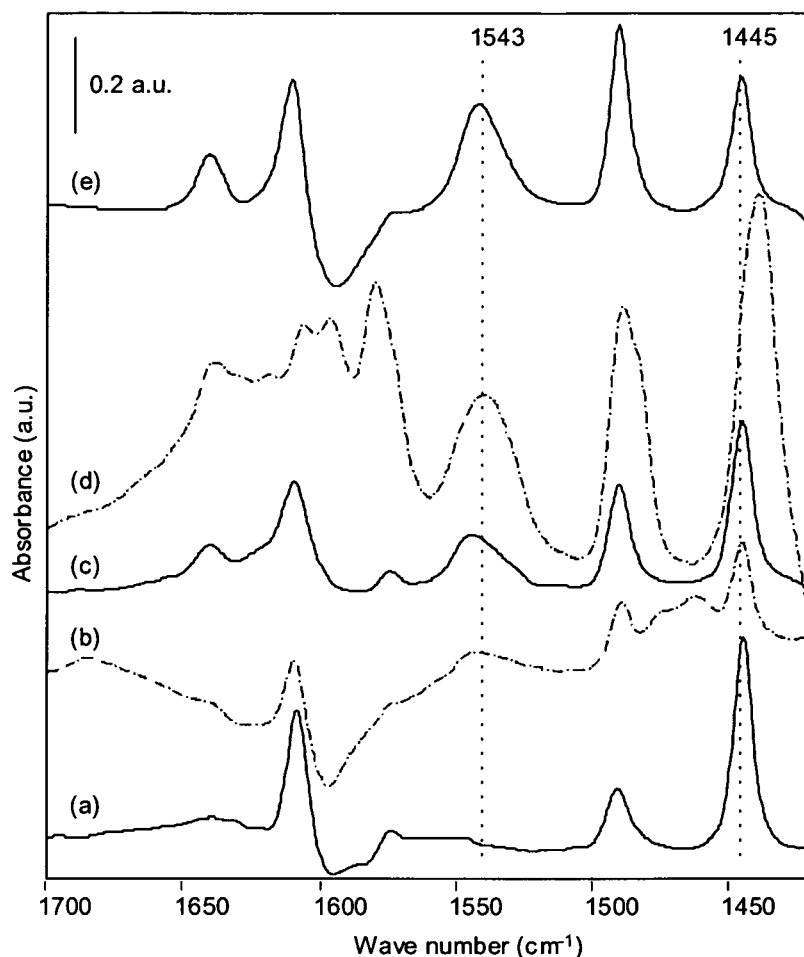


Figure 7.4: Difference spectra (obtained by subtraction of the spectrum after activation of the catalyst) after adsorption of pyridine (5 mbar, 20°C): region of bands assigned to adsorbed pyridine
(a) Pt/SZ 1, (b) Pt/SZ 2, (c) Pt/SZ 3, (d) Pt/SZ 4 and (e) Pt/Mel 2

It has been found that the relative amounts of LS and BS depend largely on the surface concentration of the sulfates [23]. At low sulfate loadings, i.e. on Pt/SZ 1 with less than half of a monolayer sulfates, only Lewis acid sites were observed. The S=O band was found at relatively low wave number (1352 cm⁻¹), which pointed to isolated sulfate species [23]. An increase in the sulfate loading to an amount exceeding half of a monolayer results in a shift of the S=O frequency to higher wave numbers and in the formation of Brønsted acid sites.

It seems that more than half a monolayer of sulfates is necessary for the formation of Brønsted acid sites. Zhang et al. [25] observed an increase of BS on the calcined sample with an increase in

7. Influence of the sulfate content on the activity of Pt containing sulfated zirconia

the sulfate concentration in the precursor, therefore the concentration of BS is directly correlated to the sulfate concentration.

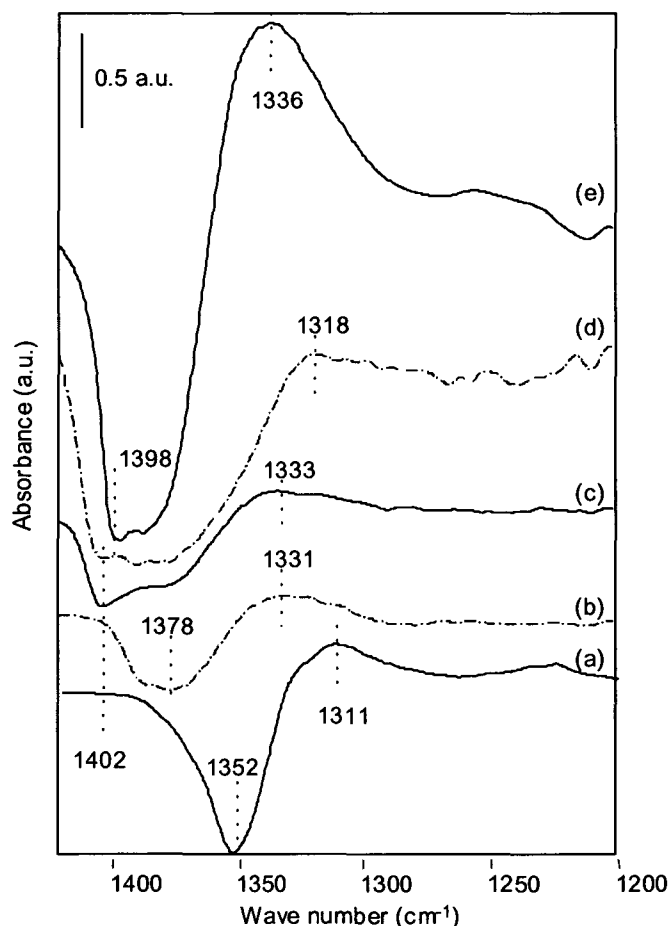


Figure 7.5: Difference spectra (obtained by subtraction of the spectrum after activation of the catalyst) after adsorption of pyridine (5 mbar, 20°C): S=O region
(a) Pt/SZ 1, (b) Pt/SZ 2, (c) Pt/SZ 3, (d) Pt/SZ 4 and (e) Pt/Mel 2

For the commercial Mel 2 sample a LS/BS ratio of 0.8 was measured, after impregnation with Pt a higher concentration of Brønsted acid sites in comparison to Lewis acid sites was found. Also Stevens et al. [26] found an increase of the B/L acid site ratio when Pt is present on SZ.

The LS/BS ratio varied between 0.52 for Pt/Mel 2 to 1.76 for the coked Mel sample, whereas the inactive Pt/Mel 2 and Pt/SZ 1 possess only Lewis acid sites. Li et al. [27] found an optimum LS/BS ratio of 2, a sample with a ratio of 0.147 was totally inactive while samples with higher

7. Influence of the sulfate content on the activity of Pt containing sulfated zirconia

ratios – activated at lower temperatures – are less active. Nascimento et al. [28] found that the fraction of BS increased with sulfur loading and that when the sulfur loading exceeds a monolayer the BS exceed LS.

Ward and Ko [29] proposed that the strong BS are the Zr-OH surface hydroxyl groups whose proton donating ability is increased by electron withdrawing effect of the S=O groups. On the other hand Kustov et al. [30] and Adeeva et al. [31] proposed that surface bi-sulfate species instead of Zr-OH are responsible for BS.

The deposition of coke does not appear to inhibit the adsorption of pyridine (Table 7.3). However, the LS/BS ratio was higher on the coked sample than on a fresh sample, indicating a loss of Brønsted acid sites. Note, that the coked sample could be reactivated after burning off the coke in air at 500°C. Under these conditions no loss of sulfates was observed.

On the inactive Pt/Mel sample only Lewis acid sites were observed and it was not possible to reactivate the sample by calcining in air. Li and Gonzalez [27] found that SZ after regeneration in N₂ at 550°C had a LS/BS ratio of 7.87. This catalyst was completely inactive and the activity could not be restored.

It seems that a certain concentration of sulfates is necessary for developing Brønsted acidity and catalytic activity.

n-Heptane conversion:

The conversion of n-heptane over all Pt free SZ catalysts (SZ 1 – SZ 4 and Mel) decreased rapidly with time on stream. The same behavior was observed when the reaction was carried out over Pt containing SZ catalysts using nitrogen or helium as carrier gas. The selectivity to isomerization was very small and main reaction products were propane and iso-butane indicating an acid catalyzed cracking mechanism.

The deactivation resulted from carbon deposition on the catalysts. The carbon content measured after 2h time on stream of n-heptane in He was 0.45 wt% and 0.90 wt% for Mel 2 and Pt/Mel 2, respectively. By burning off the coke both samples could be regenerated to their initial activity. The temperature interval of CO₂ release was between 400 and 550°C for Mel and 250 and 400°C for Pt/Mel. Note, that no sulfate loss was detected when the catalyst was regenerated in oxidizing atmosphere.

7. Influence of the sulfate content on the activity of Pt containing sulfated zirconia

Grau et al. [32] reported that the simultaneous presence of Pt and hydrogen is essential to have an active and stable catalyst. However, an additional requirement for catalytic activity should be the presence of Brønsted acid sites.

Pt/SZ 1, which has the lowest sulfate content and no Brønsted acid sites, was not active for n-heptane conversion at 200°C. Increasing the temperature to 250°C, which is the highest possible reaction temperature due to reduction of sulfate groups by hydrogen, only a small conversion with 60% selectivity to iso-heptanes and 40% cracking to propane and mainly n-butane was found. This result can be interpreted as a metal catalyzed isomerization and hydrogenolysis of n-heptane [33]. Therefore over Pt/SZ 1 the metal function prevails and no acid catalyzed reaction is possible.

In Table 7.4 the reaction rates in $\mu\text{mol}/(\text{g}\cdot\text{s})$ after 1 h time on stream at 200°C, the isomerization selectivity, the ratio of mono to multibranched isomers (Mo/Mu) and for comparison the estimated LS/BS ratio are summarized.

Table 7.4: Reaction rates after 1h time on stream at 200°C (total flow 40 ml/min, n-heptane partial pressure 15 mbar, total pressure 1 bar), isomerization selectivity, ratio of mono- to multibranched isomers (Mo/Mu) and LS/BS ratio

Catalysts	Rate ($\mu\text{mol}/(\text{g}\cdot\text{s})$)	Selectivity (%)	Mo/Mu	LS/BS
Pt/SZ 1	0	-	-	LS
Pt/SZ 2	0.55	63	3.2	1.6
Pt/SZ 3	1.76	52	3.0	1.06
Pt/SZ 4	2.11	21	2.2	1.1
Pt/Mel 2	16.3	4	1.8	0.52
Pt/Mel 2 coked	0.08	0	-	1.76
Pt/Mel 2 inactive	0	-	-	LS

The activity increased with an increasing concentration of Brønsted acid sites, but the selectivity to isomerization decreased. 2-Methylhexane and 3-methylhexane are the predominant isomerization products. Over the catalysts with more Brønsted acid sites, the fraction of multibranched isomers increased (Table 7.4) but with decreasing yields. The main cracking products are propane and iso-butane, indicative of an acid cracking process. Pt/SZ 1 and Pt/Mel 2 (inactive), which contain only Lewis acid sites, are completely inactive for the reaction, whereas

7. Influence of the sulfate content on the activity of Pt containing sulfated zirconia

over Pt/Mel 2 (coked) a small initial activity was measured. For the generation of Brønsted acid sites a threshold amount of sulfates on the surface should be necessary.

In Table 7.5 the global apparent activation energy and the apparent activation energy values for isomerization and cracking are summarized. The reaction order in hydrogen and n-heptane was found to be -0.25 and $+0.8$ respectively. In all experiments for the determination of the kinetic data, the conversion was smaller than 10%.

Table 7.5: Global apparent activation energy and apparent activation energy values for isomerization and cracking

	Global E_A (kJ/mol)	E_A isomerization (kJ/mol)	E_A cracking (kJ/mol)
Pt/SZ 2	107	105	110
Pt/SZ 3	83	68	101
Pt/SZ 4	86	62	102
Pt/Mel 2	79	33	108

The conventional bifunctional metal-acid mechanism is characterized by specific kinetic data: (i) apparent activation energies between 84 and 126 kJ/mol, (ii) hydrocarbon reaction orders near $+1$, and (iii) hydrogen reaction orders between -1 and 0 [34,35]. All these conditions are fulfilled over the different Pt containing SZ samples.

Pt/SZ catalysts are active for n-heptane conversion but not selective for isomerization. The activity is related to Brønsted acid sites, which are built up when at least half of a monolayer of sulfate groups is present on the surface. If only Lewis sites are detected by pyridine adsorption the catalysts are totally inactive. Also Li et al. [36] found that Brønsted acid sites are indispensable for n-butane isomerization over SZ whereas Lewis acid sites are insufficient for catalyzing the reaction.

The surface coverage by sulfates is similar for SZ 3, 4 and Mel 2. The latter catalyst is much more active, which can be correlated to more Brønsted acid sites in comparison to Lewis sites. It remains an open question why similar coverages by sulfate groups lead to a different content of Brønsted acid sites.

CO adsorption on Pt/Mel 2 indicated that Pt is present in a partially oxidized form, whereas on all other Pt/SZ samples only metallic Pt is found. Therefore it is assumed that for higher activity

7. Influence of the sulfate content on the activity of Pt containing sulfated zirconia

ensembles containing metallic and acidic sites – $(Pt_n H)^+$ are the active sites together with hydride ions necessary for hydrogenation and desorption of iso-alkanes.

Liu et al. [37] and Buchholz et al. [38] discussed these sites as combined metal-acid sites or compressed bifunctional sites, respectively. In all cases the close vicinity between metallic and acidic sites is essential. On these sites hydrogen is dissociated on Pt and is then transferred to adjacent acidic sites as hydride ions and reacts with surface carbenium ions to form isoalkanes. The selectivity for isomerization is high for small alkanes until n-hexane where β -cracking is not favored, but for higher alkanes the selectivity is too low.

Role of BS and LS

It is obvious from the results reported above that Brønsted acid sites are crucial for the catalytic activity and that their concentration depends on the sulfate content. These findings are summarized and visualized in Figures 7.6 and 7.7 for the samples Pt/SZ 1, 2 and 3.

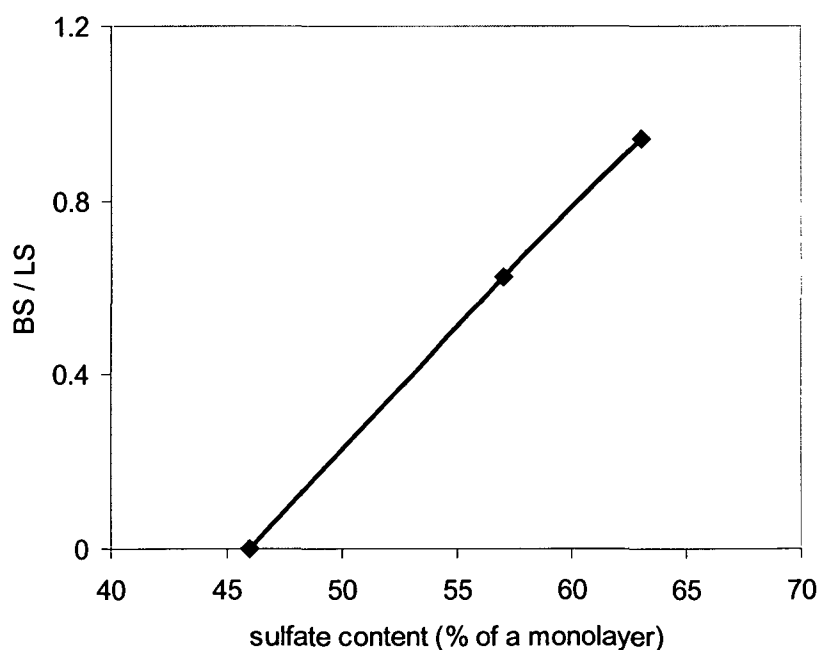


Figure 7.6: BS/LS versus surface coverage with sulfates for Pt/SZ 1, 2 and 3

7. Influence of the sulfate content on the activity of Pt containing sulfated zirconia

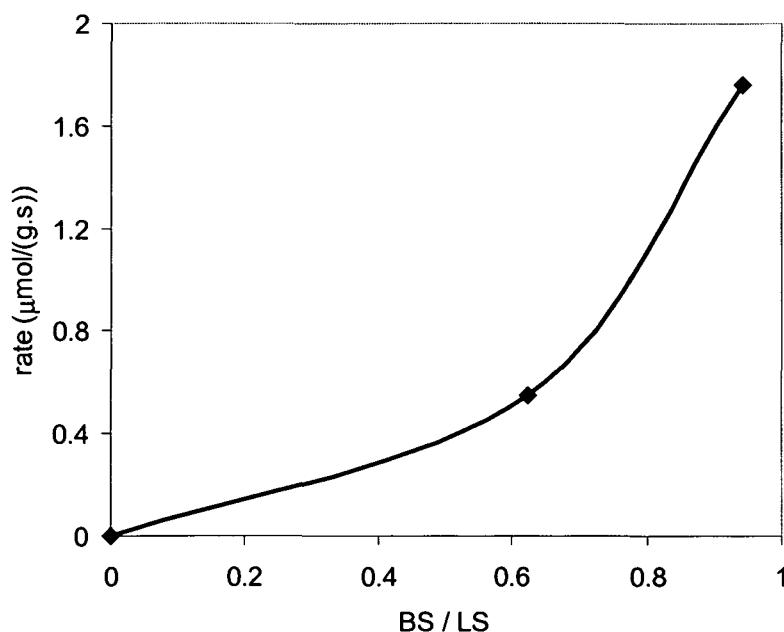


Figure 7.7: Activity for n-heptane isomerization at 1 bar and 200°C in hydrogen against the LS/BS ratio determined by FTIR after pyridine adsorption on Pt/SZ 1, 2 and 3

7.3 Conclusions

- Sulfated zirconia is only active for alkane conversion when Brønsted acid sites are present.
- The concentration of Brønsted acid sites depends on the concentration of surface sulfates.
- The formation of Brønsted acid sites starts when more than half of a monolayer of sulfates is present.
- On an inactive sample of sulfated zirconia, which has lost a part of sulfate groups, only Lewis acid sites were measured. Calcining in oxidizing atmosphere could not reactivate this sample.
- No sulfate loss but a decreasing concentration of Brønsted acid sites were found on coked sulfated zirconia. Calcining in oxidizing atmosphere could reactivate this sample.

7. Influence of the sulfate content on the activity of Pt containing sulfated zirconia

- Pt/SZ containing more than half of a monolayer sulfate groups is active for n-heptane conversion but not selective for isomerization.

References

-
- [1] M.J. Hunter, *Erdoel Erdgas Kohle* 119 (2003) OG97-OG107.
- [2] K. Ebitani, J. Konishi, H. Hattori, *J. Catal.* 130 (1991) 257.
- [3] R.A. Comelli, C.R. Vera, J.M. Parera, *J. Catal.* 151 (1995) 96.
- [4] H. Hattori, *Stud. Surf. Sci. Catal.* 77 (1993) 69.
- [5] K. Ebitani, J. Konishi, A. Horie, H. Hattori, K. Tanabe, in: K. Tanabe, H. Hattori, T. Yamaguchi, T. Tanaka /Eds.), *Acid-Base Catalysts*, Kodansha Ltd., Tokyo, 1989, p. 491.
- [6] C. Morterra, G. Cerrato, S. Di Ciero, M. Signoretto, F. Pinna, G. Strukul, *J. Catal.* 165 (1997) 172.
- [7] F. Haase, J. Sauer, *J. Am. Chem. Soc.* 120 (1998) 13503.
- [8] A. Hofmann, J. Sauer, *J. Phys. Chem. B* 108 (2004) 14652.
- [9] J. Zhang, J.B. Nicholas, J.F. Haw, *Angew. Chem. Int. Ed.* 39 (2000) 3302.
- [10] G. Resofszki, M. Muhler, S. Sprenger, U. Wild, Z. Paál, *Appl. Catalysis A* 240 (2003) 71.
- [11] C. Morterra, G. Cerrato, F. Pinna, M. Signoretto, *J. Phys. Chem.* 98 (1994) 12373.
- [12] F.R. Chen, G. Coudurier, J.F. Joly, J.C. Vedrine, *J. Catal.* 143 (1993) 616.
- [13] K. Föttinger, H. Vinek, *Catal. Lett.* 97 (2004) 55.
- [14] K. Ebitani, J. Tsuji, H. Hattori, H. Kita, *J. Catal.* 135 (1992) 609.
- [15] X. Song, A. Sayari, *Catal. Rev.-Sci. Eng.* 38 (1996) 329.
- [16] A.V. Ivanov, A.Yu. Stakheev, L.M. Kustov, *Stud. Surf. Sci. and Catal.* 130 (2000) 263.
- [17] Z. Paál, U. Wild, M. Muhler, J.M. Manoli, C. Potvin, T. Buchholz, S. Sprenger, G. Resofszki, *Appl. Catal. A* 188 (1999) 257.
- [18] J.M. Manoli, C. Potvin, M. Muhler, U. Wild, G. Resofszki, T. Buchholz, Z. Paál, *J. Catal.* 178 (1998) 338.
- [19] K. Föttinger, G. Kinger, H. Vinek, *Appl. Catal. A* 266 (2004) 195.
- [20] W.M.H. Sachtler, Z. Zhang, *Adv. Catal.* 39 (1992) 129.
- [21] J.A. Anderson, C.H. Rochester, *Catalysis Today* 10 (1991) 275.
- [22] T. Lopez, J. Navarrete, R. Gomez, O. Novaro, F. Figueras, H. Armendariz, *Appl. Catal. A* 125 (1995) 217.
- [23] C. Morterra, G. Cerrato, V. Bolis, *Catal. Today* 17 (1993) 505.
- [24] A. Clearfield, G.P.D. Serrette, A.H. Khazi-Syed, *Catal. Today* 20 (1994) 295.
- [25] C. Zhang, R. Miranda, B.H. Davis, *Catal. Lett.* 29 (1994) 349.
- [26] R.W. Stevens Jr., S.S.C. Chuang, B.H. Davis, *Appl. Catal. A* 252 (2003) 57.
- [27] B. Li, R.D. Gonzalez, *Catalysis Today* 46 (1998) 55.
- [28] P. Nascimento, C. Akrapoulou, M. Oszagyan, G. Coudrier, C. Travers, J.F. Joly, J.C. Vedrine, in "New Frontiers in Catalysis" (L. Guczi et al. Eds.) pp. 1185-1197 Elsevier Science, Amsterdam, 1993.
- [29] D.A. Ward, E.I. Ko, *J. Catal.* 150 (1994) 18.
- [30] L.M. Kustov, V.B. Kazansky, F. Figueras, D. Tichit, *J. Catal.* 150 (1994) 143.
- [31] V. Adeeva, J.W. De Haan, J. Jänchen, G.D. Lei, V. Schünemann, L.J.M. van de Ven, W.M.H. Sachtler, R.A. van Santen, *J. Catal.* 151 (1995) 364.

- [32] J.M. Grau, J.C. Yori, J.M. Parera, Appl. Catal. A 213 (2001) 247.
- [33] Z. Paál in "Hydrogen Effect in Catalysis" Eds. Z. Paál, P.G. Menon, Marcel Dekker Inc. 1988, p. 449.
- [34] J.H. Sinfelt, Adv. Chem. Eng. 5 (1964) 37.
- [35] M. Belloum, C. Travers, J.P. Burnonville, Rev. Inst. Fr. Pet. 46 (1991) 89.
- [36] X. Li, K. Nagaoka, J.A. Lercher, J. Catal. 227 (2004) 130.
- [37] H. Liu, H. Lei, W.M.H. Sachtler, Appl. Catal. A 137 (1996) 167.
- [38] T. Buchholz, U. Wild, M. Muhler, G. Resofszki, Z. Paál, Appl. Catal. A 189 (1999) 225.

8 GENERAL CONCLUSIONS

The isomerization of n-alkanes is a very important process in refining and petrochemical industry. Industrial processes use Pt supported on chlorided alumina and Pt containing zeolites as catalysts. However, the process using Pt/Cl⁻/Al₂O₃ has serious disadvantages, mainly the need for continuous introduction of chloride to maintain the catalytic activity, the corrosiveness and the high costs for catalyst disposal. The zeolite is less active, therefore higher reaction temperatures are needed. Pt promoted sulfated zirconia is believed to be a promising alternative catalyst due to its high catalytic activity at low temperatures. A thorough understanding of the mechanism of the alkane isomerization over SZ and the active sites of sulfated zirconia are helpful for the development of an effective catalyst.

In this thesis the isomerization of n-hexane and n-heptane was investigated with in situ IR and kinetic studies as well as various characterization techniques.

Activity and selectivity

Pt containing sulfated zirconia is active for n-alkane hydroconversion. Compared to zeolite HBEA the reaction temperature required to reach the same level of conversion is shifted for approximately 80°C to lower temperatures on Pt/SZ. The selectivity to isomerization was excellent for n-hexane, whereas for n-heptane it was small and the main reaction products were propane and iso-butane indicating an acid catalyzed cracking mechanism. Thus for higher hydrocarbons (> C₆) Pt/SZ is suitable for hydrocracking reactions, but not for hydroisomerization.

SZ possesses weaker acid sites than zeolite HBEA, which was shown by IR spectroscopy after adsorption of basic probe molecules, calorimetric studies and NH₃ TPD. But it remains an open question why this material is so active and shows such a high cracking selectivity.

Active sites:

The following results were found concerning the active sites of Pt/SZ:

- (i) A close vicinity of the metal and acidic sites leads to a significantly better performance of the catalyst resulting in a higher activity and a better selectivity to isomerization. This is contrary to

zeolites, where the same activity was observed for a mechanical mixture of the zeolite and Pt supported on an inert carrier material and for the Pt containing zeolite [1].

(ii) The catalytic activity is connected to a part of the sulfate groups, which are the active species and induce Brønsted acidity on SZ, probably pyrosulfate-type species.

(iii) Brønsted acid sites (BS) were identified as the sites responsible for catalytic activity. Sulfated zirconia is only active for alkane conversion when Brønsted acid sites are present. The concentration of Brønsted acid sites depends on the concentration of surface sulfates. The formation of BS starts when more than half of a monolayer of sulfates is present. Samples, which have lost a part of sulfate groups during regeneration in inert gas after a reductive step or which have less than half a monolayer sulfates on the surface, possess only Lewis acid sites and are therefore inactive.

A model, which explains all these results, are collapsed bifunctional sites $(Pt_nH)^+$ nearby the active sulfate species. Such ensembles contain BS connected to pyrosulfate species and adjacent metal sites, which provide activated hydrogen species such as hydride ions.

Sulfate groups:

There are at least two different sulfate species present on the surface of sulfated zirconia. The sulfate species, which are more weakly bonded to the surface after a reductive step and are thus evolved at lower temperatures (between 300 and 500°C) in inert gas, are essential for catalytic activity, whereas the sulfate groups, which are removed at temperatures above 600°C under the same conditions, are inactive for n-alkane conversion. The active species amount to about 15-20% of the total sulfate groups in the case of Mel 2.

The active sulfate groups show the following characteristic behaviour: (i) Reduction in hydrogen in the presence of Pt or reaction with hydrocarbons transforms them into a state, where they are more weakly bonded to the oxidic surface and thus evolve already at lower temperatures during heating in inert gas. Oxidation restores the initial state. (ii) They can be removed by washing with water at room temperature, which was observed by Li et al. [2]. (iii) They are formed when more than half a monolayer of sulfates are present on the surface of SZ. At lower coverages only the inactive species were found.

Using DFT calculations, Hofmann and Sauer [3] found that pyrosulfate species $S_2O_7^{2-}$ are a possible and stable structure over a wide temperature and partial pressure range. The formation of

pyrsosulfate groups at sulfate loadings above half of a monolayer could explain the results reported in this thesis.

Reaction mechanism:

The initiation step of alkane isomerization is different over Pt/SZ in hydrogen and over Pt/SZ and SZ in He. In the first case it is a real catalytic reaction whereas otherwise a surface reaction took place. The last reaction is interpreted as an oxidative dehydrogenation characterized by water and coke formation. For the isomerization of n-butane in helium over unpromoted SZ it was found that the concentration of traces of butenes in the feed influences the activity [4].

When the reaction is carried out in hydrogen, the obtained kinetic data point to the conventional bifunctional metal-acid mechanism, which is characterized by the following requirements: (i) apparent activation energies between 84 and 126 kJ/mol, (ii) hydrocarbon reaction orders near +1, and (iii) hydrogen reaction orders between -1 and 0. According to the classical mechanism for alkane conversion over bifunctional catalysts proposed by Weisz and Swegler [5] the n-alkanes are first dehydrogenated on the metallic sites, then isomerized or cracked at the acidic sites and the products finally desorb as alkenes and are hydrogenated on the metallic sites.

Deactivation:

Two different deactivation mechanisms were identified over Pt/SZ. Reaction in inert gas leads to a reversible deactivation via coke formation, whereas heating the catalyst in inert gas after a reduction leads to an irreversible deactivation due to a loss of sulfate groups.

In helium as carrier gas oxidative dehydrogenation of the alkanes leads to the formation of carbenium ions on the catalyst surface. When spillover hydrogen is not present, the carbenium ions remain on the surface, where they are oligomerized into coke precursors or coke. Regeneration in oxygen containing atmosphere restores the catalytic activity, whereas in inert gas the catalyst gets inactive due to a loss of the active sulfate species. Such an inactive catalyst cannot be reactivated by thermal treatment. However, it is possible to regain catalytic activity for n-alkane conversion via resulfation.

References

-
- [1] G. Kinger, Ph. D. thesis, TU Wien, 2001.
 - [2] X. Li, K. Nagaoka, J.A. Lercher, J. Catal. 227 (2004) 130.
 - [3] A. Hofmann, J. Sauer, J. Phys. Chem. B 108 (2004) 14652.
 - [4] X. Li, Ph. D. thesis, TU München, 2004.
 - [5] P.B. Weisz, E.W. Swegler, Science 126 (1957) 31.

Lebenslauf

Persönliche Daten

Name: KARIN FÖTTINGER
Geboren am: 25. Dezember 1976 in Braunau am Inn
Familienstand: ledig
Wohnhaft in: 1170 Wien, Kalvarienberggasse 18/1/1
Email: foettinger@tuwien.ac.at
Staatsbürgerschaft: Österreich

Schulausbildung

09/87 – 06/95 Bundesgymnasium Braunau am Inn
Juni 95 Matura (mit Auszeichnung)

Studium

10/95 - 10/01 Technische Chemie an der Technischen Universität Wien,
Studienzweig Analytische und Physikalische Chemie
10/00 – 10/01 Diplomarbeit zum Thema „Isomerisierung von n-Penten über Ferrierit
und Beta“ am Institut für Materialchemie unter Betreuung von Prof.
Vinek
Tätigkeit als Studienassistent
Oktober 01 2. Diplomprüfung für Technische Chemie (mit ausgezeichnetem Erfolg)
seit 10/01 Doktoratsstudium der Technischen Wissenschaften am Institut für
Materialchemie der TU Wien, Arbeitsgruppe für Heterogene Katalyse
und Photochemie bei Prof. Vinek, Gebiet „n-Alkanisomerisierung über
Pt-hältigem sulfatisierten Zirkonoxid“

Berufspraxis

10/01 – 11/03 Doktorandenstelle im Rahmen eines FWF-Projekts (P-14972) mit dem
Titel „Composites as Catalysts for the Hydroisomerization of n-Alkanes
at low Temperatures“
12/03 – dato Wissenschaftlicher Mitarbeiter in Ausbildung am Institut für
Materialchemie, Arbeitsgruppe für Heterogene Katalyse und
Photochemie

Wien am 23. Mai 2005

Publikationen

K. Föttinger, K. Zorn, H. Vinek:

"Influence of the sulfate content on the activity of Pt containing sulfated zirconia."

Applied Catalysis A: General **284** (2005) 69 – 75.

K. Föttinger, H. Vinek:

"Activation and deactivation of Pt containing sulfated zirconia and sulfated zirconia studied by in situ IR spectroscopy."

Catalysis Letters, **97** (2004) 3, 131-138.

K. Föttinger, G. Kinger, H. Vinek:

"In situ IR investigation of n-hexane isomerization over Pt containing sulfated zirconia."

Applied Catalysis A: General **266** (2004) 195 – 202.

K. Föttinger, G. Kinger, H. Vinek:

"1-Pentene isomerization over FER and BEA."

Applied Catalysis A: General **249** (2003) 205 – 212.

K. Föttinger, G. Kinger, H. Vinek:

"1-Pentene isomerization over zeolites studied by in-situ IR spectroscopy."

Catalysis Letters, **85** (2003) 1-2, 117 - 122.

B. Basnar, J. Schnöller, K. Föttinger, G. Friedbacher, U. Mayer, H. Hoffmann, L. Fabry:

"Characterization of silicon wafers through deposition of self-assembled monolayers."

Fresenius J. Anal. Chem., **368** (2000) 434 - 438.

Konferenzbeiträge

K. Föttinger, K. Zorn, H. Vinek:

Vortrag "*Isomerization of n-Alkanes over Pt promoted sulfated zirconia studied by in situ IR spectroscopy.*"

Bunsentagung 2005, Frankfurt am Main, Deutschland; 05.05.2005 – 07.05.2005

K. Föttinger, H. Vinek:

Vortrag "*Activation and deactivation of Pt containing sulfated zirconia and sulfated zirconia studied by in situ IR spectroscopy.*" (Oral Presentation Award)

7th Pannonian International Symposium on Catalysis, Srni, Tschechien; 12.09.2004 – 16.09.2004

K. Föttinger, H. Vinek:

Poster "*Isomerization of n-Alkanes over Pt-sulfated zirconia studied by in situ IR spectroscopy.*"

13th International Congress on Catalysis, Paris, Frankreich; 11.07.2004 – 16.07.2004

K. Föttinger, G. Kinger, H. Vinek:

Poster "*Hydroisomerization of n-Heptane over Pt-sulfated zirconia catalysts. An in-situ FT-IR study.*"

12. Tagung Festkörperanalytik, Wien, Österreich; 22.09.2003 – 24.09.2003

K. Föttinger, G. Kinger, H. Vinek:

Poster "*Comparison of n-alkane isomerization over Pt promoted BEA and sulfated zirconia*"

EuropaCat VI, Innsbruck, Österreich; 31.08.2003 – 04.09.2003

K. Föttinger, G. Kinger, H. Vinek:

Vortrag "*Isomerization of 1-Pentene over HFER and HBEA zeolites*"

15. Deutsche Zeolithtagung, Kaiserslautern, Deutschland; 05.03.2003 – 07.03.2003

K. Föttinger, G. Kinger, H. Vinek:

Poster "*Hydroisomerisierung von n-Heptan über Pt- und Al- hältigem sulfatisierten Zirkonoxid*"

10. Österreichische Chemietage der GÖCh, Linz, Österreich; 17.09.2002 – 19.09.2002

K. Föttinger, G. Kinger, H. Vinek:

Vortrag "*Isomerization of 1-Pentene over ferrierite and beta zeolites*"

6th Pannonian International Symposium on Catalysis, Obergurgl, Österreich; 11.09.2002 – 14.09.2002

K. Föttinger, G. Kinger, H. Vinek:

Poster "*Isomerization of 1-Pentene over 10- and 12- MR molecular sieves*"

EuropaCat V, Limerick, Irland; 02.09.2001 – 07.09.2001